Limnological Conditions in Tainter and Menomin Reservoirs: Final Report 2014-18

31 December 2019

William F. James
University of Wisconsin – Stout
Discovery Center - Center for Limnological Research and Rehabilitation
Department of Biology
Menomonie, WI 54751
715-338-4395
jamesw@uwstout.edu

EXECUTIVE SUMMARY

Seven sampling stations were established on Tainter (5 stations) and Menomin (2 stations) Lakes, respectively, in 2015-18 to examine longitudinal variations in summer physical, chemical, and biological characteristics as a function of nutrient loading and hydrology. Sampling stations were also established on existing US Geological Survey gauging stations located on the Red Cedar River near Colfax (RCR_{in}) and Menomonie (RCR_{out}) and the Hay River near Wheeler (HR). Samples for analysis of nitrogen and phosphorus species and chlorophyll were collected as surface grabs from the tributaries and 2-m integrated grabs at 1- to 2-week intervals between May and September of 2015-18. Samples were collected less frequently in 2014 as a part of the LAKES Research Experience for Undergraduates (REU) National Science Foundation (NSF) Grant awarded to the University of Wisconsin – Stout. In situ water temperature, conductivity, dissolved oxygen, and pH were also measured.

Annual and summer (May-September) flows at RCR_{out} were much greater in 2014-17 compared to long-term records while the year 2018 exhibited means that were similar to long-term trends. The summer of 2014 exhibited the highest RCR_{out} flows during the study period. Monthly RCR_{out} exceeded long-term historical flows during most summer months in 2014-17, particularly July, August, and September. In contrast, monthly RCR_{out} flows in 2018 reflected long-term averages, particularly in June, July, and August. RCR_{out} flows were also elevated during spring snowmelt periods in 2014, 2016, 2017, and 2018. Modest snowpack during the El Niño winter of 2015 was associated with minor snowmelt runoff. Overall, annual measured inflows and the outflow were similar between the 5 study years while summer inflows and the outflow were greater in 2014 compared to 2015-18. Mean summer residence time ranged between ~ 4-7 days in Tainter Lake and 3-5 days in Menomin Lake.

RCR_{in} accounted for ~ 74% of the measured annual and summer inflow to Tainter Lake. SRP loading represented ~50% (flow-weighed total P = 0.150 mg/L, SRP = 0.080 mg/L)

of the summer RCR_{in} total P load and ~ 47% (flow-weighed total P = 0.127 mg/L, SRP = 0.061 mg/L) of the summer HR total P load between 2014 and 2018. RCR_{in} contributed a mean 80,341 kg/summer total P and a mean 40,108 kg/summer. HR contributed a mean 27,739 kg/summer total P and a mean 13,062 kg/summer. The combined mean measured

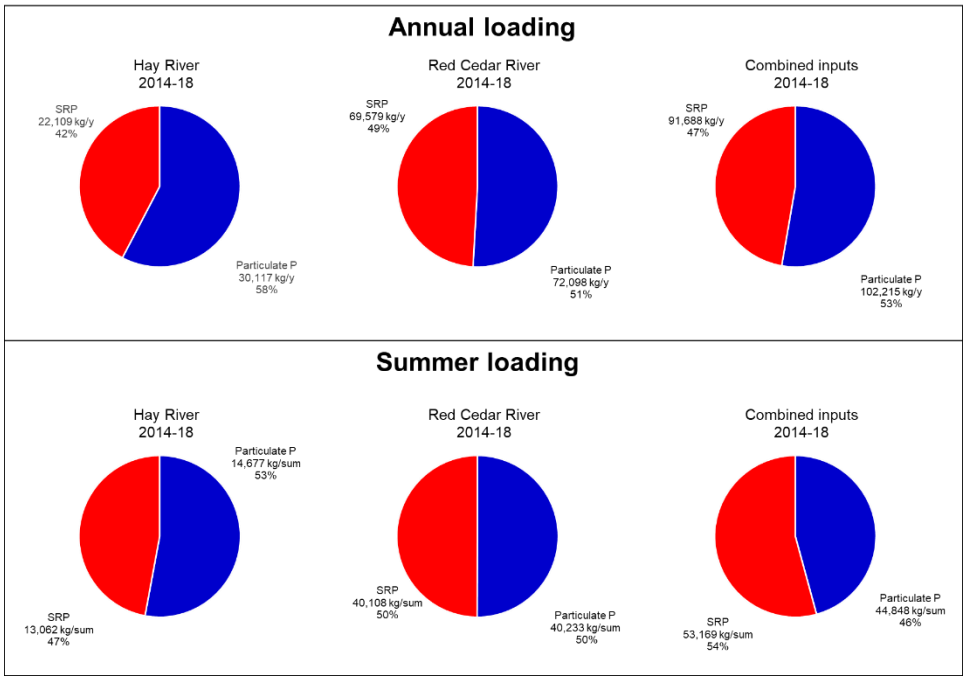

summer P input between 2014-18 was 98,017 kg/summer total P and 53,169 kg/summer SRP.

On an annual basis, the mean combined total P input between 2014-18 was 193,903 kg/y, which was ~ 16% less than the 229,654 kg/y measured in 1990 (La Liberte et al. 2013). Mean combine annual SRP loading accounted for ~ 47% of the mean combined annual

		Annual					Summer (May-September)			
Variable	Units	Annual Inflow Loading			Discharge Loading	Units	Summer Inflow Loading			Discharge Loading
		Hay R	Red Cedar R	Total	Red Cedar R		Hay R	Red Cedar R	Total	Red Cedar R
Flow	(m^3/s)	12.25	33.43	45.70	53.80	(m^3/s)	13.20	36.79	50.00	58.42
Total P	(kg/y)	52,226	141,677	**193,903**	165,106	(kg/su)	27,739	80,341	108,080	86,227
Particulate P	(kg/y)	30,117	72,098	102,215	88,689	(kg/su)	14,677	40,233	54,910	42,282
SRP	(kg/y)	22,109	69,579	91,688	76,417	(kg/su)	13,062	40,108	53,170	43,945
Total P	(mg/L)	0.101	0.124	0.118	0.092	(mg/L)	0.127	0.150	0.144	0.107
Particulate P	(mg/L)	0.055	0.058	0.057	0.054	(mg/L)	0.066	0.070	0.069	0.062
SRP	(mg/L)	0.046	0.066	0.061	0.038	(mg/L)	0.061	0.080	0.075	0.045

1990 TMDL annual total P was 229,654 kg (La Liberte et al. 2012)

total P load. The flow-weighted mean combined annual total P and SRP concentrations were 0.118 mg/L and 0.061 mg/L, respectively. The flow-weighted mean combined SRP concentration represented ~ 52% of the total P.

Vertical temperature patterns in Tainter Lake were complex and influenced by riverine inputs as well as solar radiation and heat absorption during the summer. Vertical density differences in the water column may have been due in large part to layering of cooler HR water underflow currents near the reservoir bottom. Both Tainter and Menomin Lakes exhibited periods of bottom water hypoxia near the dam region after high inflow and loading periods suggesting dissolved oxygen demand. Shortly after high inflow events, bottom water dissolved oxygen concentrations often rapidly declined to < 2 mg/L within 0.5 m of the sediment-water interface and hypoxia (i.e., < 4 mg/L) was prevalent below the 7-m and 4-m depths of TL5 and ML 5 (stations located near the dam), respectively.

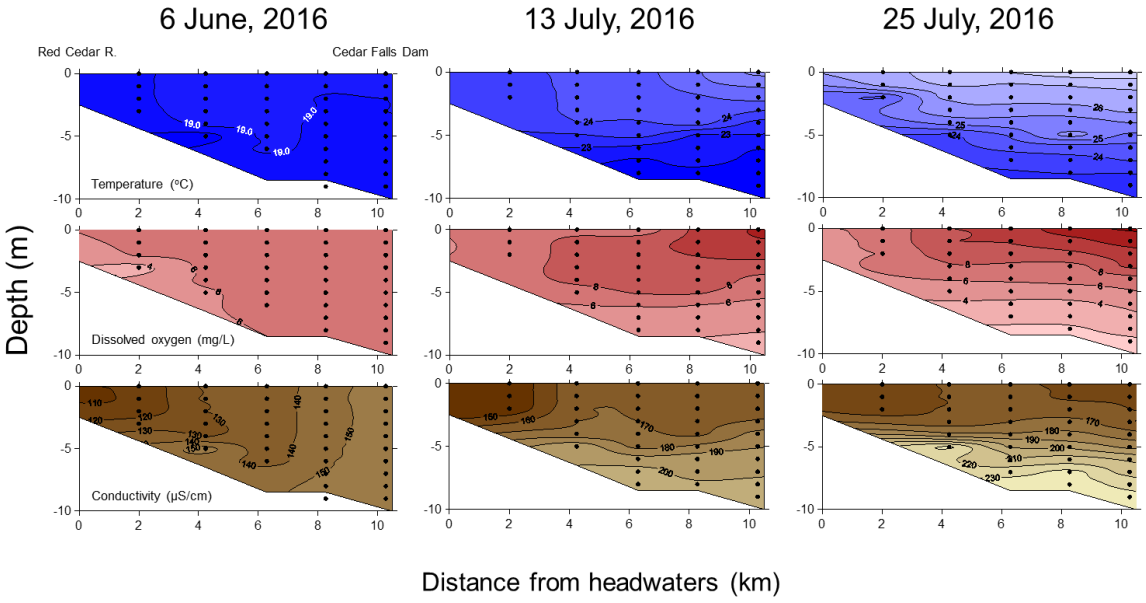

Longitudinal and depth-related variations in temperature, dissolved oxygen, and conductivity in Tainter Lake after a high inflow event in 2016. Note the intrusion of the Hay River as a cool water underflow current with higher conductivity.

Longitudinal patterns in surface water P and chlorophyll dynamics in both lakes were largely regulated by nutrient (primarily P) loading and reservoir flushing patterns during

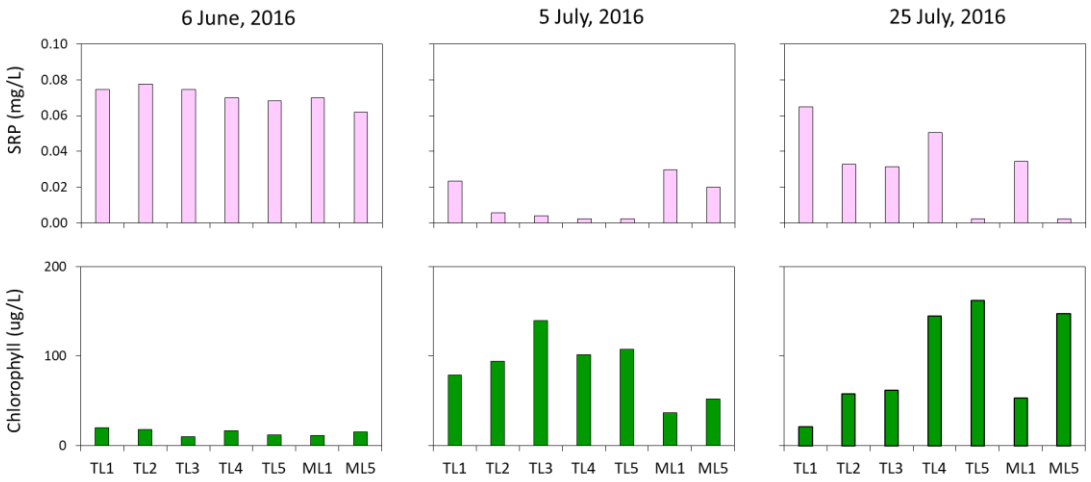

Longitudinal variations in soluble reactive phosphorus (SRP) and chlorophyll in Tainter and Menomin Lakes after a storm-related inflow in 2016. TL1 and ML1 = Headwaters to TL5 and ML5= Dam region. Short residence time and high Red Cedar and Hay River SRP loading resulted in flushing and washout of algal biomass (as chlorophyll) and input of high concentrations of SRP on 6 June. Lower inflow and longer residence times in late June through July coincided with algal uptake of SRP, growth, and bloom development.

the summer. During periods of high inflow and flushing, chlorophyll concentrations declined reservoir-wide due to rapid washout of algae in excess of cellular doubling time (i.e., rate of cellular division). Residence time was often < 2-3 d during these periods. Phosphorus concentrations increased reservoir-wide during these high inflow periods due to loading. SRP concentrations, directly available for algal uptake, were usually extraordinarily high at > 0.075 mg/L. As storm inflows subsided and residence time increased, chlorophyll increased in conjunction with declining SRP, indicating P uptake for growth.

In 2016-17, seasonal and longitudinal patterns in N species varied as a function of N loading from the Red Cedar and Hay Rivers and uptake of dissolved inorganic N by algae in Tainter Lake. Nitrate-nitrite N was often > 1.0 mg/L. During periods of higher inflow and loading, molar DIN:SRP ratios were < 25:1 from the headwaters to the dam region, reflecting Red Cedar and Hay River ratios. During periods of lower flow and higher residence time, potential uptake of DIN and SRP by algae coincided with higher

DIN:SRP ratios, usually > 35:1. These patterns suggested algal growth was probably not limited by DIN availability and, rather, approached P limitation during periods of lower flows and higher residence time. However, alkaline phosphatase activity, a surrogate measure of P deficiency, was low in Tainter and Menomin Lake, indicating minor to no P stress on cyanobacterial growth. P-deficient conditions and P stress to growth could develop during periods of extended summer drought.

Grand mean total P over all stations and summers was relatively high at 0.116 mg/L and 0.099 mg/L for Tainter and Menomin Lake, respectively. Grand mean summer SRP was also high at 0.039 mg/L and 0.031 mg/L, respectively, and represented ~ 31-34% of the total P in both lakes. Grand mean summer chlorophyll was high at 57 µg/L in Tainter Lake and 48 µg/L in Menomin Lake. However, mean Secchi transparency was deeper (i.e., clearer) relative to mean total P and chlorophyll concentrations (grand mean = ~1.1-1.2 m). These patterns were regulated, in large part, by hydrology and low residence time because Secchi transparency was usually greatest during periods of high inflow, when total P and SRP concentrations were high while chlorophyll was low. Essentially, mean summer trophic state indicator variables were not interrelated due to hydrology, P loading, and advective flow, making empirical modeling assumptions invalid. As a result, mean summer Wisconsin Trophic State Indices were higher for total P and chlorophyll but much lower for Secchi transparency.

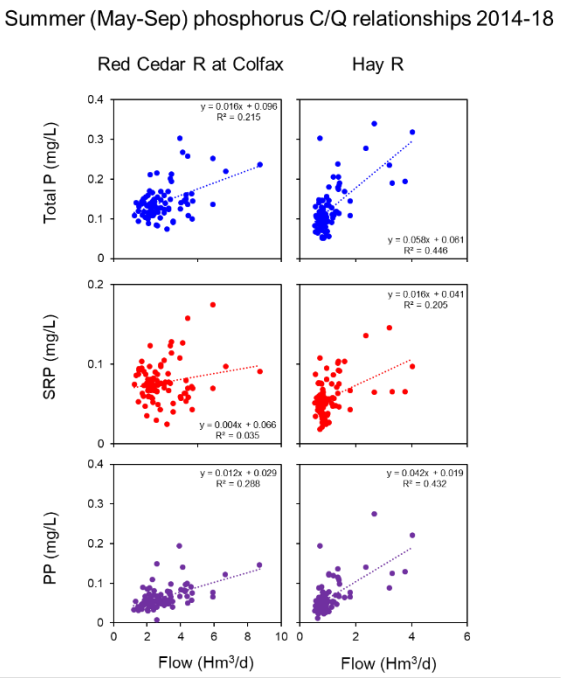

Relationships between total P, SRP, and particulate P (PP) concentration versus flow for the Red Cedar and Hay Rivers. Note that the concentration-flow relationship is stronger for total P and PP and not significant for SRP, particularly for the Red Cedar River which dominates SRP loading to the reservoirs.

The implications for P management were that in addition to soil erosion control, P loading reduction strategies need to be

considered to lower soluble P in the watershed. More information is needed on identifying the processes that are regulating high SRP concentrations and loads in the Red Cedar Watershed. Total P and particulate P concentrations tended to increase with increasing flow, suggesting increased particle erosion from the landscape as a function of increasing rainfall intensity. However, SRP concentrations did not follow this pattern but instead tended to reach a concentration asymptote as P loading increased. The latter pattern could imply that SRP concentration was being regulated to a certain extent by equilibrium between P adsorbed (i.e., loosely-bound) to soils eroded off the landscape and soluble P in the runoff water (Froelich 1988, James and Larson 2008). Thus, P adsorbed to soil particles may be regulating the concentration of SRP during runoff and transport to Tainter and Menomin Reservoirs. For instance, SRP concentration in the RCR_{in} tended to reach an asymptote concentration of ~ 0.080 mg/L as PP loading increased. SRP concentration in the HR tended to average ~ 0.060 mg/L with increasing PP loading. More research is needed to verify the possible role that P equilibrium processes may play in regulating SRP concentrations in the Red Cedar River Basin.

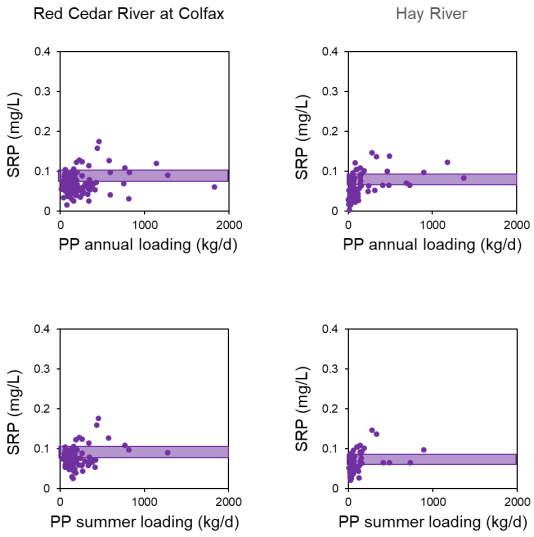

Relationships between soluble reactive phosphorus (SRP) concentration and annual particulate phosphorus (PP) loading (upper panels) or summer (May-September) PP loading (lower panels). Horizontal line denotes an equilibrium P concentration of ~ 0.080 mg/L for the Red Cedar River and ~ 0.061 mg/L for the Hay River.

OBJECTIVES

Tainter and Menomin Lakes are hypereutrophic impoundments located near the mouth of the Red Cedar River Watershed in Dunn County, WI. More information is needed to better understand and manage nutrient loading and reduce cyanobacteria blooms. The objectives of this research were to:

- *Examine interrelationships between hydrology, advection (horizontal water movement), residence time and riverine nutrient (primarily phosphorus) delivery on cyanobacteria dynamics.* Cyanobacterial bloom development in these reservoirs is driven by seasonal variations in nutrient loadings, bioavailability, and hydraulic residence time in relation to cell doubling time. High precipitation years provide abundant phosphorus loading but low hydraulic residence time, which can result in discharge of cyanobacteria before they can divide. Severe bloom development is reduced under this scenario. During lower flow years, summer nutrient loads followed by drought and longer hydraulic residence time set the stage for severe bloom development because soluble phosphorus concentrations are initially high and cellular doubling time exceeds discharge rate. Long-term monitoring information is needed to better understand these interrelationships.
- *Determine Red Cedar and Hay River soluble phosphorus (bioavailable to algae) loading and concentration as a function of storm and base flow.* Recent research on bedrock geology and groundwater in wells and has suggested that soluble phosphorus concentrations could be relatively high during base flow conditions in the Red Cedar River basin. A better understanding of soluble phosphorus dynamics and loading during base flow and storm flow conditions is needed to assess the significance of soluble phosphorus derived from surface runoff on agriculturally-managed land cover versus groundwater recharge through bedrock and soils naturally high in phosphorus. This information is needed to refine the TMDL and better target best management practices for remediation.

- *Examine soluble P loading in relation to the TMDL.* High soluble P loading and reservoir flushing complicate the original management goals. The primary objective has been to drive cyanobacteria toward phosphorus-limited growth. A better understanding of when cyanobacteria growth becomes limited by advection versus phosphorus or other nutrients is needed to refine TMDL goals.

A comprehensive research program was developed to examine nutrient and chlorophyll dynamics in Tainter and Menomin Lakes to address the above knowledge gaps and gain a better understanding of factors regulating cyanobacterial growth.

METHODS

Study site

Tainter and Menomin Lakes are hypereutrophic impoundments of the Red Cedar River (Fig. 1). Major tributary inputs to Tainter Lake include the Red Cedar River and the Hay River. Tainter Lake discharge and Wilson Creek flow into Menomin Lake. Hydraulic residence time is short at ~ 7 d and 5 d for Tainter and Menomin Lake, respectively. Watershed land use is forest (51%), croplands (28%), grass-pasture (19%), and urban (2%). Tainter and Menomin dams are managed by Xcel Energy for hydropower with a maximum pool operation range of only 0.5 ft (LaLiberte et al. 2012). Morphometric characteristics are shown in Table 1.

Hydrology and constituent loading

Existing US Geological Survey flow gauging stations on the Hay River near Wheeler, WI, (05368000), Red Cedar River near Colfax, WI (05367500), and Menomin Lake Dam (0536900) were used to estimate annual and seasonal constituent loading and hydrological budgets for each impoundment (Table 2 and Fig. 1). Reservoir pool elevation was obtained from Xcel Energy (M. Miller, Xcel Energy, Eau Claire, WI).

Water grab samples were collected at weekly to monthly intervals in 2015-18 and less frequently in 2014. Annual and seasonal loadings (kg/y or kg/d) were estimated using the Weighted Regressions on Time, Discharge, and Season (WRTDS, Hirsch et al. 2010).

In-lake monitoring

Weekly to biweekly water sampling was conducted at 5 stations in Tainter Lake and 2 stations in Menomin Lake between the May and September (Fig. 1). Frequent sampling intervals were needed to capture nutrients and chlorophyll dynamics as a function of residence time. An integrated sample over the upper 2-m was collected for analysis of variables listed in Table 3. Secchi transparency and in situ measurements (temperature, dissolved oxygen, pH, and conductivity) were collected at the surface of each station on each date. In 2015, additional vertical in situ profiles (1-m intervals) were collected at TL 5. Vertical profiles were collected at 1-m intervals at TL 1, TL 2, TL 3, TL 4, TL 5, and ML 5 in 2016-18. Recording temperature probe arrays (Onset Instruments) were deployed at TL 5 in 2016 to capture temperature stratification dynamics and river-reservoir hydrology for CE-QUAL-W2 modeling purposes.

Chemical and biological analyses

An additional integrated water sample was collected at TL 5 and ML 5 during the summer of 2016 for determination of phytoplankton identification and biovolume, and alkaline phosphatase activity (APA). Alkaline phosphatase (AP) is a competitively inhibited enzyme readily produced by algae that cleaves phosphate from dissolved organic P molecules that are otherwise not available for uptake and assimilation (Healey and Hendzel 1979). Thus, APA becomes an important recycling process when phosphate is limiting. In addition, APA is inversely related to SRP in the surrounding water and, thus, represents a very sensitive surrogate measure of P-deficiency or P-surplus and potential P limitation of algal growth (James et al. 1992; Connors et al. 1996). When growth is P-stressed or P deficient and surplus P reserves within the cell are depleted, APA and enzyme production increases substantially. Conversely, when SRP

concentrations are higher and the cellular N:P ratio declines, APA decreases according to classic Monad enzyme kinetic models. APA was determined using Turner Designs application method 998-2679. One mL of 36 μM 4-methylumbelliferyl phosphate (MUP) in 50 mM TRIS buffer was added to 4 mL of raw lake water and incubated at ~ 20 C. Changes in fluorescence were determined on a TD-700 Turner Designs fluorometer with a 300-400 nm excitation filter and 410-600 nm emission filter. Fluorescence increased as a function of enzymatic cleavage of phosphate from MUP. Linear changes in fluorescence were converted to rates of MUP hydrolysis and expressed as nM/h and nM/μg CHLa min.

Samples for P and chlorophyll analysis from RCR_{in}, RCR_{out}, HR, and all reservoir stations were analyzed at UW-Stout in 2014-18. Samples for total P were digested with potassium persulfate in an autoclave at 120 C for 1 h prior to colorimetric analysis (Ameel et al. 1990, APHA 2011). Samples for soluble reactive P (SRP) were filtered through a 0.45 μm syringe filter in the field. Total P and SRP were analyzed using the ascorbic acid method (APHA 2011) on a UV-VIS spectrophotometer (Perkin-Elmer Lambda 25) using a 1-cm cell path length. The detection limit was ~ 0.010 mg/L for total P and 0.006 mg/L for SRP. Samples for chlorophyll were filtered onto a glass fiber filter (A/E, < 2 μm pore size) and extracted in a 1:1 DMSO:Acetone solution in 2015-16 and 90% acetone in 2017-78. Chlorophyll fluorescence was determined on a TD-700 (Turner Designs). Certified chlorophyll standards (Turner Designs # 10-850) were used to calibrate the fluorometer.

Additional samples collected from RCR_{in}, RCR_{out}, HR during summer 2015 were shipped to the Wisconsin State Laboratory of Hygiene for analysis of total suspended solids (TSS), total P, total Kjeldahl nitrogen (TKN), nitrate-nitrite-N (NO_x), and ammonium-N (NH_x). During the summer of 2016-17, additional samples from all stations were sent to ARDL (Applied Research & Development Laboratory), Inc (Mount Vernon, IL) for chemical analysis of total organic carbon (TOC), dissolved organic carbon (DOC), TKN, NO_x, NH_x, and total P. Samples for organic carbon species were analyzed using infrared spectroscopy (APHA 2011). TKN and Total P were predigested with potassium

persulfate according to APHA (2011; method 4500) before analysis. DOC, NH_x, NO_x, and SRP samples were filtered through a 0.45 μm syringe filter in the field prior to analysis.

RESULTS AND DISCUSSION

Tributary Hydrology, Nutrient Concentrations, and Loading

Summer (May-September) and annual flows for RCR_{out} were higher in 2014 through 2017 compared to the long-term means (Fig. 2). The year 2018 exhibited lower summer and annual flow at RCR_{out} compared to the other study years. The 2018 summer mean RCR_{out} flow was also closer to the long-term summer means (i.e., 100 y and since 1980; Fig. 2). 2014 was the wettest year during the study period with summer and annual flows exceeding the mean since 1980 by 102% and 45%, respectively. The years 2015-17 also exhibited higher summer and annual flow compared to long-term means. Annual and summer RCR_{out} mean flows were also similar among those years.

Monthly RCR_{out} flow in 2014 exceeded long-term means for all summer months, but particularly in May, June, and September (Fig. 3). Numerous storm-related hydrograph peaks in the RCR_{in}, HR, and RCR_{out} during May through the end of June (Fig. 4) resulted in very high monthly May and June RCR_{out} flow in 2014 that exceeded long-term means by > 100% (Fig. 3). High precipitation in late summer also resulted in a substantial RCR_{in}, HR, RCR_{out} hydrograph peaks in September 2014 (Fig. 4) and a >100% increase in monthly RCR_{out} flow compared to long-term means (Fig. 3). All measured flows declined to a minimum during drought conditions between mid-July and early August 2014 (Fig. 4).

During the summer of 2015, mean monthly RCR_{out} flow was near the long-term mean in May and June (Fig. 3). Modest inflow-outflow peaks in the hydrograph were observed during this June period (Fig. 4). Monthly RCR_{out} flow increased in July 2015 (Fig. 3) in

conjunction with a series of inflow hydrograph peaks (Fig. 4). As a result, mean monthly RCR_{out} flow was high in July relative to other study years and the long-term July averages. Mean monthly RCR_{out} flow also increased in September 2015, in conjunction with storm-related inflow peaks in the hydrograph (Fig. 4).

The year 2016 was also characterized by numerous smaller inflow-outflow hydrograph peaks throughout the summer (Fig. 4). Greatest inflow-outflow hydrograph peaks occurred in late May, early June, and early September (Fig. 4). Monthly RCR_{out} flow in 2016 was high in June, July, August, and September relative to long-term means (Fig. 3). An extended period of lower inflow-outflow occurred in early and mid- to late July, 2016 (Fig. 4).

The maximum inflow during the summer years of 2014-18 was observed in late May 2017 (Fig. 4). Prominent peaks in the inflow hydrograph were also observed in early May and mid-June 2017. Inflows declined between July and August 2017 in conjunction with diminished precipitation. Smaller peaks in the inflow hydrograph occurred in mid- and late August. Monthly RCR_{out} flow in 2017 was well above long-term averages in May and elevated in June, July, and August (Fig. 3). Monthly flow was near the long-term mean in September 2017.

Monthly RCR_{out} flow in 2018 was relatively low in July and August in contrast to the other study years (Fig. 3). Means during these months were also similar to long-term means since 1980 (Fig. 3). Monthly RCR_{out} flow was also nominal in May and June 2018 due to lower inflow hydrograph peaks (Fig. 4). In addition, inflow-outflow peaks were modest and less frequent throughout the summer period of 2018 (Fig. 4). Peaks in the inflow and outflow hydrograph occurred in early May, early and lay June, mid-July, early and late August and early and late September 2018 (Fig. 4). Base inflow and outflow between storm events also tended to be lower during the summer of 2018 compared to other study years.

On an annual basis, inflows and the outflow were nominal in January through mid-March 2014, then increased to a peak in early April 2014 in conjunction with snowmelt (Fig. 5). The April 2014 snowmelt period was characterized by very high RCR_{in}, HR, and RCR_{out} flows. The modest snow pack during the 2015 El Niño winter resulted in minor March-April inflow-outflow hydrograph peaks. Greater snow pack during the winter of 2016 coincided with high snowmelt runoff and peaks in the inflow-outflow hydrograph in March 2016. Early winter storm-related inflow-outflow hydrograph peaks were also most frequent in 2015 compared to the other study years. Snowmelt and accompanying elevated runoff occurred in February 2017. Record high winter snowfall in February coupled with snow additions in March and April led to very high flows in late April 2018.

RCR_{in} was the dominant measured inflow to Tainter Lake during all years, accounting for ~ 74% of the measured inflow to Tainter Lake (Fig. 6). Annual measured inflows and the outflow were similar between the five study years while summer flows were much greater in 2014 compared to 2015-18 (Fig. 6). During these latter summers, inflow and outflow was greatest in 2017 due primarily to the very high flows that occurred in May of that year. In contrast, annual and summer inflow and outflow were lowest in 2018.

In addition, measured total inflow, including direct precipitation, was lower than RCR_{out} on both a summer and annual basis (Fig. 6). In general, total inflow accounted for ~ 85% to 90% of RCR_{out} flow during the 5-year period. Inflow-outflow differences may be attributed to numerous unmeasured flows from smaller tributary inputs (i.e., Bronken Creek, Eighteen-mile Creek, Lambs Creek, Otter Creek, and Wilson Creek), some possible groundwater inputs, and overland runoff located downstream of the gauging stations. More detailed hydrological modeling is needed to provide more insight into these differences.

Hydraulic residence times were relatively low for Tainter and Menomin Lakes, ranging between 1 and 13 d and < 1and 10 d, respectively, over the 5-year period (Fig. 4 and 5). Mean summer residence time was lowest in 2014 at ~ 4 d for Tainter Lake and 3 d for

Menomin Lake in conjunction with higher summer inflows (Fig. 7). In 2015-17, the mean summer residence times were slightly higher at ~ 6 d and 4 d for Tainter and Menomin Lakes, respectively. Mean summer residence time was highest during the lower inflow period of 2018 at 7.5 d for Tainter Lake and 5.25 d for Menomin Lake.

Over the summer period, residence time increased in both lakes to maxima during a period of lower inflows in late July-early August 2014 (Fig. 4). Residence time approached 8.5 d in Tainter Lake and 5.5 d in Menomin Lake during this period. In contrast, residence time was much lower in both lakes during higher inflow periods between May and mid-July and early September 2014 (Fig. 4). Residence time exhibited more frequent peaks and troughs in 2015-17 in conjunction with a series of smaller hydrograph inflow peaks scattered throughout the summer. Shortest residence times (~ 0.8 to 1.1 day) occurred during peak inflow in May 2017 (Fig. 4). Otherwise, summer residence times were generally higher in 2015-17 compared to 2014 due to more moderate summer inflow peaks during the former summers. Residence times were maximal in both lakes during the lower inflow summer of 2018 (Fig. 4). In particular, residence time exceeded 13 d and 9 d in Tainter and Menomin Lake, respectively, in late July 2018.

Seasonal variations in TP, SRP, and PP (i.e., particulate P or the difference between TP and SRP) concentrations in RCR_{in} and HR were complex and weakly correlated with flow, particularly patterns for RCR_{in} (Fig. 8). RCR_{in} TP and PP concentrations tended to increase with increasing flow, suggesting greater particle erosion from the landscape as a function of precipitation intensity. However, RCR_{in} SRP concentrations tended to vary more with season compared to flow, increasing during summer period and declining to lower values during lower flow winter periods (Fig. 8). During snowmelt runoff periods in March of 2015 and 2016 P concentrations tended to decline to minima, suggesting probable concentration dilution by melt water (Fig. 8). P concentration dilution also occurred on RCR_{in} during peak flows in May 2017 (Fig. 8). A similar seasonal concentration pattern occurred in the HR. Overall summer ranges in concentration are shown in Table 4. Maximum summer TP concentrations were 0.34 mg/L and 0.27 mg/L

in the HR and RCR_{in}, respectively. Maximum summer SRP concentrations were also high, ranging between 0.146 mg/L in the HR and 0.175 mg/L in RCR_{in}. Maximum summer PP concentrations were 0.275 mg/L for RCR_{in} and 0.195 mg/L for HR.

Annual concentration versus flow (C/Q) relationships over the entire 2014-18 study period suggested weak to no positive relationships between TP, PP, and SRP versus flow for RCR_{in} and stronger C/Q relationships for HR (Fig. 9 and 10). For the HR, flow explained ~ 57%, 24%, and 60% of the increase in TP, SRP, and PP concentration, respectively (Fig. 10). Relationships between HR P concentration and flow also indicated that much of the variation in TP was due to increases in PP, suggesting increased particle erosion from the landscape as a function of increasing precipitation intensity and runoff (Fig. 10). Similarly, RCR_{in} flow explained 21% of the positive variation in TP and 38% of the increase in PP (Fig. 9 and 10). For HR, SRP concentrations were weakly related to flow on an annual basis. Although variation was high, these patterns suggested some potential extraction or desorption (i.e., the release of soluble P that was weakly attached to soil surfaces) of soluble P from soils during precipitation and runoff. In contrast, seasonal differences in land use practices (i.e., summer versus other seasons), cover vegetation, soil management with fertilizer, and soil conditions may have been responsible for the lack of correlation between RCR_{in} flow and SRP concentration.

Summer (May-Sep) C/Q relationships exhibited similar patterns; namely, they were weak to not significant for RCR_{in} and stronger for HR (Fig. 11 and 12). Variations in RCR_{in} flow only explained ~ 22% and 29% of the increase in TP and PP concentration (Fig. 12). The RCR_{in} C/Q relationship was not significant for SRP. In contrast, flow explained ~ 45% and 43% of the TP and PP concentration increase, respectively, and ~ 21% of the SRP concentration increase in HR (Fig. 12).

Overall, mean monthly TP, PP, and SRP concentrations also tended to vary on a seasonal basis (Fig. 13). Concentrations of these constituents in RCR_{in} tended to be lower during the winter months of December and January and increased to maxima in June through September, particularly mean monthly SRP (Fig. 13). Mean monthly SRP concentrations

also declined during the high flow snowmelt runoff period of April, suggesting some dilution of SRP. Although more variable, similar seasonal trends in mean monthly TP, PP, and SRP occurred in HR (Fig. 13).

Total P and PP loads increased nonlinearly with respect to increasing flow on an annual and summer basis in RCR_{in} and HR (Fig. 14 and 15) because concentration also increased as flows increased. This pattern of PP concentration increase could be related to increasing soil particle erosion from the landscape as a function of increasing rainfall and splash drop intensity. However, SRP loading from both rivers did not follow this nonlinear pattern as concentration either remained relatively constant or only weakly increased with increasing flow.

Relatively constant SRP, particularly at higher flows, could imply that concentration was being regulated to a certain extent by equilibrium between P adsorbed (i.e., loosely-bound) to soils and soluble P in the runoff water (Froelich 1988, James and Larson 2008). Thus, PP adsorbed to soil particles may regulate the concentration of SRP during runoff and transport to the reservoirs. For instance, SRP concentration in the RCR_{in} tended to reach an asymptote concentration of ~ 0.080 mg/L as PP loading increased (Fig. 16). SRP concentration in the HR tended to average ~ 0.060 mg/L with increasing PP loading (Fig. 16). More research is needed to verify the possible role that P equilibrium processes may play in regulating SRP concentrations in the Red Cedar River Basin.

Seasonal variations in estimated P loading for RCR_{in}, HR, and RCR_{out} are shown in Figures 17-19. Annual and summer TP and SRP loading from RCR_{in} and HR varied as a function of mean summer flow (Table 5). Loading of both constituents was greatest during the wetter summer of 2014 and nearly 2X lower during the lower flow summers of 2015-18. On an annual basis, combined (i.e., the sum of RCR_{in} and HR) TP loading ranged between 281,951 kg/y (2014) and 150,042 kg/y (2018, Table 5). The 4-year (2014-2018) mean TP load of 193,903 kg/y represented ~ 84% of the TP load of 229,654 kg/y estimated in 1990 (La Liberte et al. 2012).

Annual combined SRP loading represented ~ 47% of the annual combined TP load (Fig. 20). In contrast, summer (May-September) combined SRP loading accounted for a greater portion of the summer combined TP load at 54% (Fig. 20). This latter pattern reflected the occurrence of higher mean monthly SRP concentrations during the summer period (Fig. 13). The summer flow-weighted mean SRP concentration was relatively high in the HR and RCR_{in} at 0.061 mg/L and 0.080 mg/L, respectively (Table 5). The combined (i.e., the sum of RCR_{in} and HR loads) flow-weighted SRP concentration of loads entering Tainter Lake was also very high at 0.075 mg/L (Table 5) and directly available for algal assimilation and growth.

Overall, only ~ 15% of the mean annual and 20% of the mean summer total P load was retained in the Tainter-Menomin reservoir system during the 2014-18 study period (Table 6). As discussed in more detail below, low P retention was due to several factors. In brief, short residence time and high flushing rates promoted particle advection through the reservoirs and out the discharge resulting low sedimentation of fine silts and clays. SRP loads retained in the reservoirs were rapidly converted to particulate P as algal biomass during periods of longer residence time and lower flushing rate. A large portion of this particulate P was then flushed out during periods of high inflow and short residence time. In contrast, higher grain—sized sand loads have been retained in the headwaters of Tainter Lake (not measured in this study), resulting in loss of volume and depth.

Summer nitrogen concentration patterns in 2015-17 are shown in more detail in Figures 21 and 22. $N0_x$ was the dominant N species in both rivers. Concentrations were moderate. ranging between 0.5 mg/L and 2.5 mg/L (Table 4). TKN was the next dominant N species and concentrations ranged between 0.2 mg/L and 1.4 mg/L. NHx concentrations were relatively low at near the detection limit to ~ 0.26 mg/L. More summer concentration-flow (C/Q) information is needed; but current patterns suggested that NOx concentrations declined with increasing flow in both river systems because of concentration dilution (Fig. 23). In contrast, distinct C/Q relationships were not detected for TKN and NHx, although TKN concentration tended to increase slightly with increasing flow in the HR.

The molar stoichiometric ratio between dissolved inorganic N (DIN; sum of NO_x and NH_x) and SRP (i.e., DIN:SRP ratio) of the inflows to Tainter Lake (HR and RCR_{in}) provided an indication of the proportion of available N and P inputs to the algal community and the potential for nutrient deficiency or limitation of growth. Generally, freshwater algae can be exposed to a range of DIN and SRP inputs and physiologically adapt their uptake requirements (Klausmeier et al. 2004a and b, 2008). Under optimal growth conditions, the cellular N:P ratio in cyanobacteria can range between 22:1 and 30:1 on a molar basis (Hillebrand et al. 2013).

Summer molar DIN:SRP ratios were usually > 20:1 in the RCR_{in} and much higher in the HR (Fig. 24). Thus, although SRP concentrations were relatively high in both river systems, the molar DIN:SRP ratio suggested DIN concentrations, primarily in the form of NO_x, were in higher proportion relative to SRP. Weak inverse relationships were observed between summer flow and the molar DIN:SRP ratio of both river inflows (Fig. 25) and in the combined inflow to the headwater region of Tainter Lake (Fig. 26). As flow increased, the molar ratio tended to decrease. This pattern was related to differences in the C/Q relationship for NO_x and SRP (Fig. 11 and 23). As summer flow increased, NO_x concentration declined while SRP concentration tended to remain constant or slightly increase, resulting in lower molar DIN:SRP ratios. More concentration information is needed at flows > 80 m^3/s to better understand stoichiometric DIN:SRP ratio patterns during periods of very low residence time and rapid reservoir flushing. However, these results suggested that the DIN:SRP ratio approached optimal ranges for cyanobacteria uptake and growth during periods of high inflow and loading.

Reservoir Limnological Trends

Vertical temperature patterns in Tainter Lake at station TL 5 were complex in 2016 and influenced by riverine inputs as well as solar radiation and heat absorption during the summer. Despite oftentimes very low residence time and a high flushing rate during storm inflows, time series variations in water temperature versus depth also suggested

some periods of vertical temperature differences and very weak stratification throughout the summer of 2016 (Fig. 27). As discussed in more detail below, vertical density differences in the water column at station TL 5 could have been due in large part to layering of cooler HR water underflow currents near the reservoir bottom. Cooler groundwater intrusion may have also contributed to these bottom temperature patterns.

Periods of partial and complete water column mixing in 2016 were usually associated with peak inflow events, suggesting that rapid flushing and replacement with river water caused entrainment and water column mixing. Similar temperature patterns were observed at TL 5 in 2015-18 during storm inflow periods (Fig. 28). Bottom temperatures at station TL 5 initially increased during flushing periods due to entrainment of surface with bottom water and inflows of river water dominated by the Red Cedar River (Fig. 27). However, bottom temperatures then declined rapidly after these high flushing events due to HR inflows. Although the RCR_{in} dominated measured inflow, HR water temperatures were lower than RCR_{in} and surface temperatures at station TL 1 (Fig. 29), which resulted in plunging of HR river water to the bottom and movement through Tainter Lake as a cooler underflow density current.

Specific conductivity differences between RCR_{in} and HR provided distinct end points that could be used to track HR flow for a better understanding of hydrodynamics in Tainter Lake. Conductivity was very high at ~ 300 µS/cm in HR versus much a lower average of ~ 150 µS/cm in RCR_{in} (Fig. 29). For example, during the moderate inflow period of late May - early June 2016 Tainter Lake was flushed rapidly and water temperatures were nearly uniform both longitudinally and vertically on 6 June (Fig. 30). Conductivity was low in the headwaters on that date, reflecting intrusion of the RCR_{in} and entrainment with Tainter Lake water. Higher conductivities of HR inflows were masked on 6 June because RCR_{in} overwhelmingly dominated inflow. Conductivity may have also been lower in the HR during high inflow if dilution with low conductivity precipitation occurred. More conductivity information during high inflows are needed to examine this contention. As flows subsided, an underflow current characterized by higher conductivity values that approached those in HR was observed on 13 and 25 July 2016

(Fig. 30). This underflow probably represented cooler flow intrusion of HR water into Tainter Lake after the higher inflow event in early June. As a result, bottom temperatures were lower longitudinally in the lake downstream of TL 2 on 13 and 25 July in conjunction with the HR underflow current. Apparent heating of surface waters by solar radiation, combined with cooler underflow current intrusions, resulted in subtle vertical temperature differences by 25 July.

Longitudinal development of the bottom water dissolved oxygen demand in 2016-18 is shown in Figure 31-33. For instance, bottom water dissolved oxygen declined in concentration in mid-June 2016, approximately 2 weeks after storm inflows in early June 2016. Longitudinal gradients of declining concentration were observed from kilometer 4 to the dam during this period (Fig. 31). Moderate storm inflows in late June and mid-July 2016 disrupted bottom water dissolved oxygen gradients. But they redeveloped during periods of lower inflow in early and late July 2016. Bottom water dissolved oxygen depletion also coincided with elevated conductivity, further suggesting intrusion of the HR. Similar patterns occurred in 2017 and 2018 (Fig. 32-33). Dissolved oxygen demand in the HR underflow current by microbial communities may be playing a role in the development of bottom water hypoxia after storm inflows.

Longitudinal patterns in surface water P and chlorophyll dynamics in both lakes were largely regulated by P loading and flushing patterns during the summer. For instance, during periods of high inflow and flushing in Tainter Lake, chlorophyll concentrations declined reservoir-wide due to rapid washout of algae in excess of cellular doubling time (i.e., rate of cellular division, Fig. 34-37). Residence time was often < 5 d during these periods. Phosphorus concentrations increased reservoir-wide during these high inflow periods and SRP concentrations, directly available for algal uptake, were usually extraordinarily high at > 0.050 mg/L. As storm inflows subsided and residence time increased, chlorophyll increased in conjunction with declining SRP, indicating P uptake for growth.

Chlorophyll increases during periods of higher residence time were generally greatest and developed most rapidly near the dam region of Tainter and Menomin Lake, which is likely related to morphometry (Fig. 34-37). The headwaters of each reservoir are characterized by lower surface area, water volume, mean depth, and thus, shorter residence time and greater flushing. Larger water volume, greater surface area, and longer residence time favor more rapid bloom development in the dam region. During periods of lower flow and higher residence time, as in Tainter Lake in late June, late July, and mid-August 2015 (Fig. 34), late June, July, and late August, 2016 (Fig. 35), early and late July 2017 (Fig. 36), and June through August 2018 (Fig. 37) chlorophyll blooms often extended from the dam to the near the headwaters.

Variations in P and chlorophyll patterns at the headwater (i.e., TL 1 and ML 1) and dam (i.e., TL 5 and ML 5) stations of each lake more clearly illustrate the complex longitudinal patterns related to inflow, residence time, and algal uptake of P (Fig. 38 and 39). During periods of higher inflow, higher flushing, and lower residence time, SRP increased and chlorophyll decreased in both lakes, resulting in homogeneous concentrations with minimal longitudinal variation. As inflow subsided and residence time increased, SRP concentrations declined in the lacustrine dam region, often to near detection, in conjunction with increases in chlorophyll.

Three dates during the summer of 2016 show the dynamic changes in chlorophyll and SRP as a function of inflow and residence time (Fig. 40). High inflow and low residence time led to high SRP concentration throughout Tainter and Menomin on 6 June 2016 as reservoir water was rapidly replaced with river inflows. Rapid flushing also led to algal washout and low concentrations of chlorophyll. Chlorophyll concentrations increased while SRP declined as flows subsided and residence times lengthened by 5 July 2016, indicating assimilation of P by algae for growth. Longitudinal variations in chlorophyll and SRP captured on 25 July 2016 in Tainter Lake appeared to be related to lower storm-related inflows that occurred between 8 and 20 July 2016. Apparent flushing in the headwaters resulted in elevated SRP and low chlorophyll but impacts on these variables

had not yet reached the dam region at the time of sampling as an algal bloom was observed at TL5 and SRP concentrations were minor due to uptake for growth.

During a period of long residence time and lower inflow between 23 July 2018 and 14 August 2018, SRP concentrations were highest in the headwaters (TL1 and ML1) and declined to near detection limits downstream in both reservoirs in conjunction with high chlorophyll, indicating SRP assimilation by algae (Fig. 40). High SRP concentrations at ML1 on each date in 2018 reflected subsurface penstock withdrawal from Tainter Lake. SRP concentrations were apparently high below the euphotic zone in the vicinity of the penstock withdrawal of Tainter Lake, reflecting inflow concentrations. This pattern suggested that algal biomass and uptake of SRP for growth was confined to the surface waters of Tainter Lake. Lower concentrations of chlorophyll at ML1 suggested that algal biomass was also usually lower in the vicinity of the penstock withdrawal in Tainter Lake.

Chlorophyll concentrations were highest in both lakes on 23 July 2018, coinciding with a prior storm-related peak in the hydrograph and input of SRP that occurred in mid-July 2018 (Fig. 38-39), suggesting SRP uptake and growth (Fig. 40). However, apart from a minor peak the hydrograph in early August 2018 (Fig. 38-39), inflows and SRP loadings were relatively low and residence times exceeded 7 to 10 days. Chlorophyll concentrations generally declined in Tainter and Menomin Lakes from 23 July to 14 August. Some of this biomass decrease could be due to flushing and washout from the reservoirs. More likely, however, algal growth could have become P limited during this period of lower inflow and SRP loading, resulting in senescence and population decline. During algal senescence, winds could have moved dying algae into bays and coves, resulting in severe water quality issues such as odor problems and dissolved oxygen depletion.

Overall, weak relationships existed between chlorophyll and SRP near the lacustrine dam region of each lake and hydrological variables (Fig. 41 and 42). Time of travel of nutrients from headwaters to dam and algal flushing rate from the system, not accounted

for in these analyses, likely explained the moderate to weak statistical correlation between variables. Generally, there was a negative relationship between chlorophyll and SRP for both lakes. High chlorophyll was associated with lower SRP, suggesting uptake for growth. Conversely, chlorophyll concentrations were low as a function of high SRP due to rapid flushing, washout of algae, and replacement with inflows high in SRP concentration. Chlorophyll-SRP-residence time relationships were usually weaker for Menomin Lake (Fig. 42). This pattern may have been related to influences from Tainter Lake discharges and more rapid flushing in Menomin Lake. For instance, chlorophyll concentrations in Menomin may have been impacted by lower residence time compared to Tainter Lake.

While there was much variability, relationships between RCR_{out} or residence time and chlorophyll concentration at TL5 or ML5 suggested that blooms began to develop as RCR_{out} declined below ~ 90 m^3/s and as residence time increased above ~ 2-3 days (Fig. 43). Variability was likely due to the concentration of chlorophyll relative to inflow hydrograph history and travel time within each reservoir.

Seasonal and longitudinal patterns in N species varied as a function of N loading from the Red Cedar and Hay Rivers and uptake of dissolved inorganic N by algae (Figure 44). During periods of moderate flow and N loading, dissolved inorganic N concentrations, primarily as NO_x, increased in Tainter Lake. Nitrate-nitrate concentrations were relatively high during these periods at > 1.0 mg/L, which may be related to nitrification of NHx to N0x in watershed agricultural soils. During periods of higher residence time and lower flushing rate, as in late June-early July and August 2016 and late July through early August 2017 NH_x and NO_x concentrations declined, particularly in the dam region of Tainter Lake, because of algal uptake (Fig. 45). In particular, NHx concentrations, the preferred dissolved inorganic N species for algal uptake, tended to decline more rapidly than N0x in conjunction with chlorophyll increases.

Longitudinal and seasonal variations in the molar DIN:SRP ratio were examined in Tainter Lake in 2016-17 to provide insight into algal nutrient uptake and the potential

nutrient limitation during periods of extended growth (Fig. 46). Generally, during periods of higher inflow and loading as in late May of 2016 and 2017, DIN:SRP ratios were < 35:1 in the headwaters, reflecting Red Cedar and Hay River ratios, and extended longitudinally to the dam region. During periods of lower flow and higher residence time, potential uptake of DIN and SRP by algae coincided with higher DIN:SRP ratios, usually > 35:1 from TL 2 to TL 5. These patterns suggested algal growth was probably not limited by DIN availability and, rather, approached P limitation during periods of lower flows and higher residence time.

Alkaline phosphatase activity (APA) at TL 5 and ML 5 provided an additional indication of potential P limitation of cyanobacterial growth in 2016 (Fig. 47 and 48). In both lakes, APA activity was highest in July through early August 2016, coinciding with periods of low SRP concentration in the water column. It declined in mid-August through September in conjunction with storm inflows and SRP loading from the watershed. APA was negatively related to SRP in Tainter Lake but not in Menomin Lake (Fig. 49). As SRP concentration increased APA decreased and reached a minimum asymptote in both lakes. Because APA is competitively inhibited by phosphate, enzyme activity decreased at relatively high SRP concentration in both lakes. There was some evidence of potential P limitation of algal growth at low SRP concentrations in Tainter Lake. However, similar low SRP concentrations were not observed in Menomin Lake. Compared to other lakes and reservoirs, APA was very low in both Tainter and Menomin, often by an order of magnitude compared to APA reported for other systems with much lower SRP (Table 7). Thus, algal growth was probably not P limited, and certainly not P deficient, between July and September 2016 in both lakes. While summer watershed SRP loading was frequent and supplied more than sufficient P for algal growth in 2015-17, P-deficient growth could occur during drought summers (Fig. 50).

Mean summer concentrations of total P, SRP, chlorophyll, and Secchi transparency for Tainter and Menomin Lakes in 2015-18 are shown in Figure 51. Grand mean total P over all stations and summers was relatively high at 0.116 mg/L and 0.099 mg/L for Tainter and Menomin Lake, respectively. Grand mean summer SRP was also high at 0.039 mg/L

and 0.031 mg/L, respectively, and represented ~ 32% of the total P in both lakes. Grand mean summer chlorophyll was relatively high at 57 µg/L in Tainter Lake and 48 µg/L in Menomin Lake. However, mean Secchi transparency was higher relative to mean total P and chlorophyll. These patterns were regulated, in large part, by hydrology and low residence time because Secchi transparency was usually greatest during periods of high inflow, high total P and SRP concentration, and low chlorophyll, which were frequent in 2015-16.

Essentially, mean summer trophic state indicator variables were not interrelated due to hydrology and advective flow, making empirical modeling assumptions invalid. As a result, mean summer Carlson and Wisconsin Trophic State Indices were generally higher for total P and chlorophyll but much lower for Secchi transparency (Figure 52).
For instance, stations TL 1 and ML 1 reflected a riverine environment where higher turbidity coupled with higher flushing limited algal growth. The trophic state indicator variables tended to converge downstream in each lake toward the dam region, reflecting more lacustrine characteristics and incorporation of P into algal biomass. Low TSI-SD (i.e., high Secchi transparency relative to chlorophyll and total P) most likely reflected dominance by filamentous and flake-forming cyanobacteria which tend to allow for greater light penetration than colonial communities.

CONCLUSIONS AND IMPLICATIONS

Tainter and Menomin Lakes are hypereutrophic and usually exhibit periods of massive cyanobacterial blooms during summer. Phytoplankton dynamics appeared to be regulated in large part by high soluble P inputs from the watershed and hydrological advection. Periods of high watershed inflow resulted in rapid reservoir flushing and discharge of algae coupled with the input of high concentrations of soluble P (directly available for cyanobacterial uptake and growth). As inflows subsided and residence times increased, chlorophyll concentrations increased substantially in conjunction with declines in soluble P, suggesting cyanobacterial nutrient assimilation for growth. Soluble P appeared to be

diving cyanobacterial growth versus dissolved inorganic N in 2014-18. However, these summers were characterized by frequent periods of summer inflow and rapid flushing. More information is needed during periods of extended summer drought to better understand to role of available N and P on cyanobacterial blooms in these reservoirs.

Mean summer soluble P concentrations in the RCR_{in} and HR were high at 0.080 mg/L and 0.061 mg/L, respectively, resulting in the input to Tainter Lake of ~ 53 mtonnes/summer. Measured summer total P inputs from these rivers were ~ 98 mtonnes/summer. Soluble reactive P accounted for ~ 54% of the summer total P load to the reservoirs. While the particulate P load can be managed via soil erosion control, SRP load reduction may be more difficult if equilibrium exchanges between particulate and aqueous phases are regulating SRP concentration in the RCR_{in} and HR. P loading reduction management should consider BMPs to lower soluble P concentrations from the watershed. These BMPs include soil management to reduce P buildup at the surface, reducing overall soil P concentrations, increasing hydrological infiltration, sequestering soluble P in detention ponds, iron-enhanced sand benches, trapping soluble P using structures containing P binding materials (Al and Fe), and Nutrient Reduction Facilities (NuRF). Potential soluble P inputs from the groundwater watershed also need to be quantified and factored into P management.

ACKNOWLEDGMENTS

N. Paulson and C. Ferguson are gratefully acknowledged for funding support through the NSF LAKES Research Experience for Undergraduates (REU) in 2014 and 2015. The U.S. Army Engineer District – St. Paul, N. Campbell, Coordinator, provided funding for this research in 2016-17 under Section 22 of the Water Resources Development Act. Dunn County provided funding for winter sampling and research in 2015-16. M. Kuchta and S. Nold were LAKES REU Mentors and researchers on the project. The following students worked on the limnological portion of this project under the LAKES REU

program in 2014 and 2015: L. Anderson N. Loeven, P. Vang, and C. Worthington. Center for Limnological Research and Rehabilitation (CLRR, University of Wisconsin – Stout) students and personnel conducting limnological research on this project during 2014-18 included: J. Bauer, C. Dougherty, R. Fleck, M. Librande, H. Lieffort, E. Petska, L. Provos, M. Vandenberg, M.L. Vang, R. Veith, A. Wilson. R. Hulke was Director of the Discovery Center at UW – Stout. L. Profaizer coordinated the Red Cedar Basin Assessment committee. B. Cox, C. Ferguson, T. Gruetzmacher, M. Hazuga, W. James, C. Kozik, D. Lamers, S. McGovern, B. Neeb, J. Olmstead, L. Olson, N. Paulson, A. Quilling, A. Smith, B. Sorge, R. Verdon, R. Walter, D. Zerr, and T. Zien were Red Cedar Basin Assessment committee members. M. Diebel, Wisconsin Department of Natural Resources, is gratefully acknowledged for calculating final loadings using the computer model WRTDS.

REFERENCES

Ameel JJ, Axler RP, Owen CJ. 1993. Persulfate digestion for determination of total nitrogen and phosphorus in low nutrient water. Amer Environ Lab (October, 1993):8-10.

APHA (American Public Health Association). 2011. Standard Methods for the Examination of Water and Wastewater. 22st ed. Washington (DC).

Carlson RE. 1977. A trophic state index for Lakes. Limnol Oceanogr 22:361-369.

Connors SD, Auer MT, Effler SW. 1996. Phosphorus pools, alkaline phosphatase activity, and phosphorus limitation in hypereutrophic Onondaga Lake. Lake Reserv Manage 12:47-57.

Healey FP, Hendzel LL. 1979. Fluorometric measurement of alkaline phosphatase activity in algae. Freshwat Biol 9:429-439.

Hillebrand H, Steinert G, Boersma M, Malzahn A, Léo Meunier C, Plum Cm Ptacnik R. 2013. Goldman revisited: Faster-growing phytoplankton has lower N:P and lower stoichiometric flexibility. Limnol Oceanogr 58:2076-2088.

Hirsch RM, Moyer DL, Archfield SA. 2010. Weighted regressions on time, discharge, and season (WRTDS), with application to Chesapeake Bay river inputs. J Amer Wat Resourc Assoc 46:857-880.

James WF, Taylor WD, Barko JW. 1992. Production and vertical migration of *Ceratium hirundinella* in relation to phosphorus availability in Eau Galle Reservoir, Wisconsin. Can J Fish Aquat Sci 49:694-700.

Klausmeier CA, Litchman E, Levin SA. 2004a. Phytoplankton growth and stoichiometry under multiple nutrient limitation. Limnol Oceanogr 49:1463–1470.

Klausmeier CA, Litchman E, Daufresne T, Levin SA. 2004b. Optimal nitrogen-to-phosphorus stoichiometry of phytoplankton. Nature 429:171–174

Klausmeier CA, Litchman E, Daufresne T, Levin SA. 2008. Phytoplankton stoichiometry. Ecol Res 23:479-485.

La Liberte P, Oldenburg P, Schreiber K, Voss K, Simonson D, Bartilson K, Clayton N. 2012. Phosphorus Total Maximum Daily Loads (TMDLs) Tainter Lake and Lake Menomin Dunn County, Wisconsin – 31 May 2012. Wisconsin Department of Natural Resources. http://naturalresources.uwex.edu/redcedar/pdf/Final_Tainter_TMDL_May29_2012.pdf

Walker WW. 1996. Simplified procedures for eutrophication assessment and prediction: User manual. Instruction Report W-96-2, September, 1996, U.S. Army Engineer Waterways Experiment Station, Vicksburg, Mississippi, USA.

Welschmeyer NA. 1994. Fluorometric analysis of chlorophyll a in the presence of chlorophyll b and pheaopigments. Limnol Oceanogr 39:1985-1992.

Table 1. Morphometric characteristics of Tainter and Menomin Lakes.

Morphometric Variable	English			Metric		
	Tainter	Menomin	Unit	Tainter	Menomin	Unit
Surface area	1,608.2	1,325.4	ac	6,508,160	5,363,708	m^2
Volume	20,242.0	14,183.7	ac-ft	24,968,102	17,495,310	m^3
Mean depth	12.6	10.7	ft	3.84	3.26	m
Max depth	36.0	30.0	ft	10.97	9.14	m
Shoreline length	24.4	26.7	mi	39.30	42.97	km

Table 2. Hay and Red Cedar River sampling station locations and variable list.

Variable	Hay River near Wheeler, WI (05368000)	Red Cedar River near Colfax, WI (5367500)	Red Cedar River near Menomonie, WI (0536900)
Total organic carbon	X	X	X
Dissolved organic carbon	X	X	X
Total Kjeldahl nitrogen	X	X	X
Ammonium-N	X	X	X
Nitrate-nitrite-N	X	X	X
Total phosphorus	X	X	X
Soluble reactive phosphorus	X	X	X
Chlorophyll	X	X	X

Table 3. Tainter and Menomin Lake sampling stations and water chemistry variable list. AlkPAct = alkaline phosphatase activity.

Station	Coordinates		Total P	SRP	Chla	TKN	NHx	NOx	Phyto ID	AlkPAct
	North	West	(mg/L)	(mg/L)	(mg/L)	(mg/L)	(mg/L)	(mg/L)		(ug/g min)
Tainter Lake 1 (TL 1)	44.9889	-91.8361	X	X	X	X	X	X		
Tainter Lake 2 (TL 2)	44.9822	-91.8603	X	X	X	X	X	X		
Tainter Lake 3 (TL 3)	44.9657	-91.8783	X	X	X	X	X	X		
Tainter Lake 4 (TL 4)	44.9536	-91.8917	X	X	X	X	X	X		
Tainter Lake 5 (TL 5)	44.9384	-91.8913	X	X	X	X	X	X	X	X
Menomin Lake 1 (ML 1)	44.8808	-91.9239	X	X	X	X	X	X		
Menomin Lake 5 (ML 5)	44.9332	-91.8879	X	X	X	X	X	X	X	X

Table 4. Variations in minimum and maximum constituent concentrations the the Hay River at Wheeler, WI, and the Red Cedar River at Colfax, WI, for the summer period (May - September) during the years 2014-18. P = phosphorus, SRP = soluble reactive P, TN = total nitrogen, TKN = total Kjeldahl N, NOx = nitrate-nitrite-N, NHx = ammonium-N, CHLa = chlorophyll.

	Hay River															
Summer	Total P		SRP		Part P		TN		TKN		N0x		NHx		CHLa	
	Min	Max	Min	Max	Min	Max	Min	Max	Min	Max	Min	Max	Min	Max	Min	Max
2014	0.052	0.277	0.021	0.146	0.031	0.141					No Data					
2015	0.067	0.339	0.018	0.104	0.029	0.275	1.860	2.940	0.521	1.430	0.913	2.340	0.018	0.051	2.1	34.7
2016	0.052	0.302	0.025	0.108	0.012	0.194	2.130	3.000	0.200	0.730	1.900	2.500	0.030	0.130	3.1	15.7
2017	0.071	0.319	0.035	0.097	0.028	0.222	1.538	2.669	0.200	0.711	0.827	2.370	0.020	0.185	3.0	21.1
2018	0.055	0.238	0.026	0.102	0.028	0.137					No Data				2.4	12.4
	Red Cedar River															
Summer	Total P		SRP		Part P		TN		TKN		N0x		NHx		CHLa	
	Min	Max	Min	Max	Min	Max	Min	Max	Min	Max	Min	Max	Min	Max	Min	Max
2014	0.089	0.258	0.059	0.175	0.030	0.100					No Data					
2015	0.108	0.268	0.035	0.127	0.035	0.150	1.563	2.840	0.647	1.370	0.693	1.470	0.129	0.262	2.6	33.3
2016	0.074	0.160	0.025	0.091	0.008	0.096	1.390	2.290	0.300	1.000	0.720	1.800	0.030	0.130	4.7	45.5
2017	0.091	0.237	0.043	0.097	0.040	0.146	0.995	2.638	0.303	0.658	0.528	2.210	0.020	0.176	6.0	30.8
2018	0.094	0.303	0.041	0.124	0.031	0.195					No Data				2.7	20.5

Table 5a. Summer (May - September) mean flow and constituent loading from the Hay River at Wheeler, WI, and the Red Cedar River at Colfax, WI. P = phosphorus, SRP = soluble reactive P. Loading was estimated statistically using Weighted Regression on Time, Discharge, and Season (WRTDS, Hirsch et al. 2010).

Hay River

Year	Flow		Total P			SRP		
MAY-SEP)	(ft^3/s)	(m^3/s)	(kg/sum)	(kg/d)	(mg/L)	(kg/sum)	(kg/d)	(mg/L)
2014	698.4	19.78	50,628	326	0.153	24,516	132	0.073
2015	461.1	13.06	30,348	167	0.132	14,550	73	0.064
2016	387.4	10.97	17,448	117	0.111	8,775	55	0.056
2017	442.0	12.51	24,358	151	0.123	9,990	68	0.057
2018	342.8	9.71	15,914	104	0.115	7,477	49	0.056
Mean	466.32	13.20	27,739	173	0.127	13,062	75	0.061

Red Cedar River

Year	Flow		Total P			SRP		
MAY-SEP)	(ft^3/s)	(m^3/s)	(kg/sum)	(kg/d)	(mg/L)	(kg/sum)	(kg/d)	(mg/L)
2014	1840.0	52.10	144,662	946	0.198	70,806	463	0.103
2015	1115.6	31.59	61,223	400	0.141	32,225	211	0.076
2016	1271.5	36.00	65,458	428	0.133	33,423	218	0.070
2017	1334.9	37.80	79,729	521	0.140	36,621	239	0.073
2018	935.0	26.48	50,630	331	0.139	27,463	179	0.079
Mean	1,299.40	36.79	80,341	525	0.150	40,108	262	0.080

Total Measured

Year	Flow		Total P			SRP		
MAY-SEP)	(ft^3/s)	(m^3/s)	(kg/sum)	(kg/d)	(mg/L)	(kg/sum)	(kg/d)	(mg/L)
2014	2538.4	71.88	160,141	1,047	0.169	95,322	594	0.095
2015	1576.7	44.65	83,370	545	0.141	46,774	284	0.073
2016	1658.4	46.96	84,240	551	0.136	42,199	273	0.067
2017	1776.8	50.31	95,793	626	0.144	46,611	307	0.069
2018	1277.8	36.18	66,544	435	0.132	34,940	228	0.072
Mean	1,765.6	50.00	98,017	641	0.144	53,169	337	0.075

Table 5b. Annual (January - December) mean flow and constituent loading from the Hay River at Wheeler, WI, and the Red Cedar River at Colfax, WI. P = phosphorus, SRP = soluble reactive P. Loading was estimated statistically using Weighted Regression on Time, Discharge, and Season (WRTDS, Hirsch et al. 2010).

Hay River

Year	Flow		Total P			SRP		
	(ft^3/s)	(m^3/s)	(kg/y)	(kg/d)	(mg/L)	(kg/y)	(kg/d)	(mg/L)
2014	510.7	14.46	81,735	224	0.115	34,398	94	0.049
2015	438.5	12.42	54,762	150	0.102	23,480	64	0.045
2016	421.3	11.93	39,955	109	0.091	16,928	46	0.041
2017	404.5	11.46	42,857	117	0.093	17,791	49	0.043
2018	387.7	10.98	41,820	115	0.105	17,947	49	0.051
Mean	432.55	12.25	52,226	143	0.101	22,109	61	0.046

Red Cedar River

Year	Flow		Total P			SRP		
	(ft^3/s)	(m^3/s)	(kg/y)	(kg/d)	(mg/L)	(kg/y)	(kg/d)	(mg/L)
2014	1322.0	37.43	200,214	549	0.140	94,308	258	0.073
2015	1105.0	31.29	119,846	328	0.115	60,414	166	0.062
2016	1262.1	35.74	136,715	375	0.116	66,679	183	0.060
2017	1191.9	33.75	143,391	393	0.120	69,863	191	0.064
2018	1022.7	28.96	108,222	296	0.126	56,631	155	0.072
Mean	1,180.73	33.43	141,677	388	0.124	69,579	191	0.066

Total Measured

Year	Flow		Total P			SRP		
	(ft^3/s)	(m^3/s)	(kg/y)	(kg/d)	(mg/L)	(kg/y)	(kg/d)	(mg/L)
2014	1832.7	51.90	281,950	772	0.133	128,706	353	0.067
2015	1543.5	43.71	174,608	478	0.112	83,895	230	0.057
2016	1683.4	47.67	176,669	484	0.110	83,608	229	0.055
2017	1596.5	45.21	186,248	510	0.114	87,654	240	0.059
2018	1410.4	39.94	150,042	411	0.120	74,578	204	0.067
Mean	1,613.3	45.7	193,903	531	0.118	91,688	251	0.061

Table 6. Mean annual and summer flow and total phosphorus (P), particulate P, and soluble reactive P (SRP) loading anf flow-weighted concentrations. Balance/retention = total measured income divided by discharge. For instance Tainter-Menomin reservoirs retained 15%, 13%, and 17% of the annual total P, particulate P, and SRP load.

		Annual						**Summer (May-September)**				
Variable	Units	Annual Inflow Loading			Discharge Loading	Balance/ retention	Units	Summer Inflow Loading			Discharge Loading	Balance /retention
		Hay R	Red Cedar R	Total	Red Cedar R	(%)		Hay R	Red Cedar R	Total	Red Cedar R	(%)
Flow	(m^3/s)	12.25	33.43	45.70	53.80		(m^3/s)	13.20	36.79	50.00	58.42	
Total P	(kg/y)	52,226	141,677	**193,903**	165,106	15%	(kg/su)	27,739	80,341	108,080	86,227	20%
Particulate P	(kg/y)	30,117	72,098	102,215	88,689	13%	(kg/su)	14,677	40,233	54,910	42,282	23%
SRP	(kg/y)	22,109	69,579	91,688	76,417	17%	(kg/su)	13,062	40,108	53,170	43,945	17%
Total P	(mg/L)	0.101	0.124	0.118	0.092		(mg/L)	0.127	0.150	0.144	0.107	
Particulate P	(mg/L)	0.055	0.058	0.057	0.054		(mg/L)	0.066	0.070	0.069	0.062	
SRP	(mg/L)	0.046	0.066	0.061	0.038		(mg/L)	0.061	0.080	0.075	0.045	

1990 TMDL annual total P was 229,654 kg (La Liberte et al. 2012)

Table 7. Ranges in alkaline phosphatase activity (nM/hr) and specific activity (nM/ug CHLa hr) reported in various lakes and reservoirs.

System	nM/hr			nM/ug CHLa hr			Reference
	Mean	Min	Max	Mean	Min	Max	
Tainter Lake	67.5	18.5	151.5	0.73	0.16	1.58	This study
Menomin Lake	56.2	18.8	118.5	0.58	0.14	1.24	This study
Ford Lake 2004-5			1200	13			Lehman et al (2013)
Ford Lake 2006			400	11.1			Lehman et al (2013)
Ford Lake 2012			1200	4.7		59	Lehman et al (2013)
Lake Champlain	12						Levine et al (1997)
Lake Memphremagog				4			Smith and Kalff (1981)
Lake Ontario			250				Pick (1987)
Lake Superior near shore				8.425	2.1	13.3	Rose and Axler (1998)

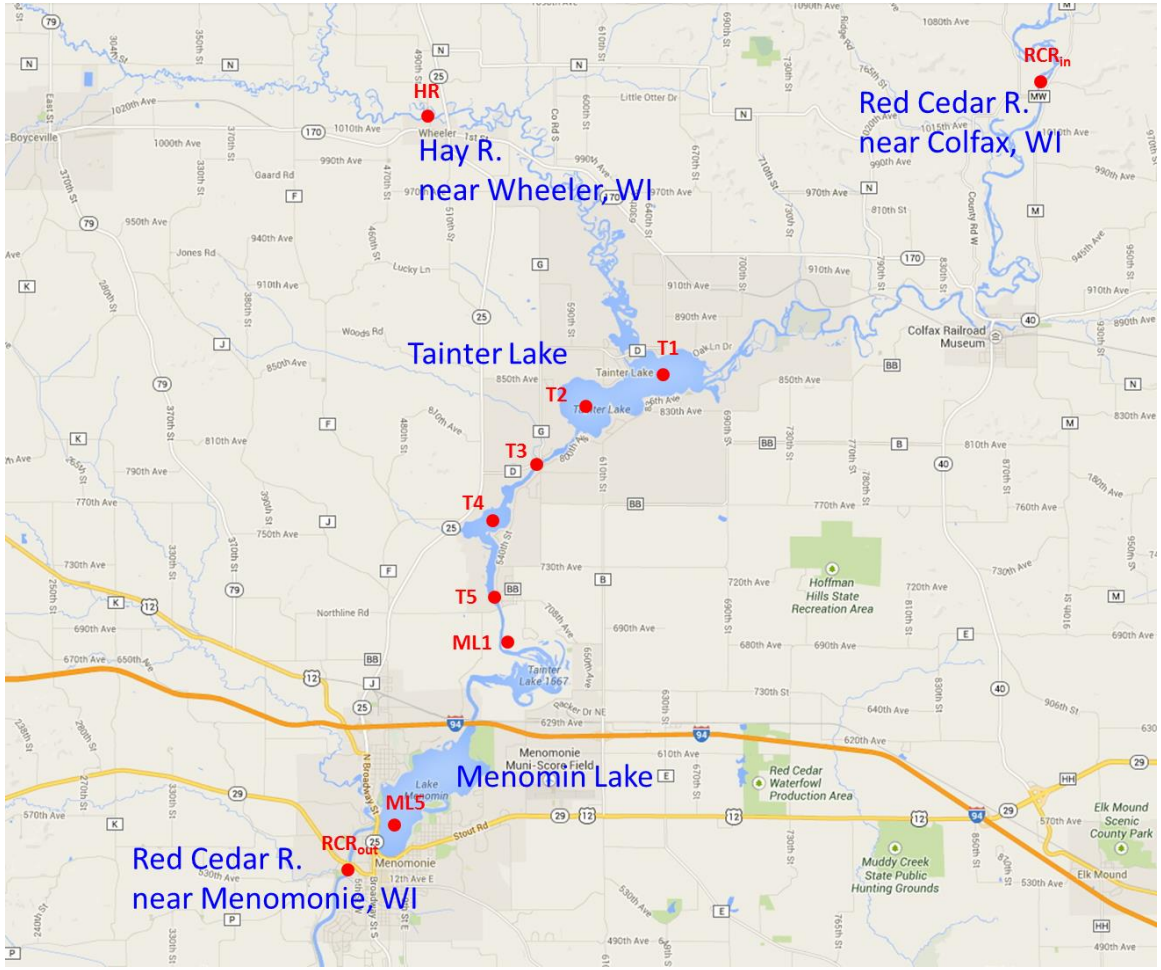

Figure 1. Station locations. HR = Hay River at Wheeler, WI, RCR_{in} = Red Cedar River at Colfax, WI, RCR_{out} = Red Cedar River at Menomonie, WI, TL = Tainter Lake, ML = Menomin Lake.

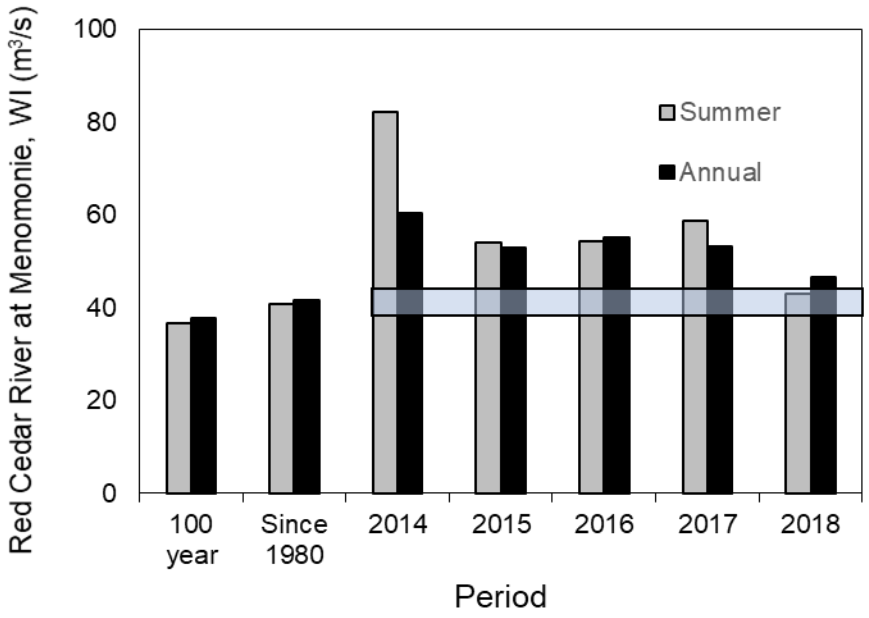

Figure 2. A comparison of mean summer (May – September) and annual (January – December) flow for the Red Cedar River at Menomonie WI in 2014-18 versus since 1980 and over a 100-year record.

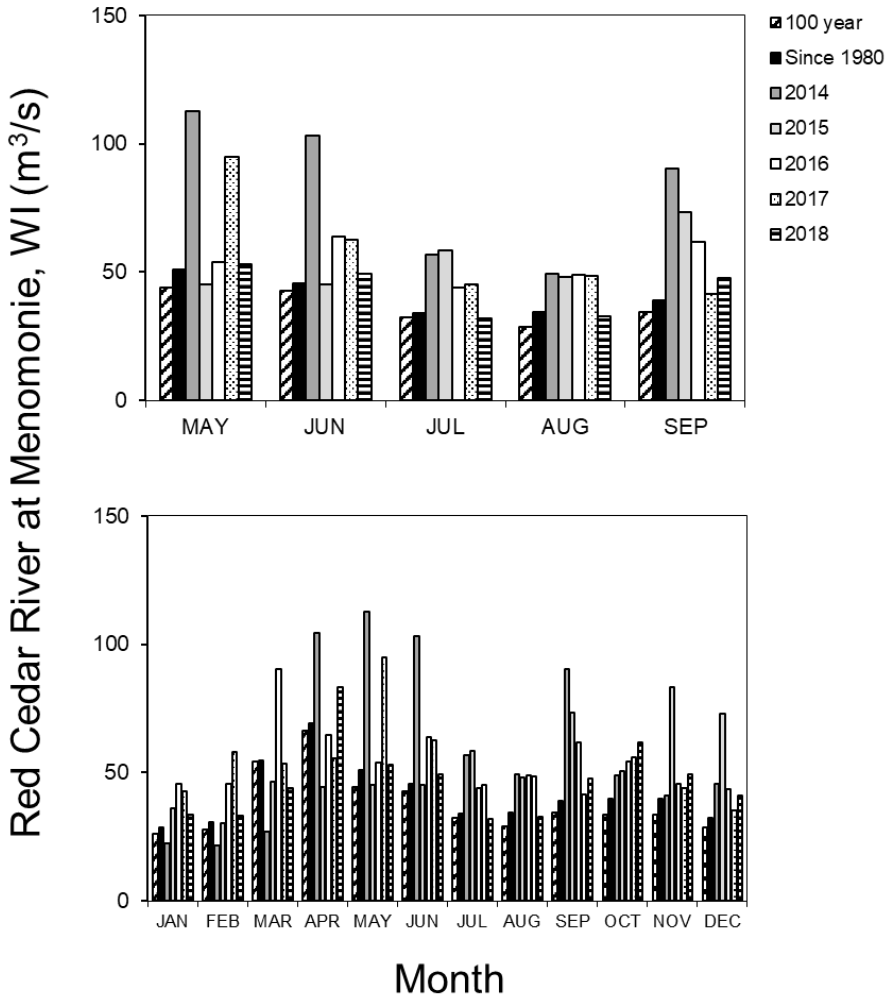

Figure 3. A comparison of mean monthly flows for the Red Cedar River at Menomonie WI in 2014-17 versus since 1980 and over a 100-year record.

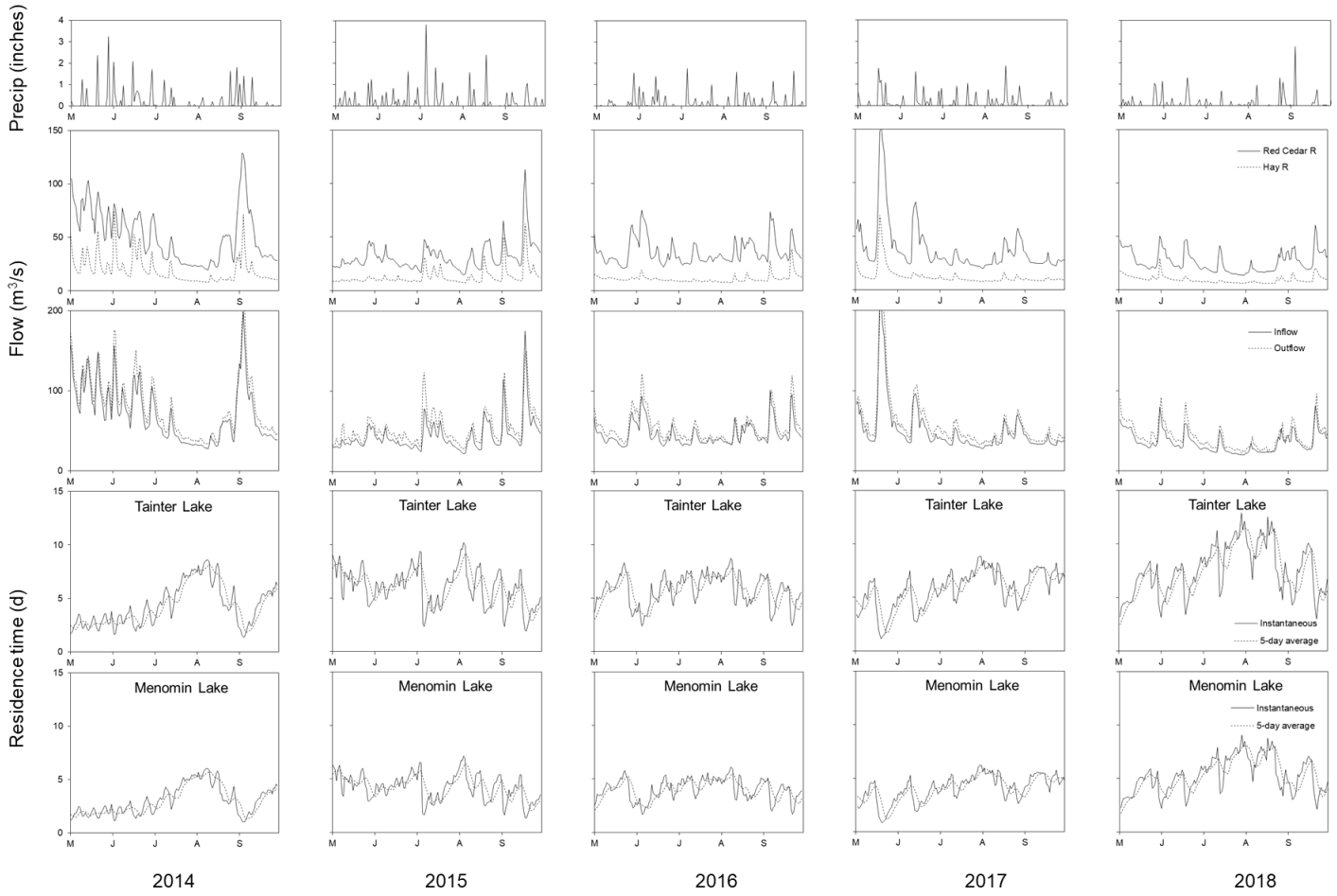

Figure 4. Summer (May – September) variations in precipitation, daily flows for the Red Cedar River at Menomonie, WI, and the Hay River at Wheeler, WI, combined inflow from the Red Cedar and Hay Rivers versus the Red Cedar River outflow at Menomonie, WI, and instantaneous and 5-day average residence times from Tainter and Menomin Lake in 2014-18.

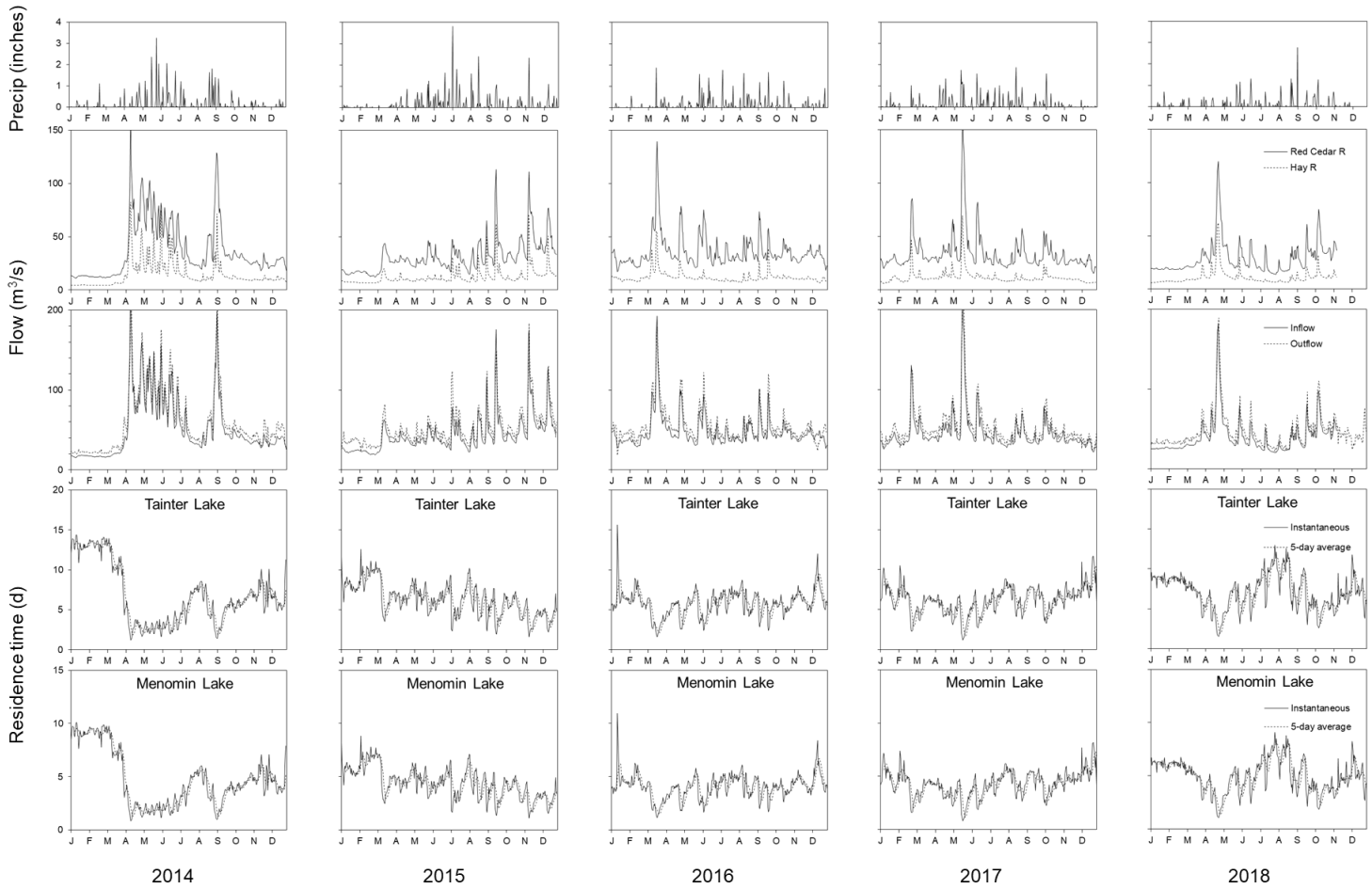

Figure 5. Annual (January – December) variations in precipitation, daily flows for the Red Cedar River at Menomonie, WI, and the Hay River at Wheeler, WI, combined inflow from the Red Cedar and Hay Rivers versus the Red Cedar River outflow at Menomonie, WI, and instantaneous and 5-day average residence times from Tainter and Menomin Lake in 2014-18.

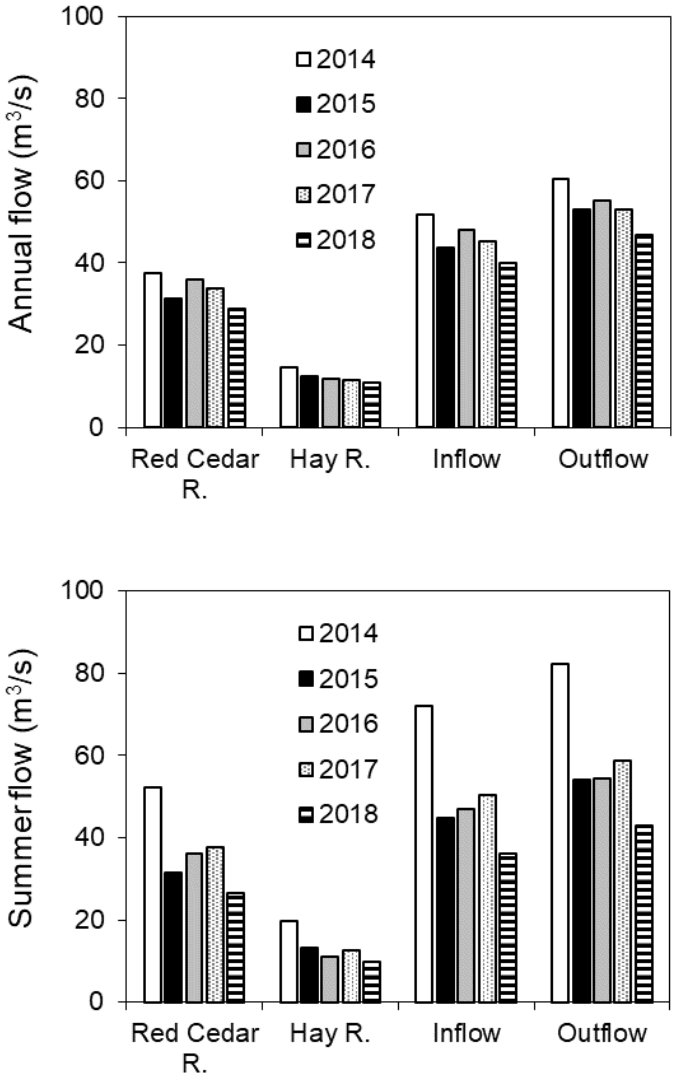

Figure 6. A comparison of mean annual (January – December, upper panel) and summer (May – September, lower panel) flow for the Red Cedar River at Colfax, WI, the Hay River at Wheeler, WI, combined inflow (i.e., Red Cedar + Hay River) and the Red Cedar River outflow at Menomonie, WI in 2014-18.

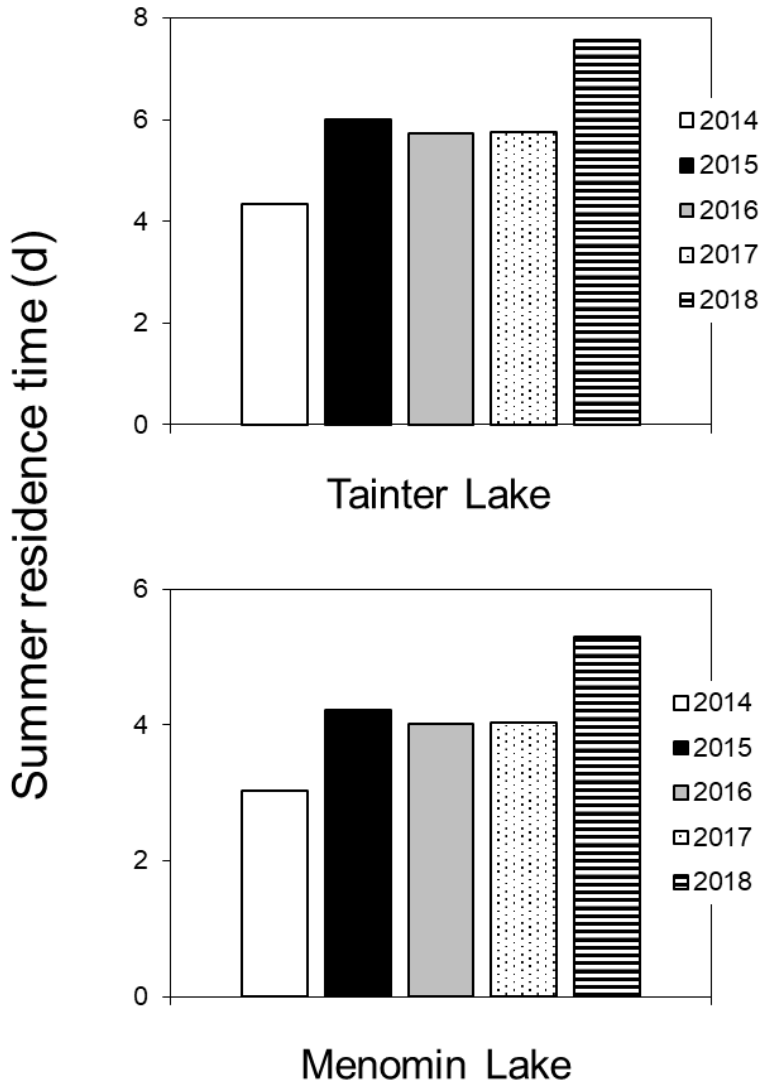

Figure 7. Mean summer (May – September) residence time of Tainter and Menomin Lake in 2014-18.

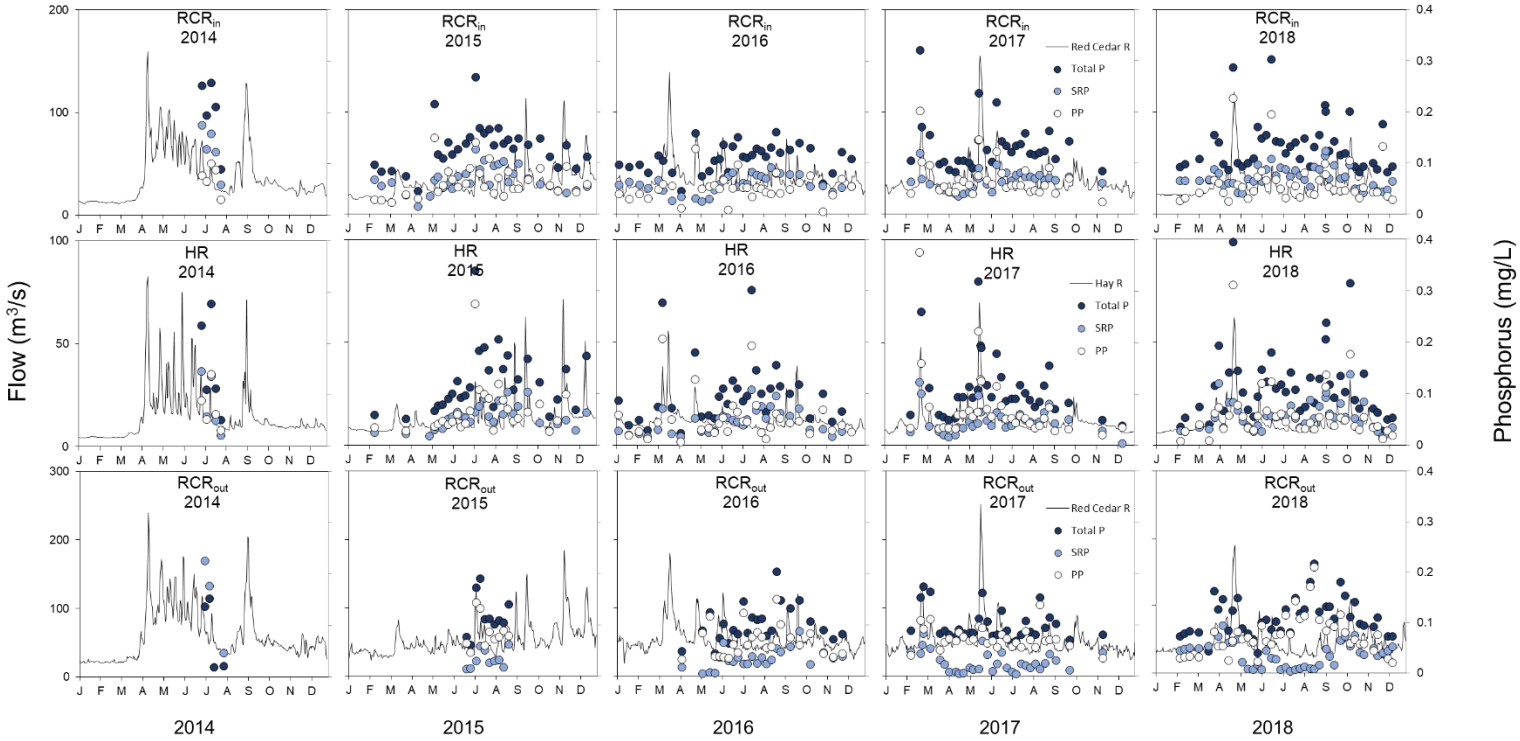

Figure 8. Annual time series of mean daily flow, total phosphorus (P), and soluble reactive P (SRP) for the Red Cedar River at Colfax, WI (upper panels) and the Hay River at Wheeler, WI (lower panels) in 2014-18.

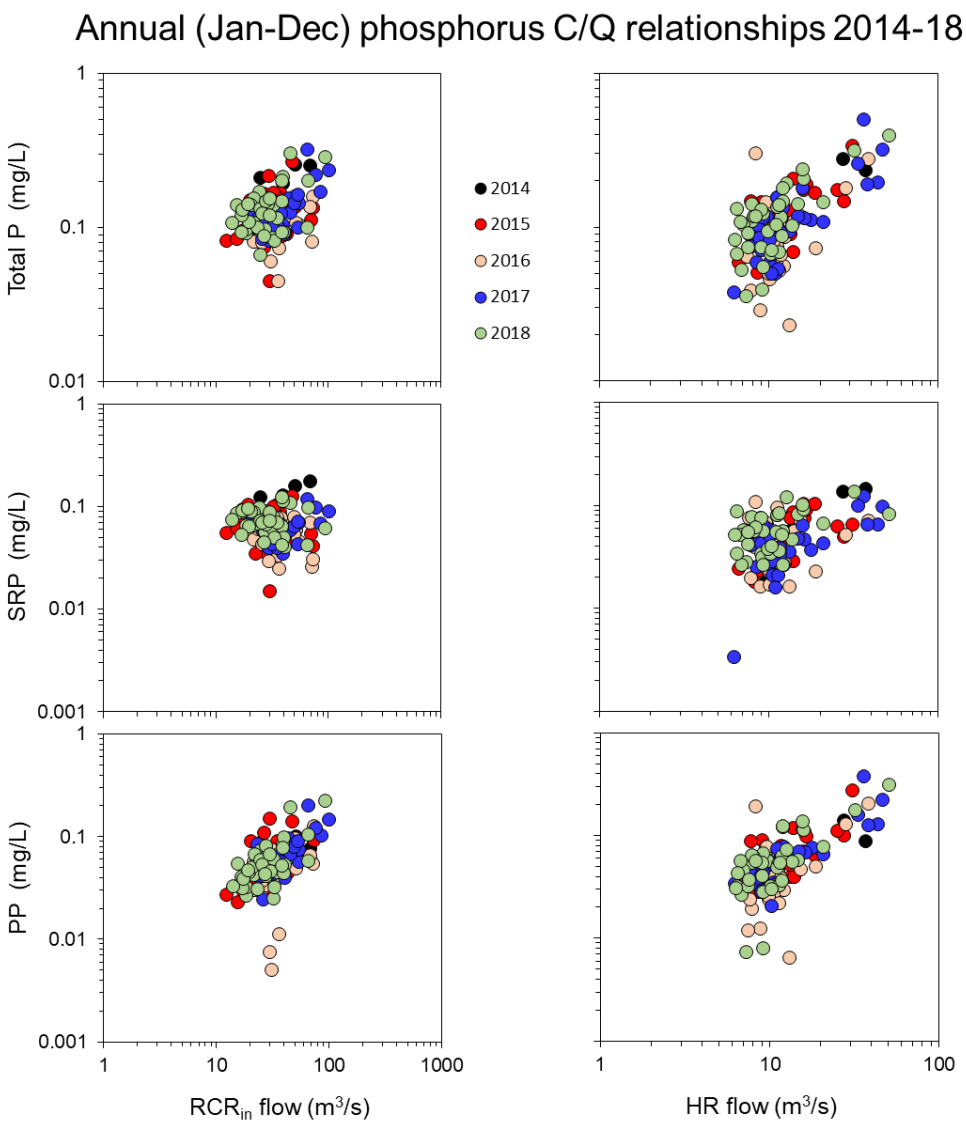

Fig. 9. Relationships between annual mean daily flow (Q) and concentration (C) in the Red Cedar River at Colfax, WI, and the Hay River at Wheeler, WI between 2014 and 2018. total P = total phosphorus and SRP = soluble reactive P.

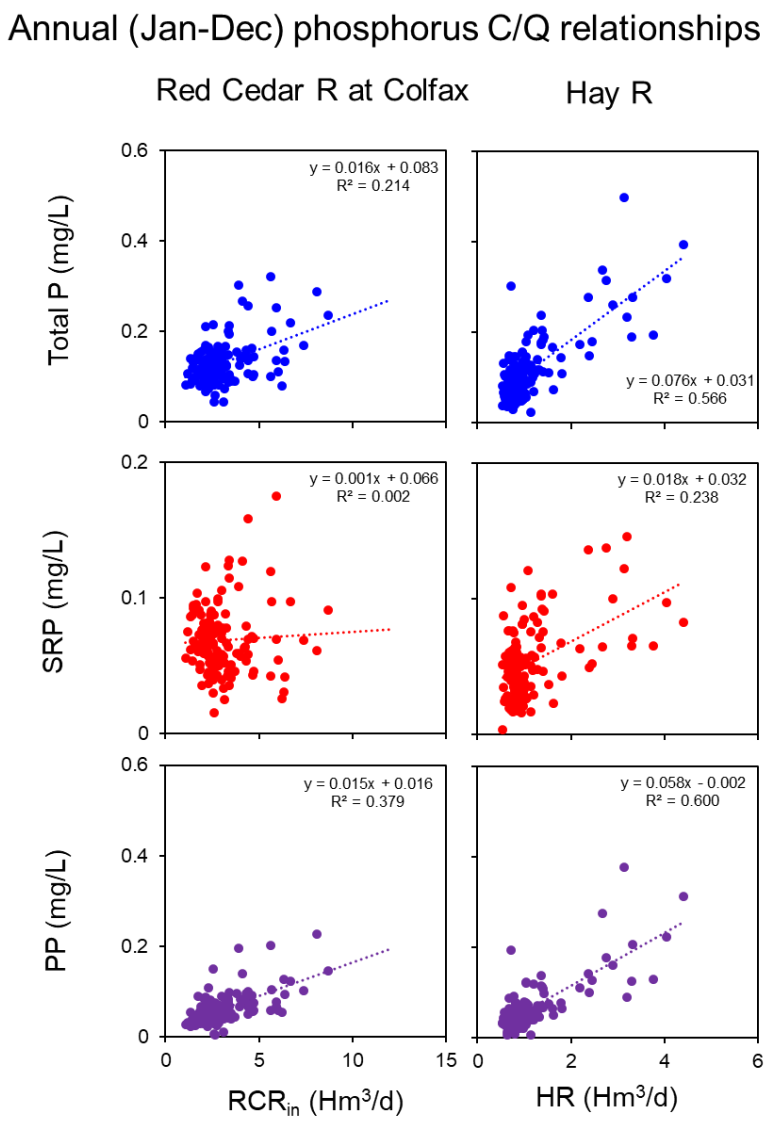

Fig. 10. Regressions relationships between annual mean daily flow (Q) and concentration (C) in the Red Cedar River at Colfax, WI, and the Hay River at Wheeler, WI between 2014 and 2018. total P = total phosphorus and SRP = soluble reactive P.

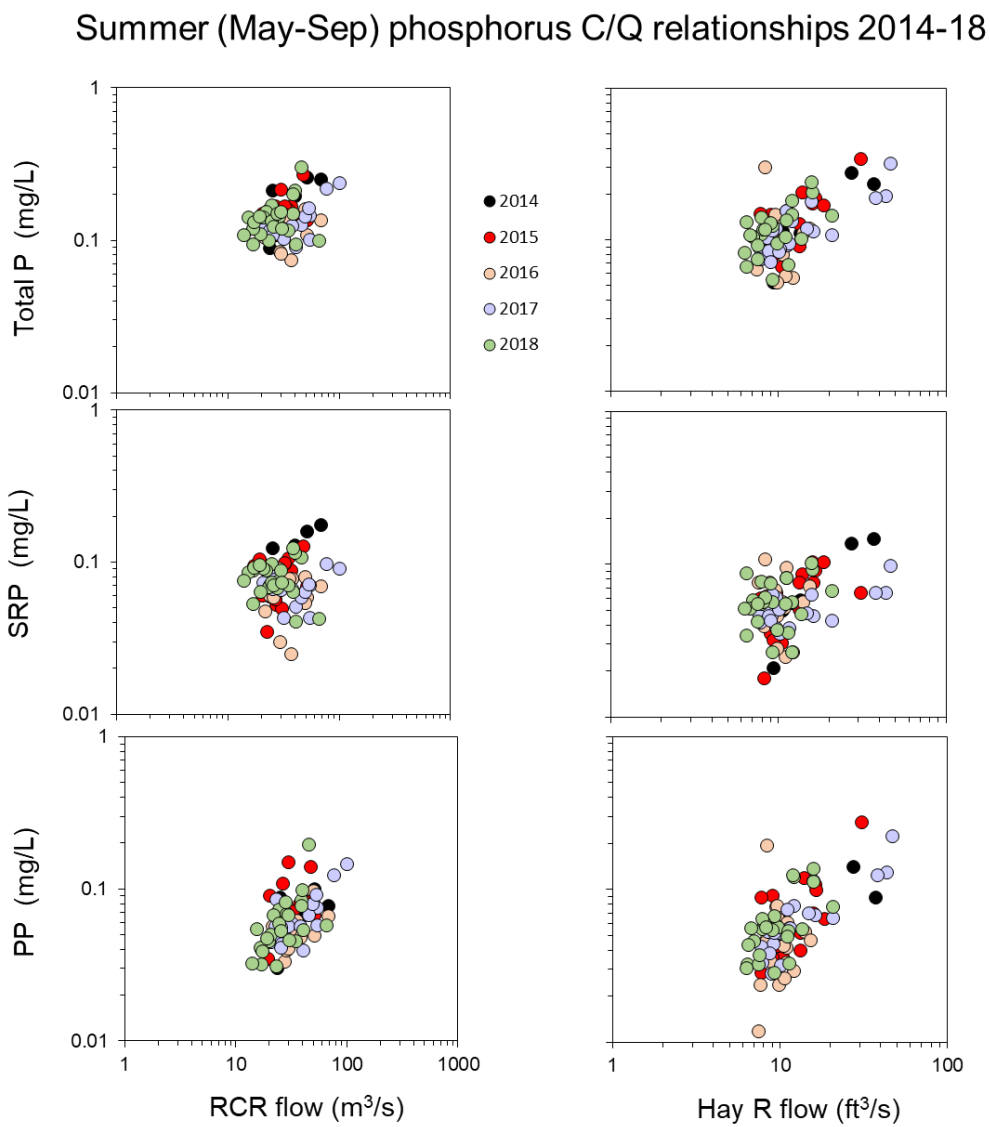

Fig. 11. Relationships between summer mean daily flow (Q) and concentration (C) in the Red Cedar River at Colfax, WI, and the Hay River at Wheeler, WI between 2014 and 2018. total P = total phosphorus and SRP = soluble reactive P.

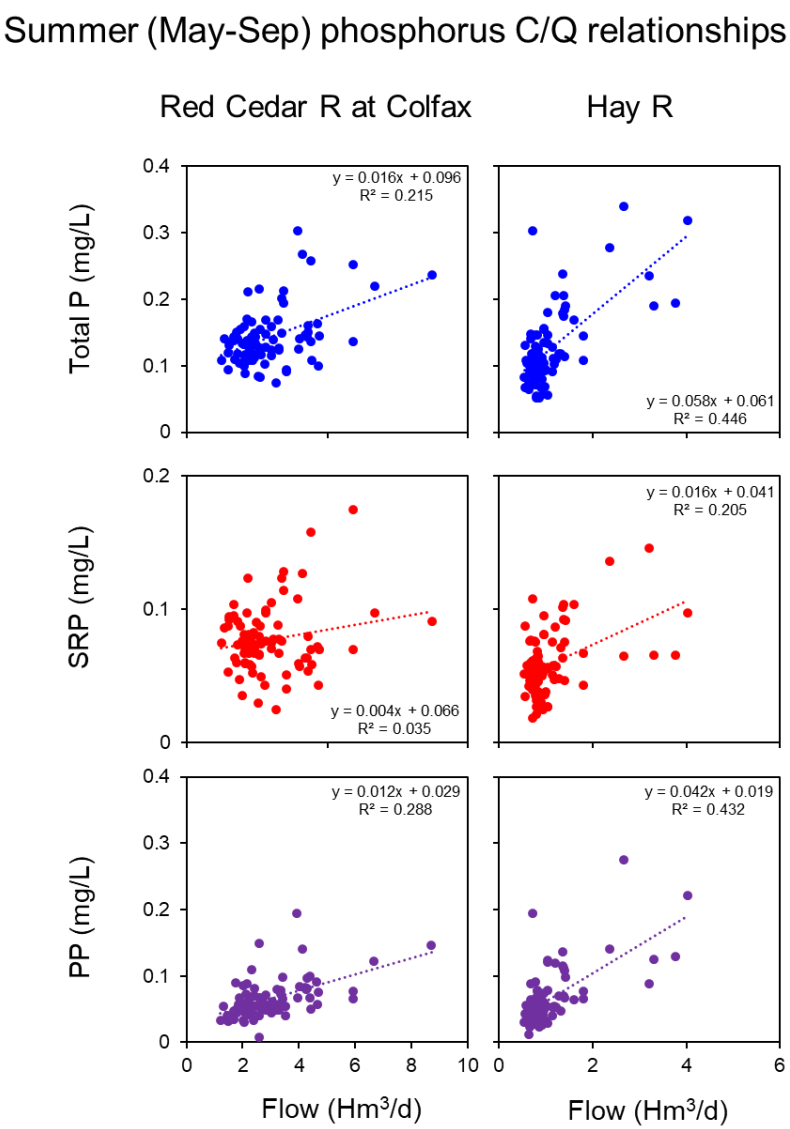

Fig. 12. Regressions relationships between summer mean daily flow (Q) and concentration (C) in the Red Cedar River at Colfax, WI, and the Hay River at Wheeler, WI between 2014 and 2018. total P = total phosphorus and SRP = soluble reactive P.

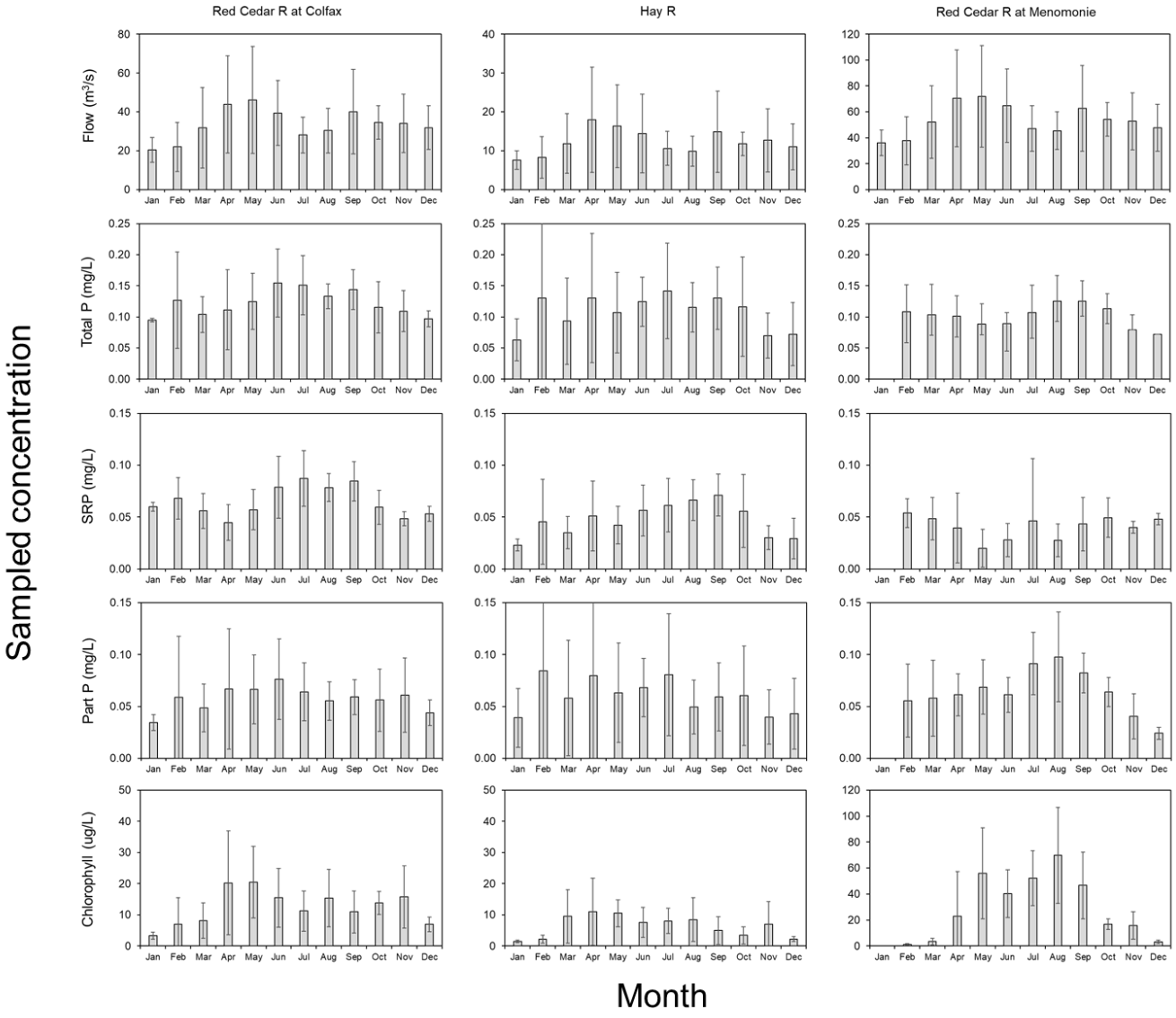

Fig. 13. Variations in mean monthly flow, total phosphorus (P), soluble reactive P (SRP), particulate P, and chlorophyll for the Red Cedar River at Colfax and Menomonie WI and the Hay River at Wheeler WI. Vertical lines denote ± 1 standard deviation.

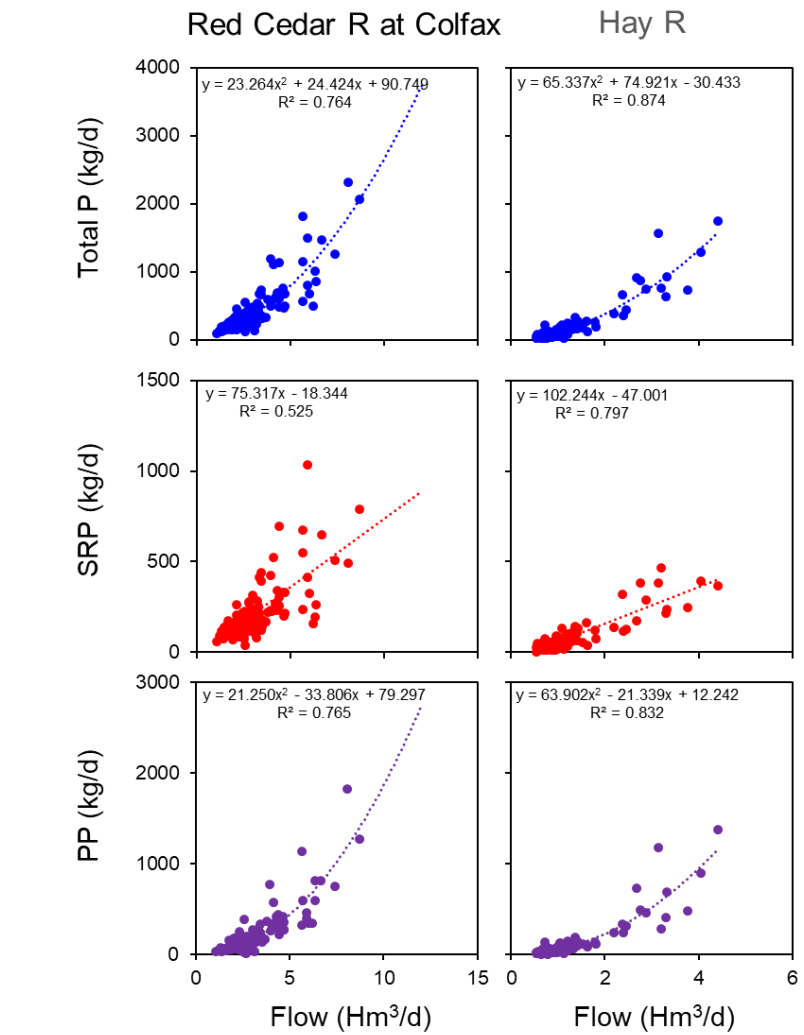

Fig. 14. Annual regression relationships between total phosphorus (P), soluble reactive P (SRP), or particulate P (PP) loading versus flow.

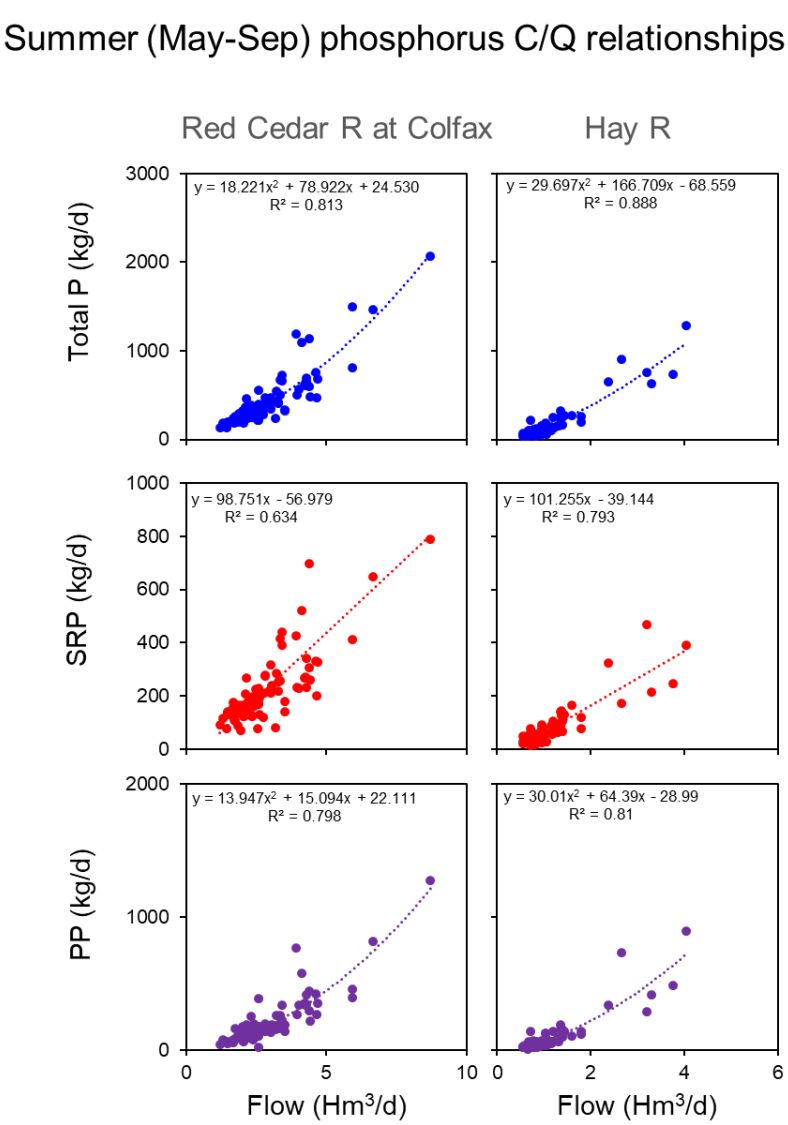

Fig. 15. Summer regression relationships between total phosphorus (P), soluble reactive P (SRP), or particulate P (PP) loading versus flow.

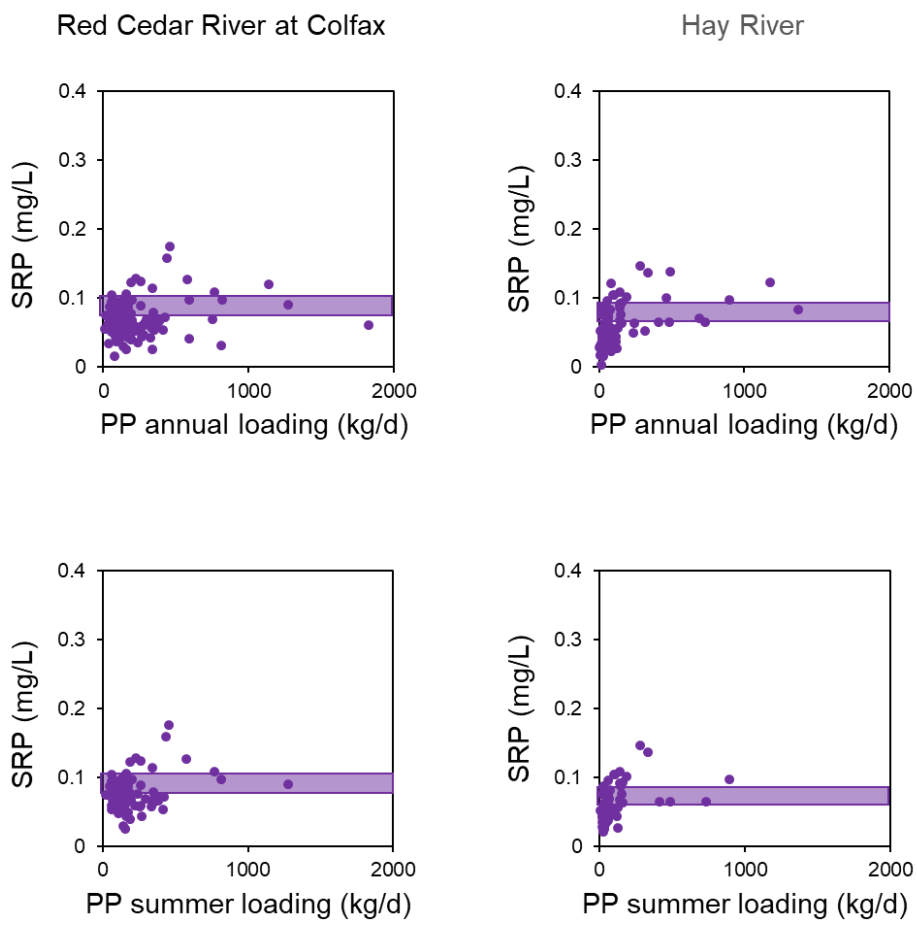

Fig. 16. Relationships between soluble reactive phosphorus (SRP) concentration and annual particulate phosphorus (PP) loading (upper panels) or summer (May-September) PP loading (lower panels). Horizontal line denotes an equilibrium P concentration of ~ 0.080 mg/L for the Red Cedar River and ~ 0.061 mg/L for the Hay River.

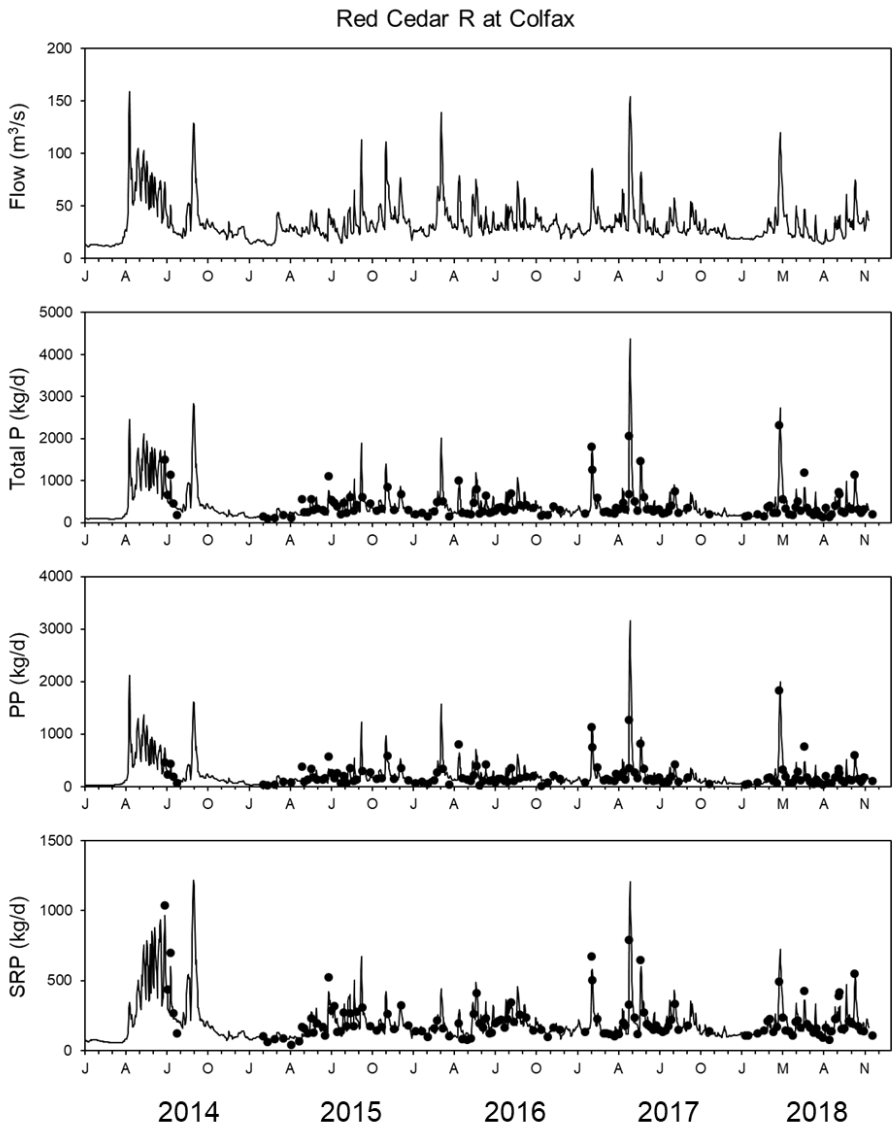

Fig. 17. Variations in flow and modeled (line) versus estimated (black dot) total phosphorus (P), particulate P (PP), and soluble reactive P (SRP) loading from the Red Cedar River at Colfax WI.

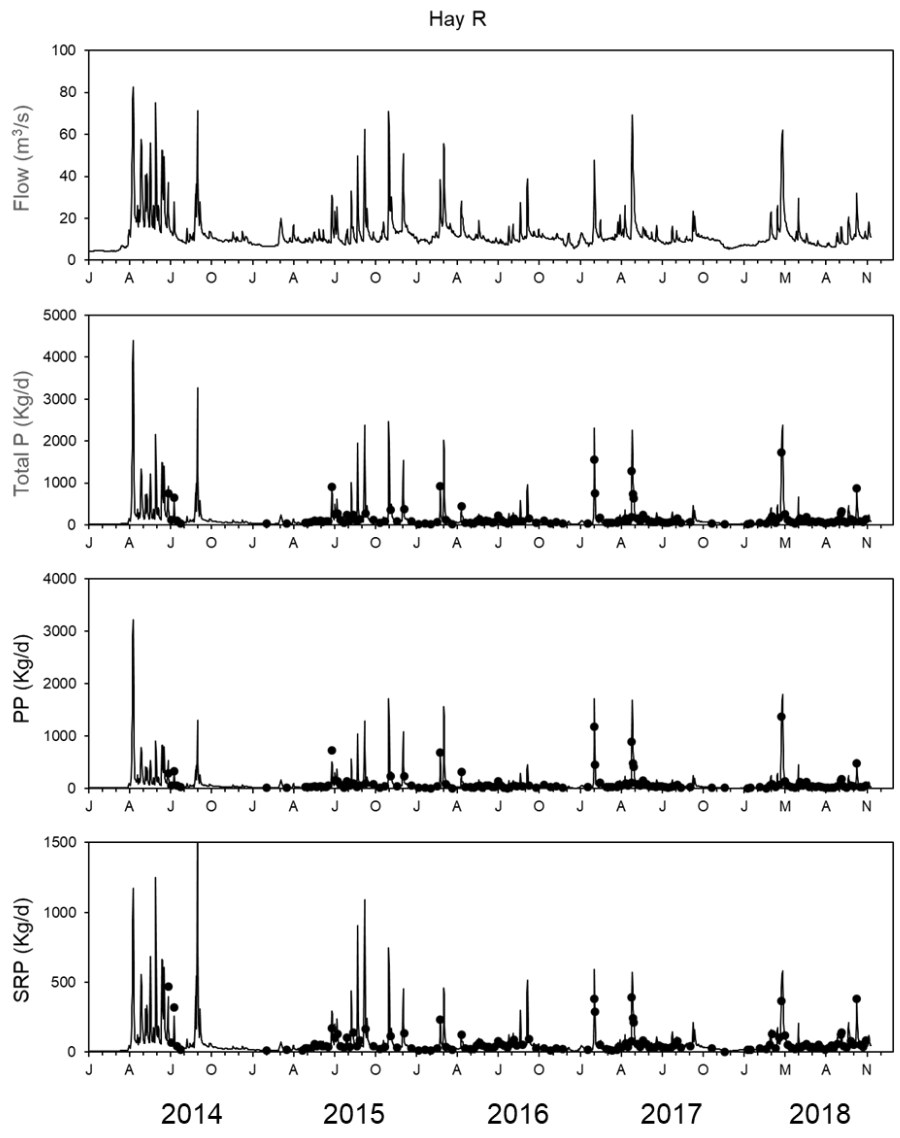

Fig. 18. Variations in flow and modeled (line) versus estimated (black dot) total phosphorus (P), particulate P (PP), and soluble reactive P (SRP) loading from the Hay River at Wheeler WI.

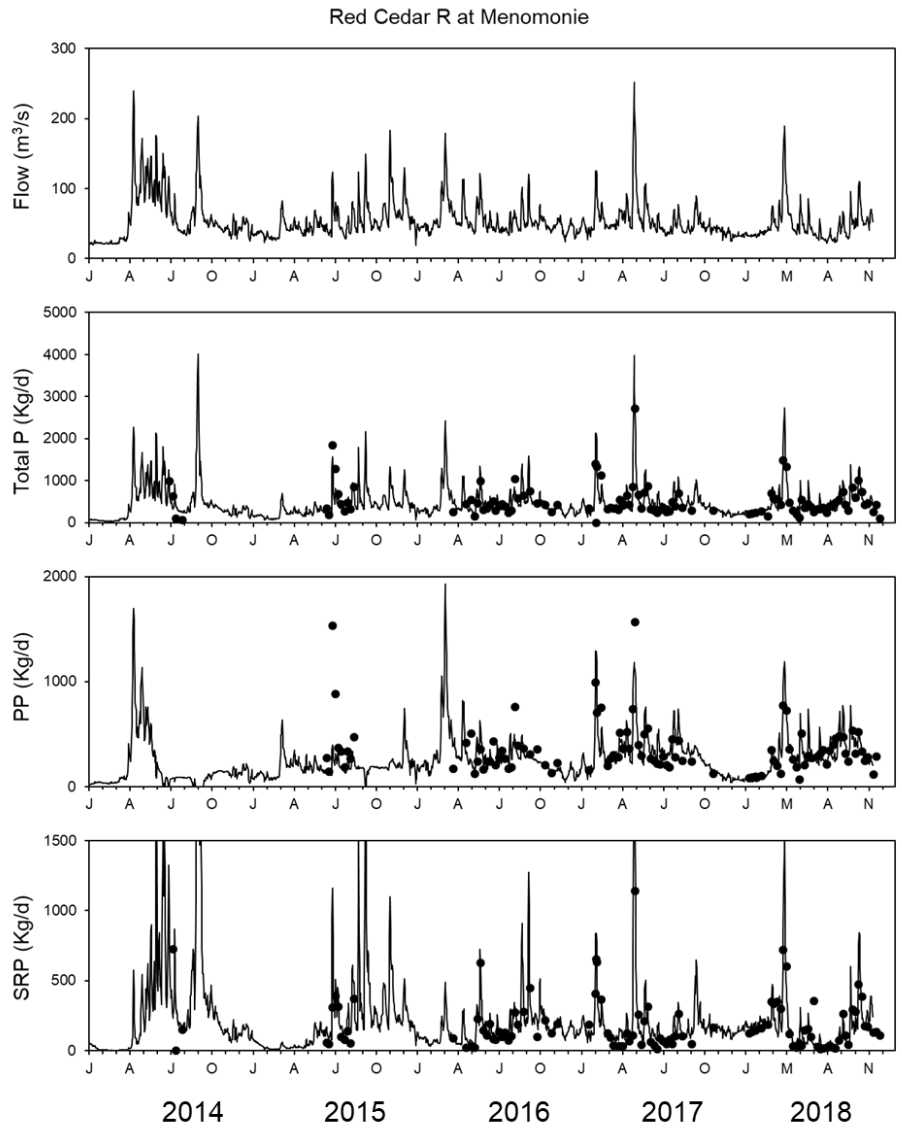

Fig. 19. Variations in flow and modeled (line) versus estimated (black dot) total phosphorus (P), particulate P (PP), and soluble reactive P (SRP) loading from the Red Cedar River at Menomonie WI.

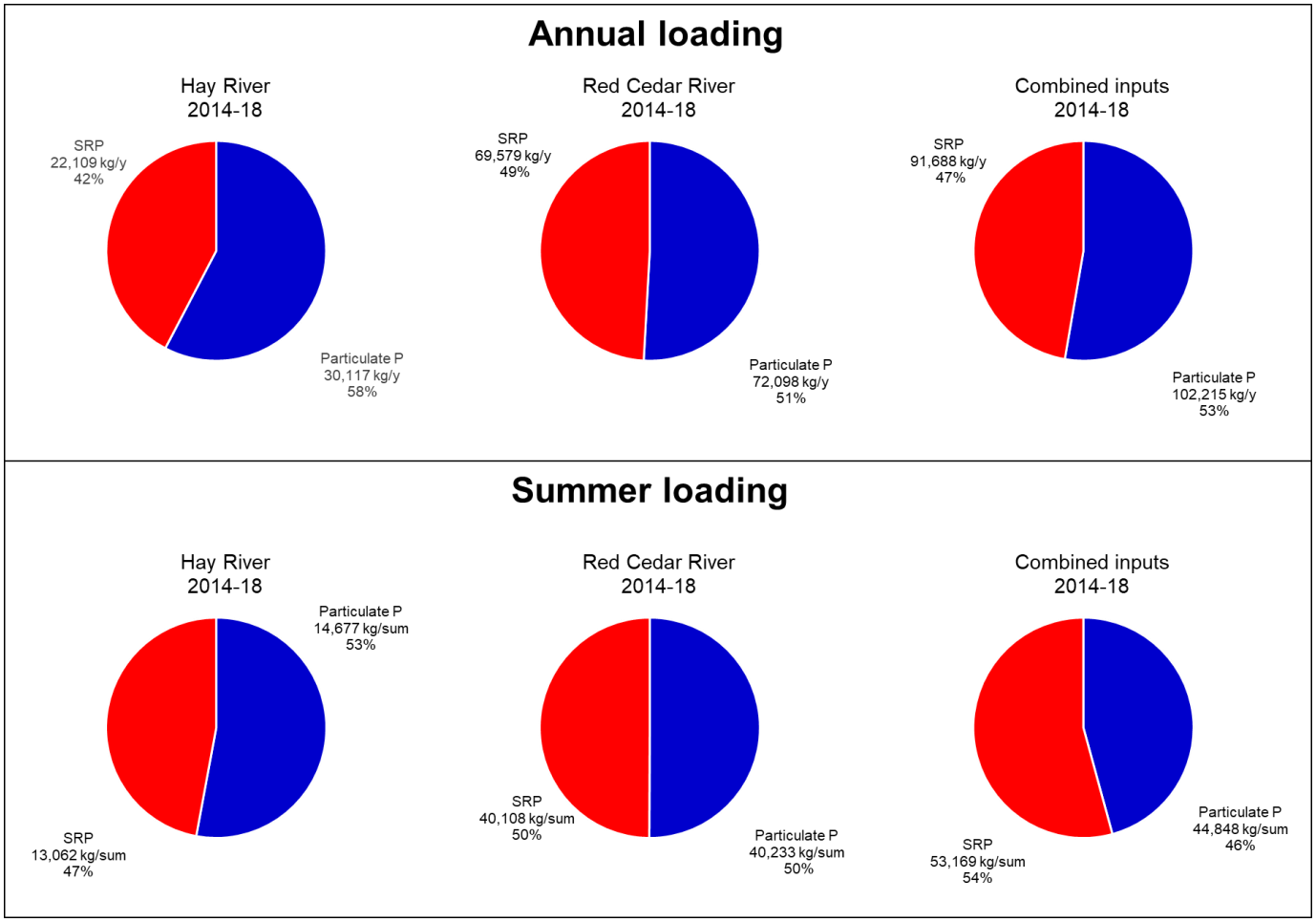

Fig. 20. Pie chart showing the composition of annual and summer total phosphorus (P) loading from the Hay River at Wheeler WI, the Red Cedar River at Colfax WI, and combined inputs over the period 2014-18.

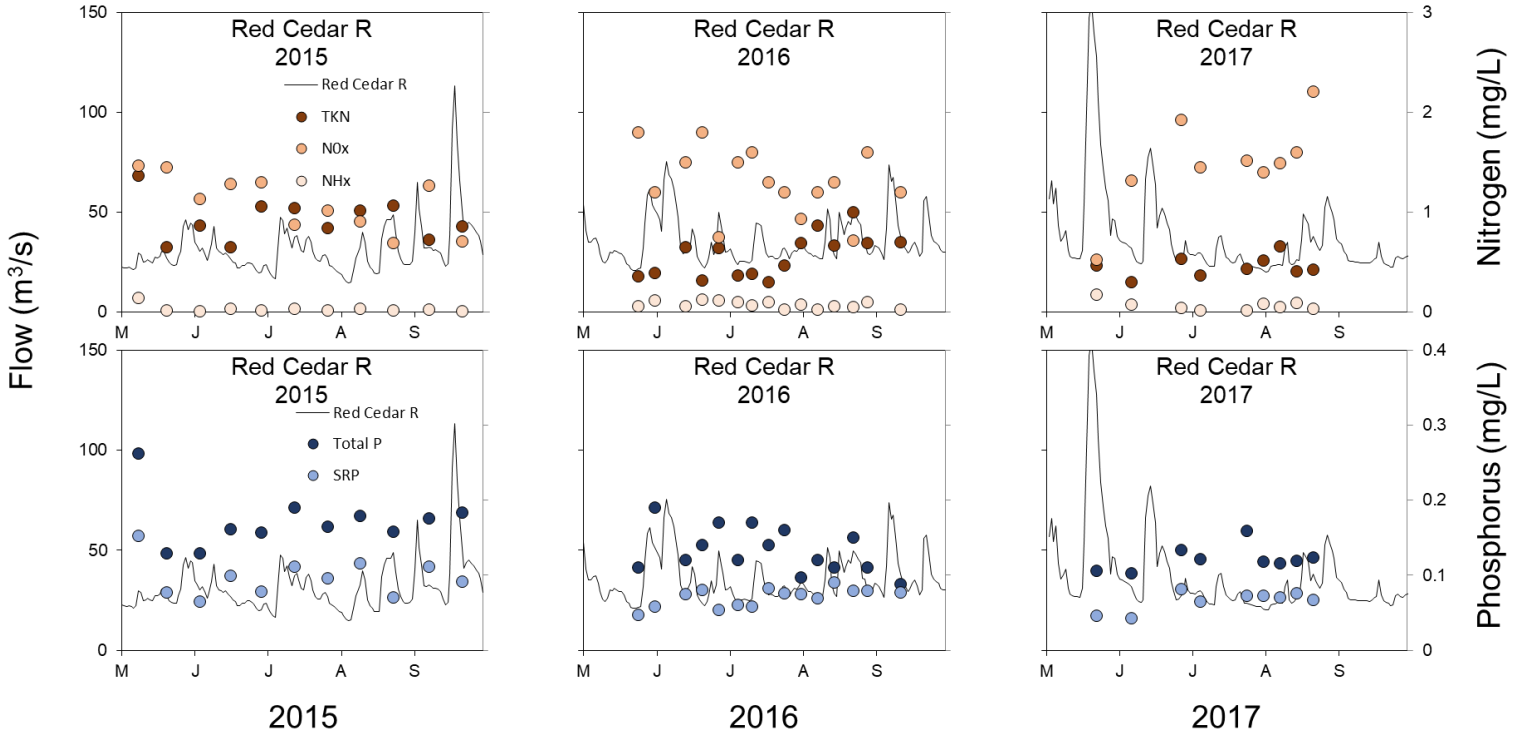

Figure 21. Summer time series of mean daily flow, total Kjeldahl nitrogen (TKN), nitrate-nitrite-N (NO_x), and ammonium-N (NH_x, upper panel) and total phosphorus (P) and soluble reactive P (SRP) for the Red Cedar River at Colfax WI in 2015-17.

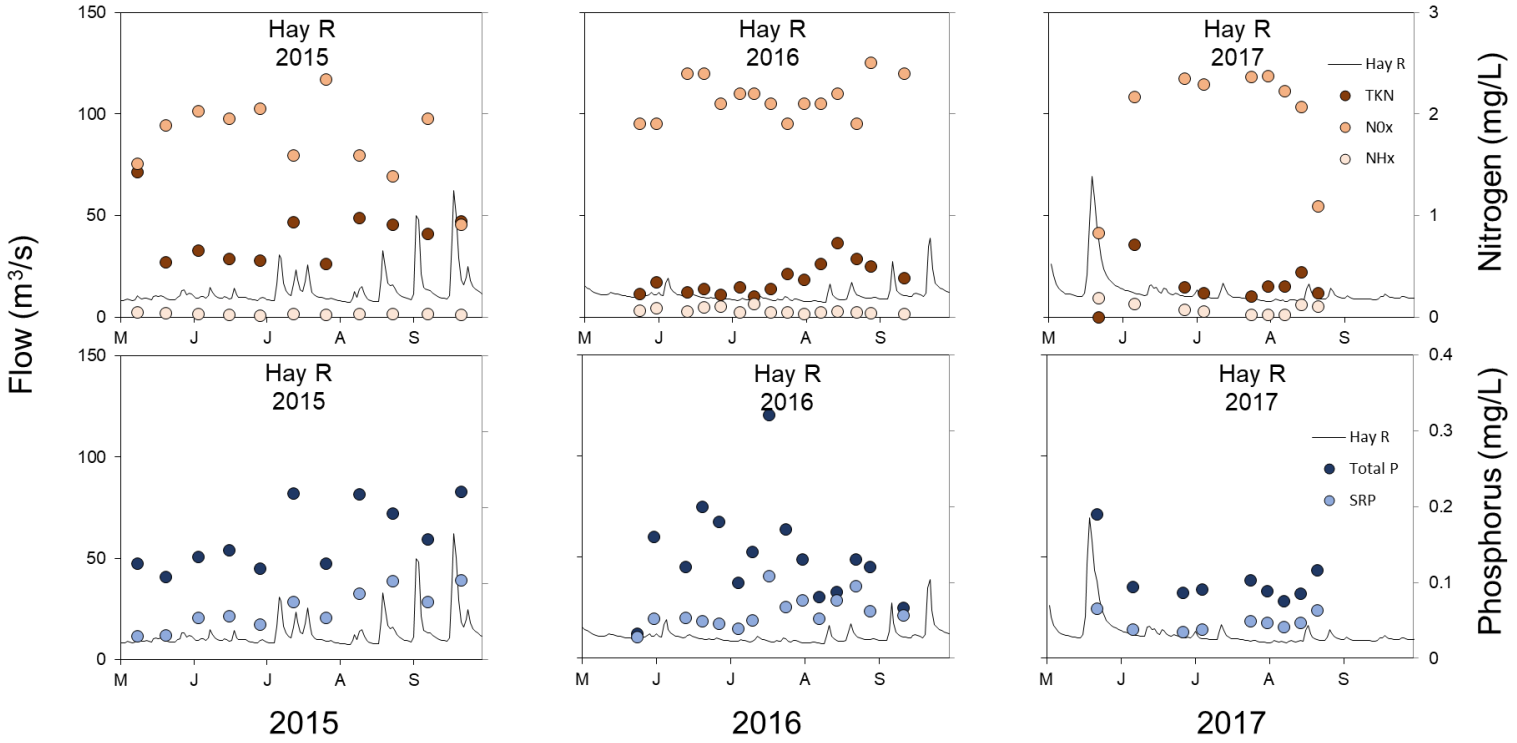

Figure 22. Summer time series of mean daily flow, total Kjeldahl nitrogen (TKN), nitrate-nitrite-N (NO_x), and ammonium-N (NH_x, upper panel) and total phosphorus (P) and soluble reactive P (SRP) for the Hay River at Wheeler WI in 2015-17.

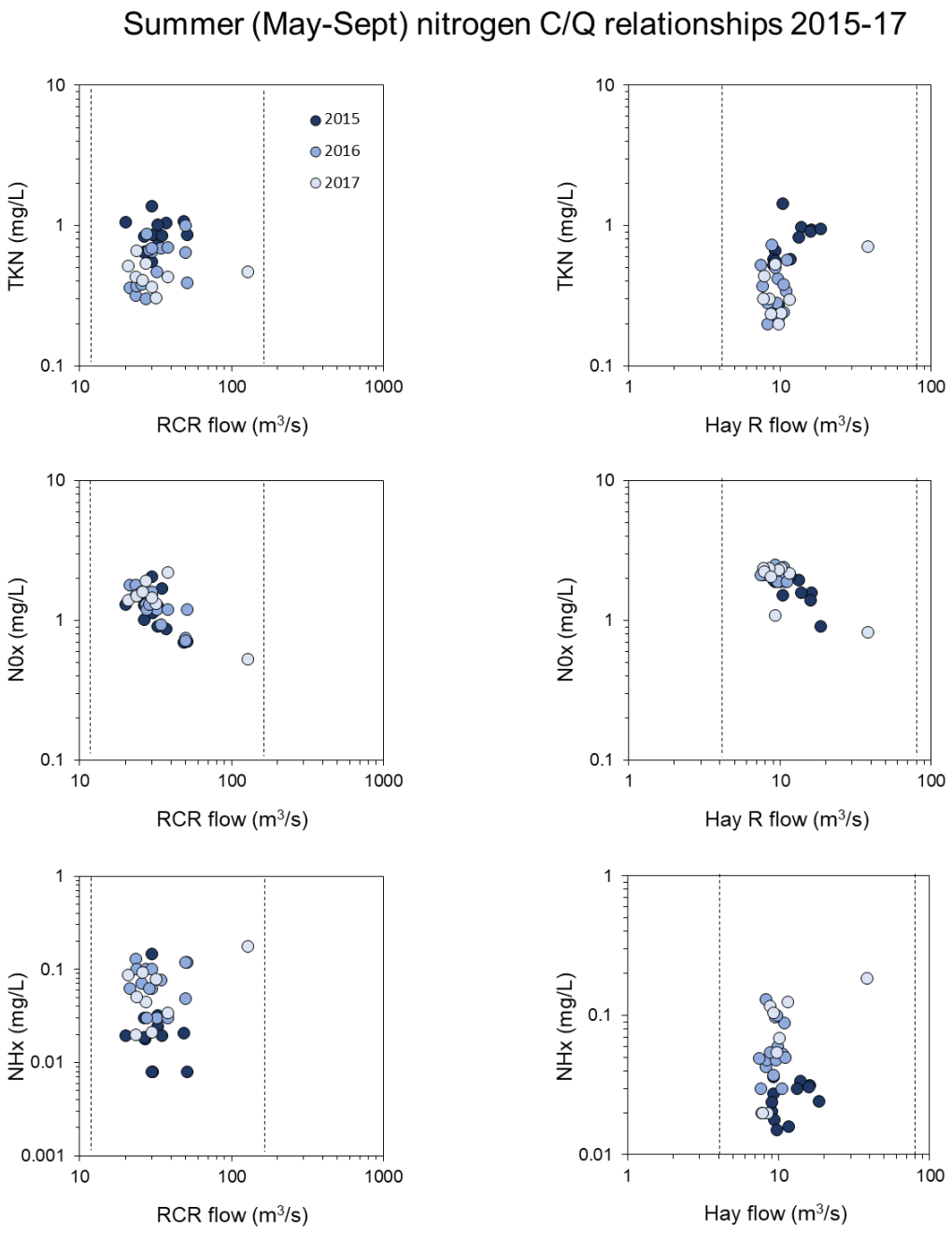

Figure 23. Relationships between summer mean daily flow (Q) and concentration (C) in the Red Cedar River (RCR_{in}) at Colfax, WI and the Hay River at Wheeler, WI. TKN = total Kjeldahl nitrogen, NO_x = nitrate-nitrite-N, NH_x = ammonium-N. Dotted line denotes the maximum mean daily flow during the period 2014-17.

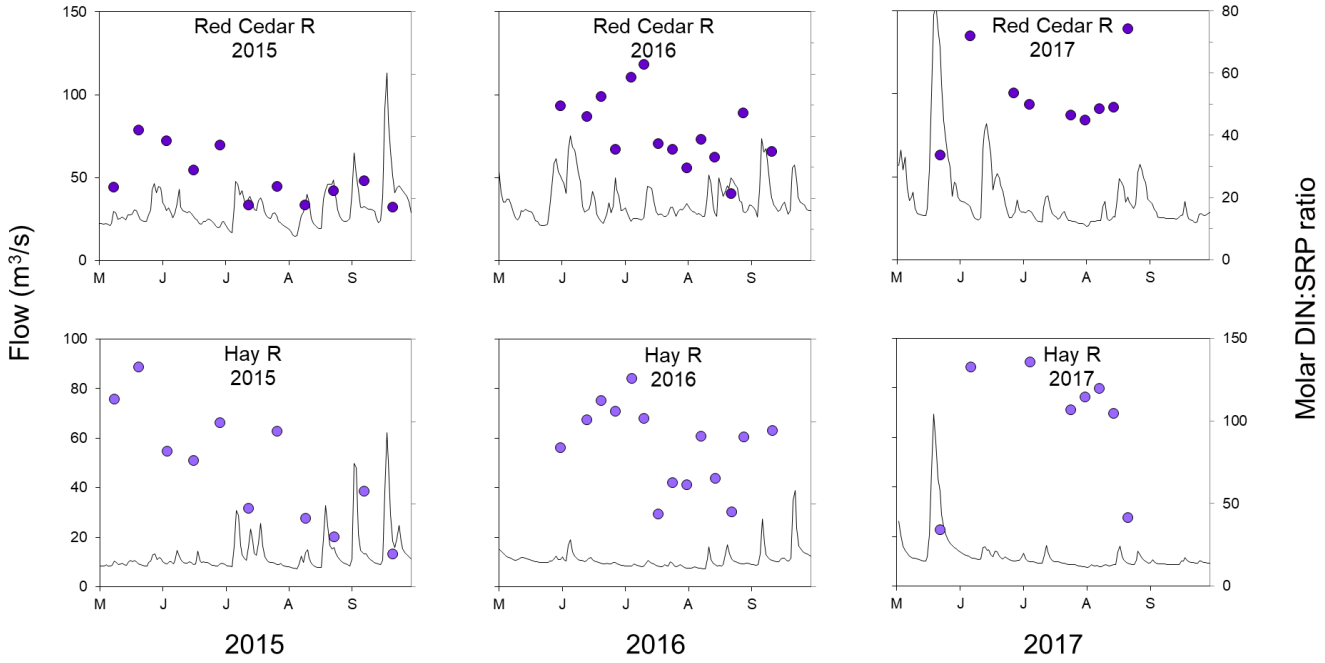

Figure 24. Variations in the molar dissolved inorganic nitrogen to soluble reactive phosphorus ratio (DIN:SRP) in the Red Cedar River at Colfax WI and the Hay River at Wheeler WI during the summers of 2015-17. DIN = the sum of nitrate-nitrite-N and ammonium-N.

Figure 25. Relationships between mean daily flow and the molar dissolved inorganic nitrogen to soluble reactive phosphorus ratio (DIN:SRP) in the Red Cedar River at Colfax WI and the Hay River at Wheeler WI during the summers of 2015-17. DIN = the sum of nitrate-nitrite-N and ammonium-N.

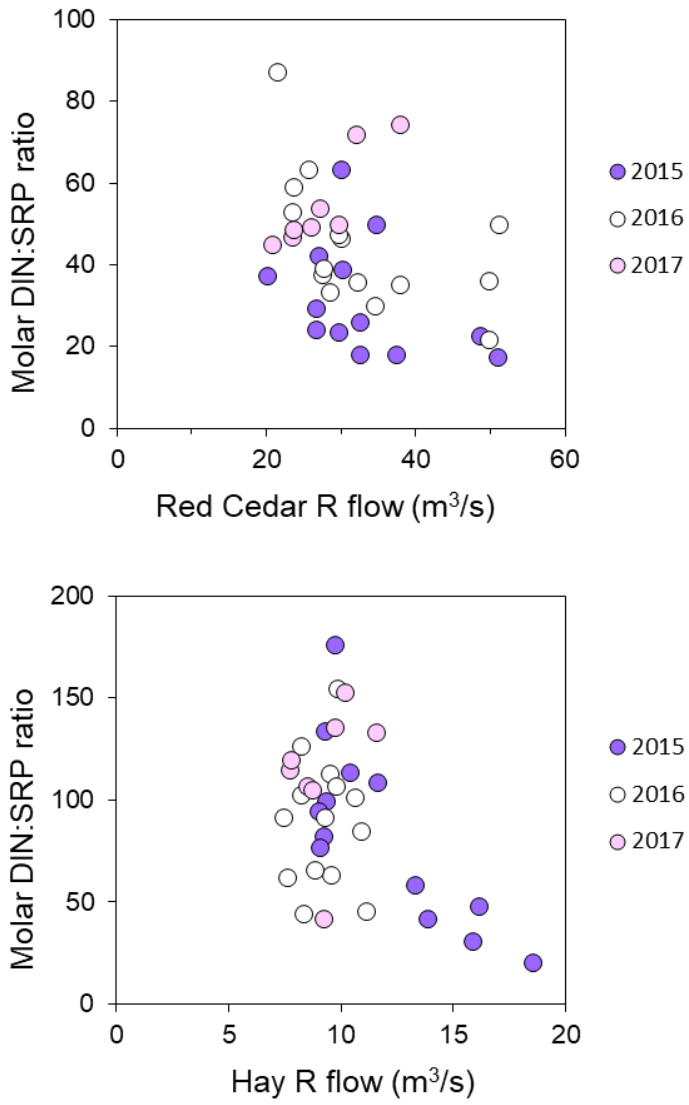

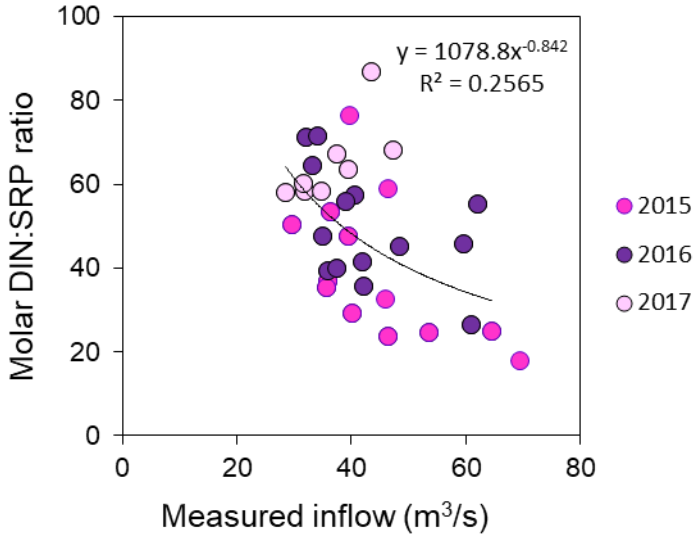

Figure 26. Relationships between mean daily flow and the molar dissolved inorganic nitrogen to soluble reactive phosphorus ratio (DIN:SRP) in the combined inflow (i.e., Red Cedar River at Colfax WI and the Hay River at Wheeler WI) during the summers of 2015-17. DIN = the sum of nitrate-nitrite-N and ammonium-N.

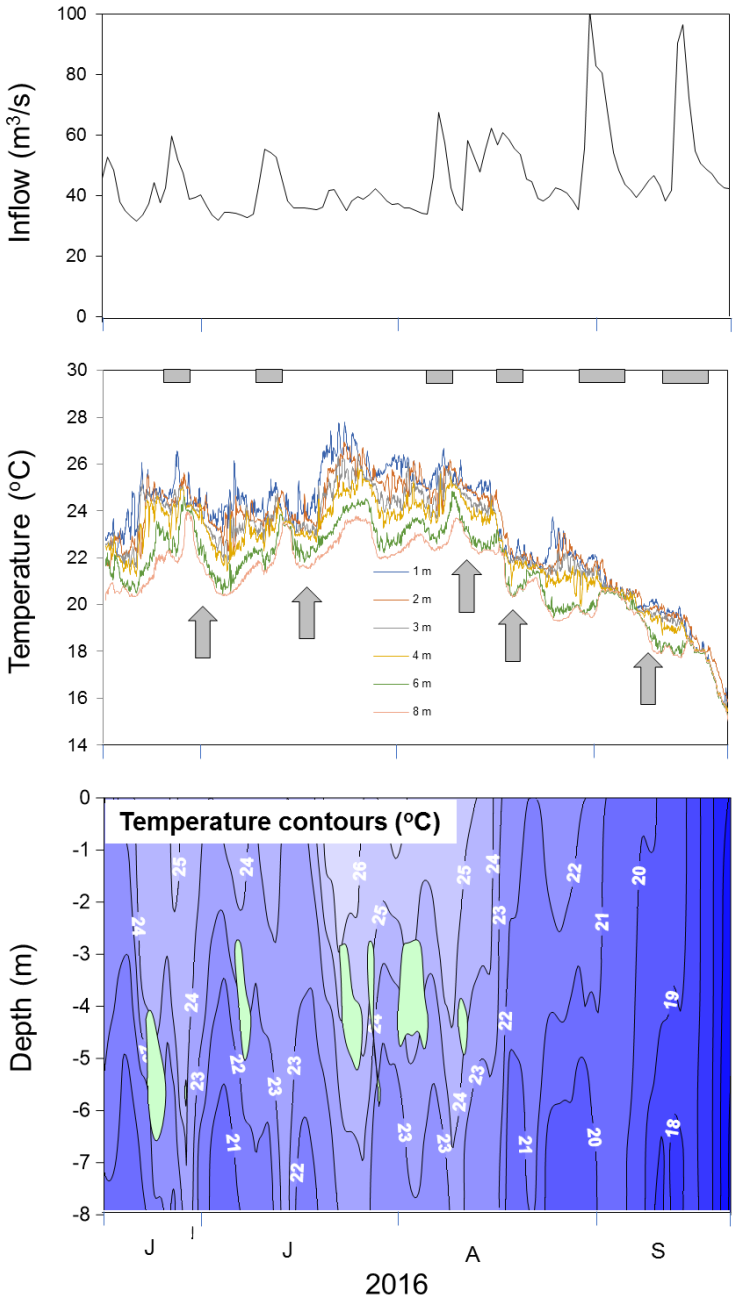

Figure 27. Seasonal variations in combined mean daily inflow (upper panel) versus water temperature at 1-m intervals (middle panel) and temperature contours (lower panel) in Tainter Lake at station TL 5 in 2016. Gray horizontal bars denote periods of elevated inflow while gray arrows represent periods of Hay River water intrusion into Tainter Lake as an underflow current. Green areas in the lower panel represent weak metalimnion development.

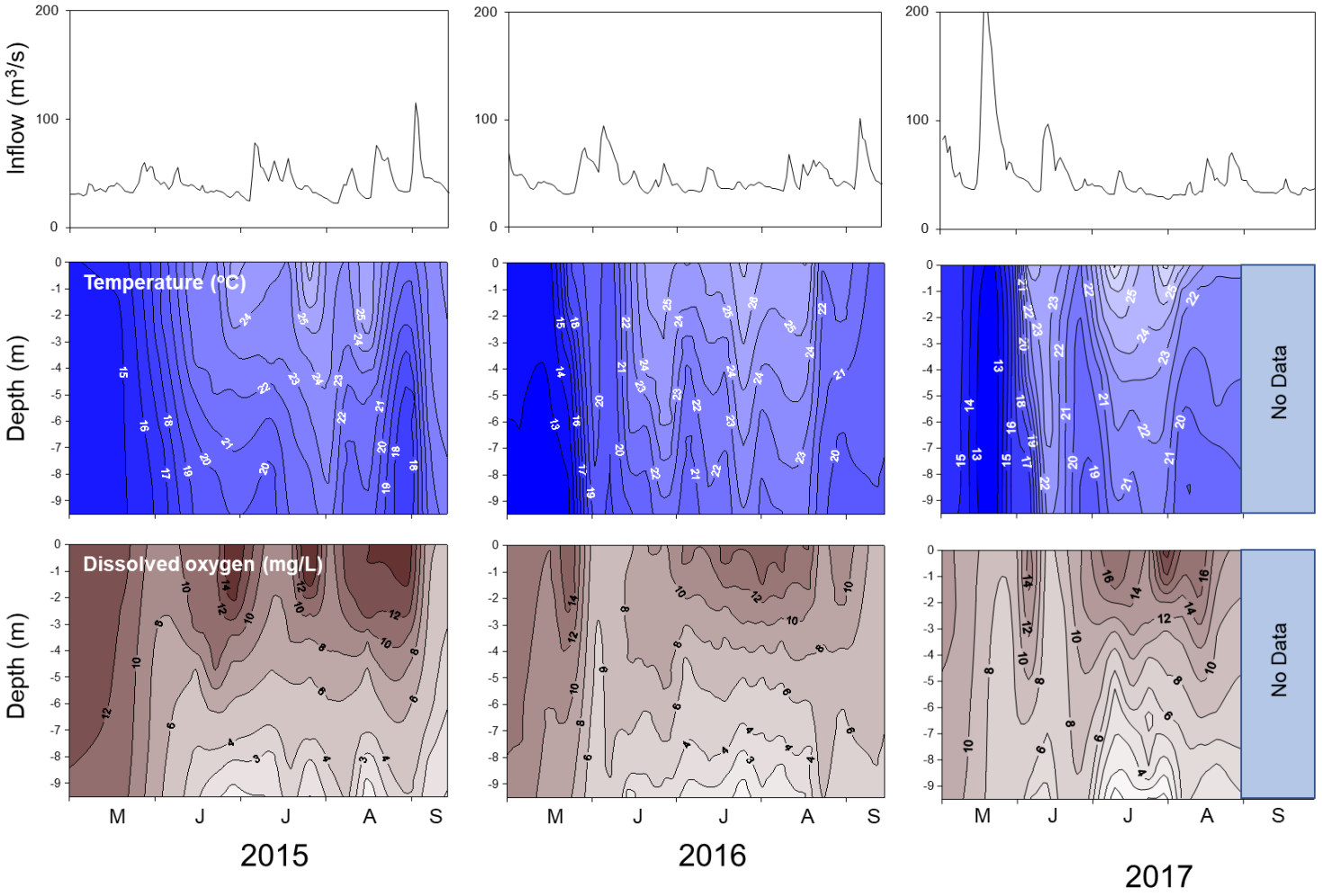

Figure 28. Seasonal variations in mean daily combined (i.e., Red Cedar and Hay Rivers) flow (upper panel) and seasonal and vertical variations in water temperature (middle panel) and dissolved oxygen (lower panel) at station TL 5 in Tainter Lake in 2015-17.

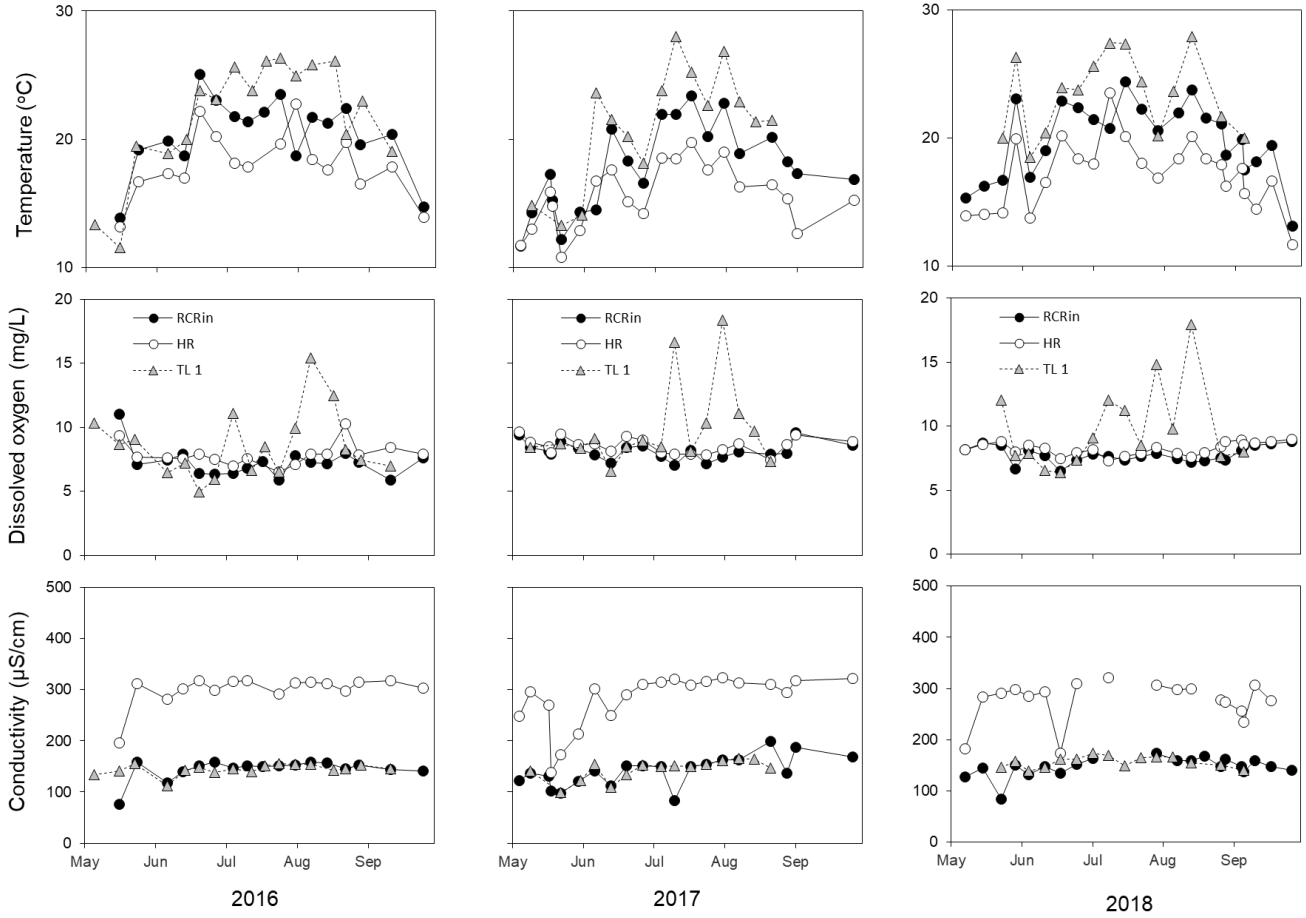

Figure 29. Seasonal variations in water temperature (upper panel), dissolved oxygen (middle panel), and conductivity (lower panel) in the Red Cedar River at Colfax, WI (RCR_{in}), the Hay River (HR), and station TL 1 in Tainter Lake in 2016-18.

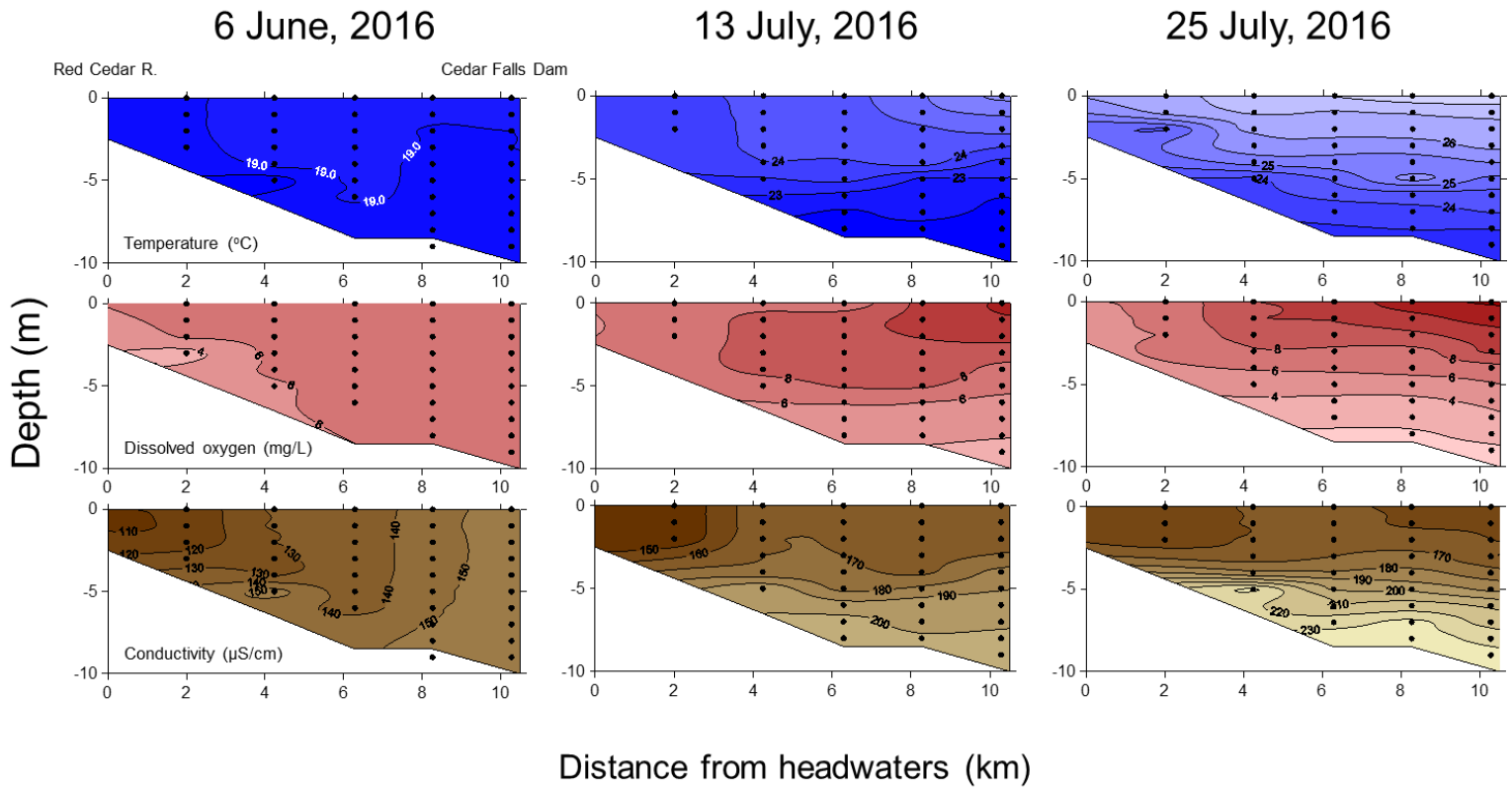

Figure 30. Longitudinal and vertical variations in water temperature, dissolved oxygen, and conductivity contours in Tainter Lake on selected dates in 2016.

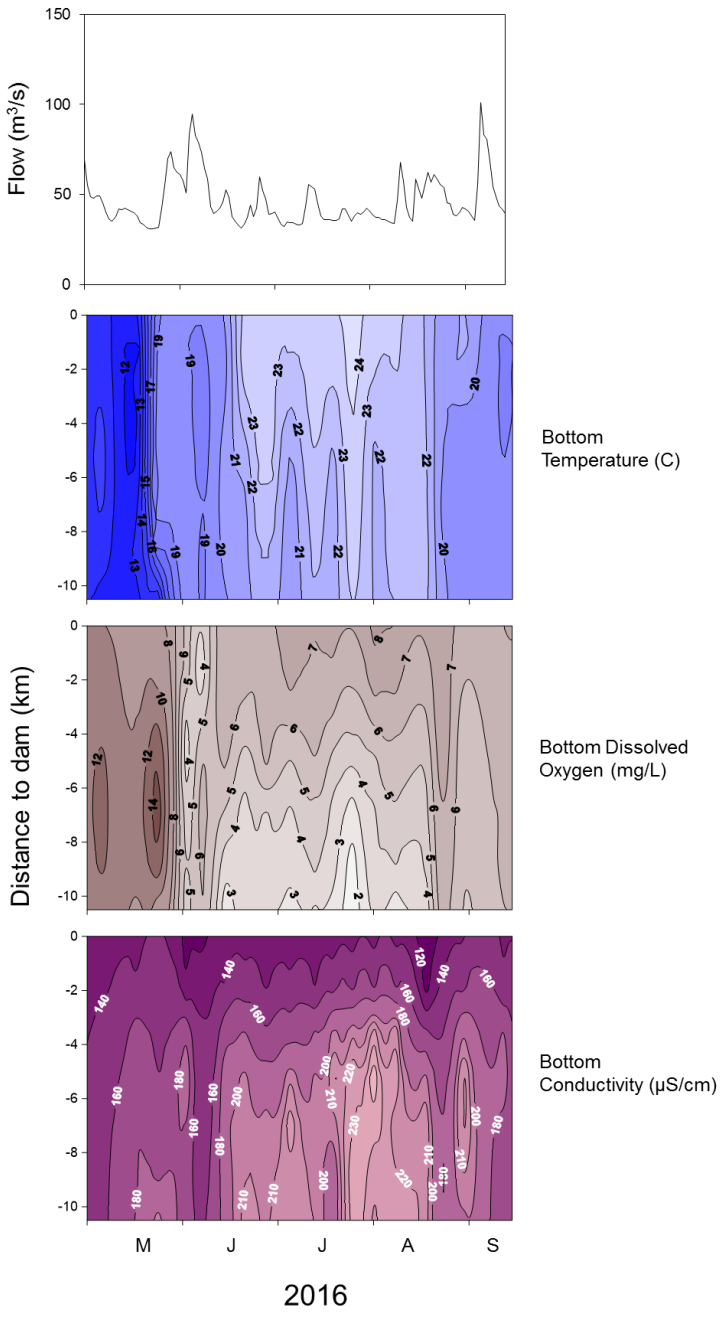

Figure 31. Seasonal variations in mean daily combined (i.e., Red Cedar and Hay Rivers) flow (upper panel) and seasonal and longitudinal variations in bottom water temperature (upper middle panel), bottom dissolved oxygen (lower middle panel), and bottom conductivity (lower panel) in Tainter Lake, 2016.

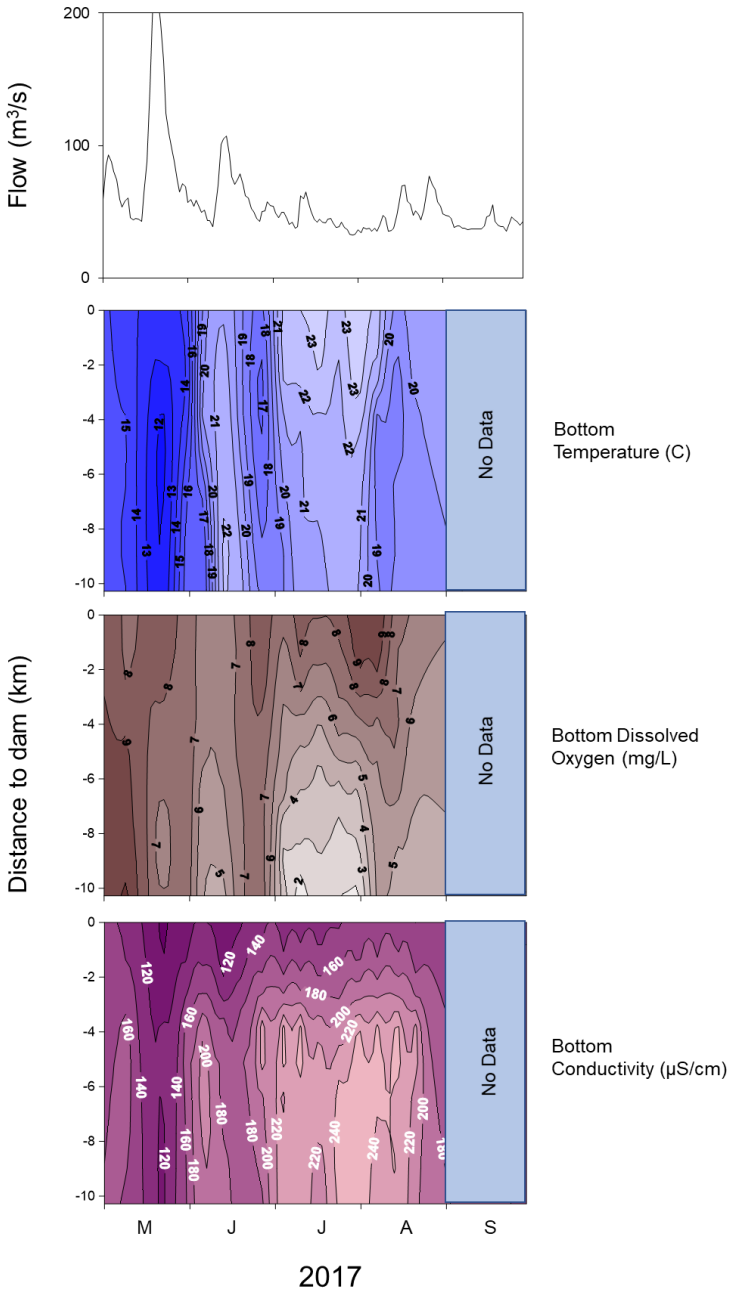

Figure 32. Seasonal variations in mean daily combined (i.e., Red Cedar and Hay Rivers) flow (upper panel) and seasonal and longitudinal variations in bottom water temperature (upper middle panel), bottom dissolved oxygen (lower middle panel), and bottom conductivity (lower panel) in Tainter Lake, 2017.

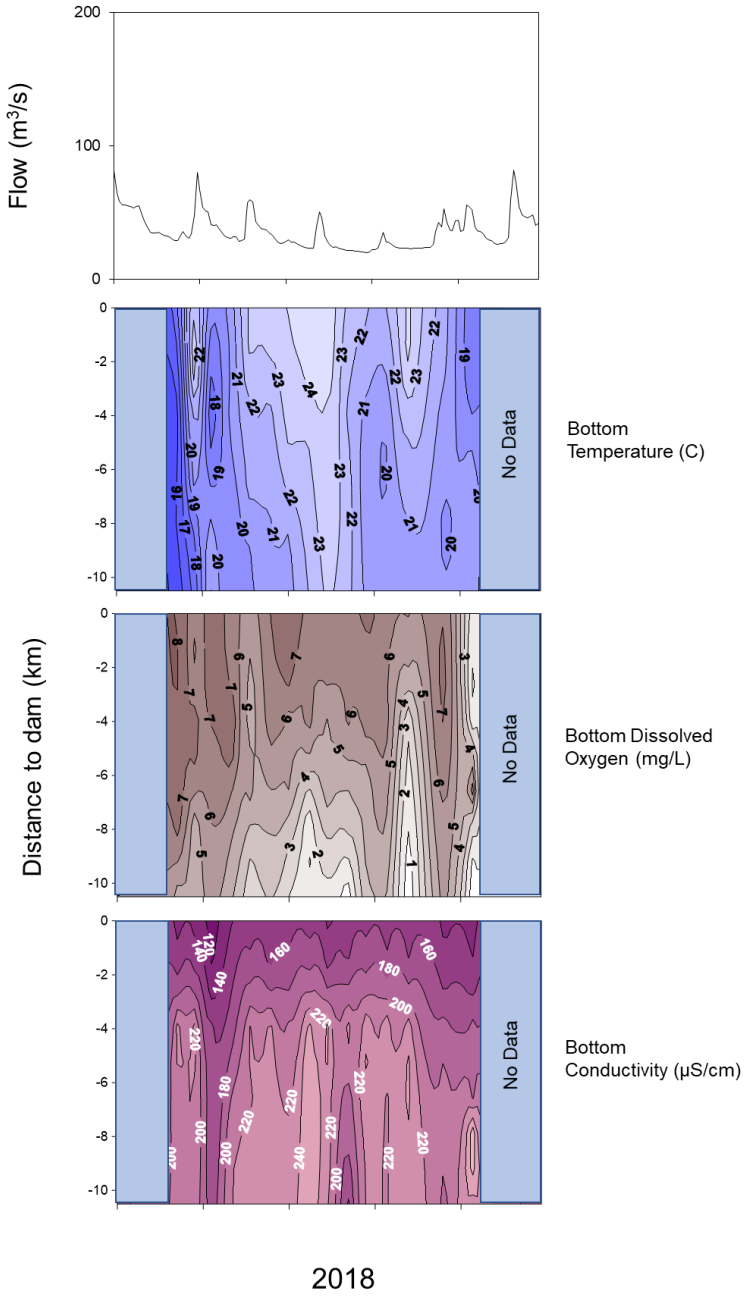

Figure 33. Seasonal variations in mean daily combined (i.e., Red Cedar and Hay Rivers) flow (upper panel) and seasonal and longitudinal variations in bottom water temperature (upper middle panel), bottom dissolved oxygen (lower middle panel), and bottom conductivity (lower panel) in Tainter Lake, 2018.

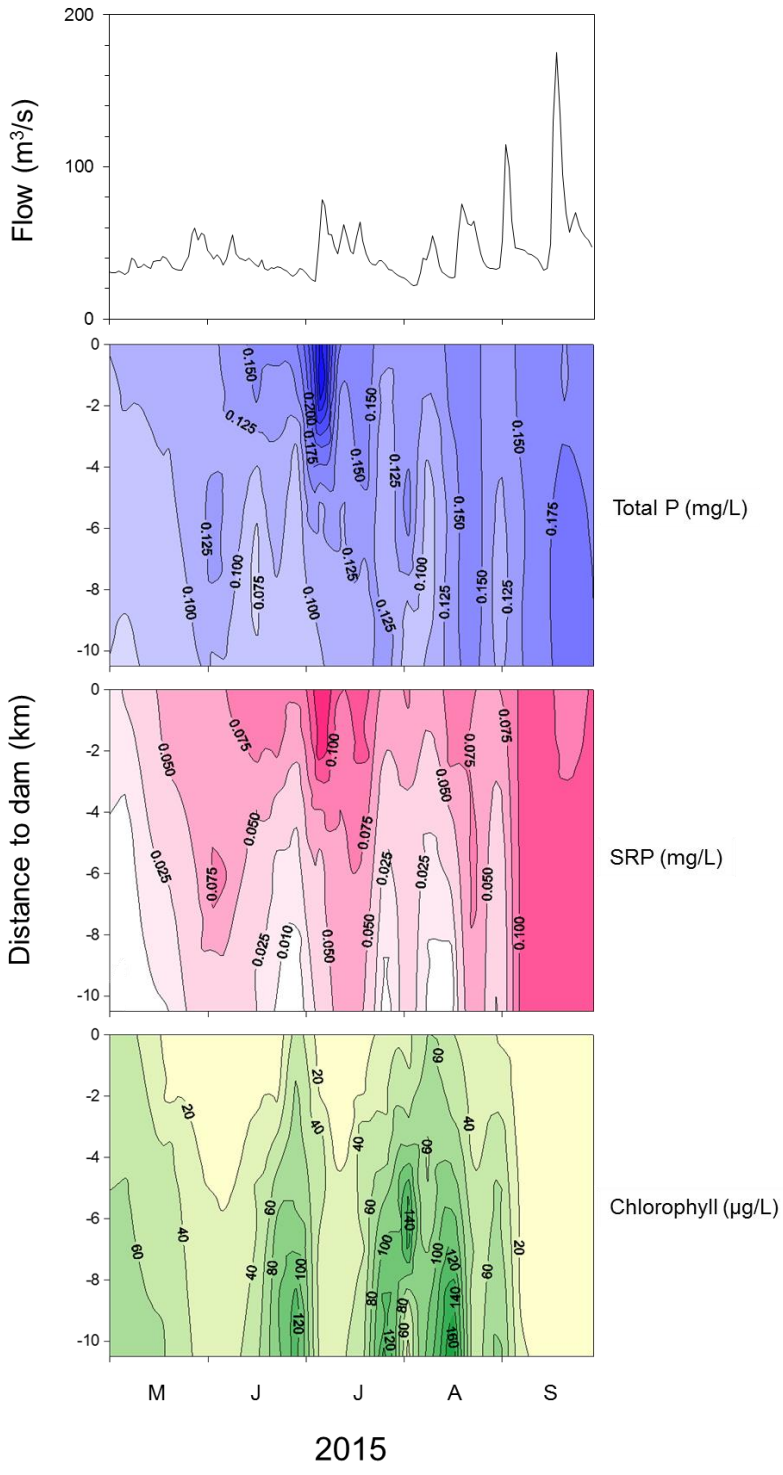

Figure 34. Seasonal variations in mean daily combined (i.e., Red Cedar and Hay Rivers) flow (upper panel) and seasonal and longitudinal variations in surface total phosphorus (P, upper middle panel), surface soluble reactive P (SRP, lower middle panel), and surface chlorophyll (lower panel) in Tainter Lake, 2015.

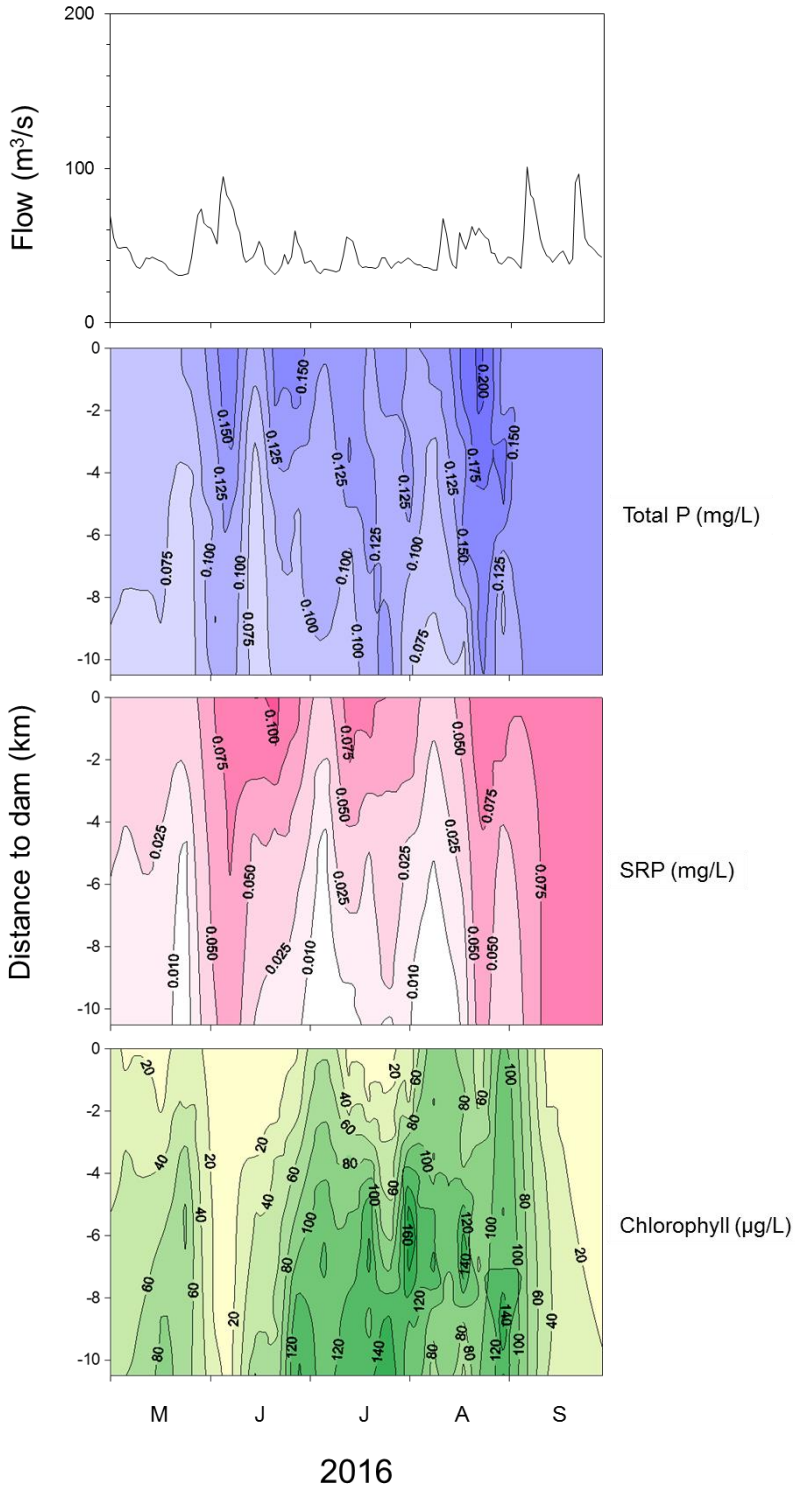

Figure 35. Seasonal variations in mean daily combined (i.e., Red Cedar and Hay Rivers) flow (upper panel) and seasonal and longitudinal variations in surface total phosphorus (P, upper middle panel), surface soluble reactive P (SRP, lower middle panel), and surface chlorophyll (lower panel) in Tainter Lake, 2016.

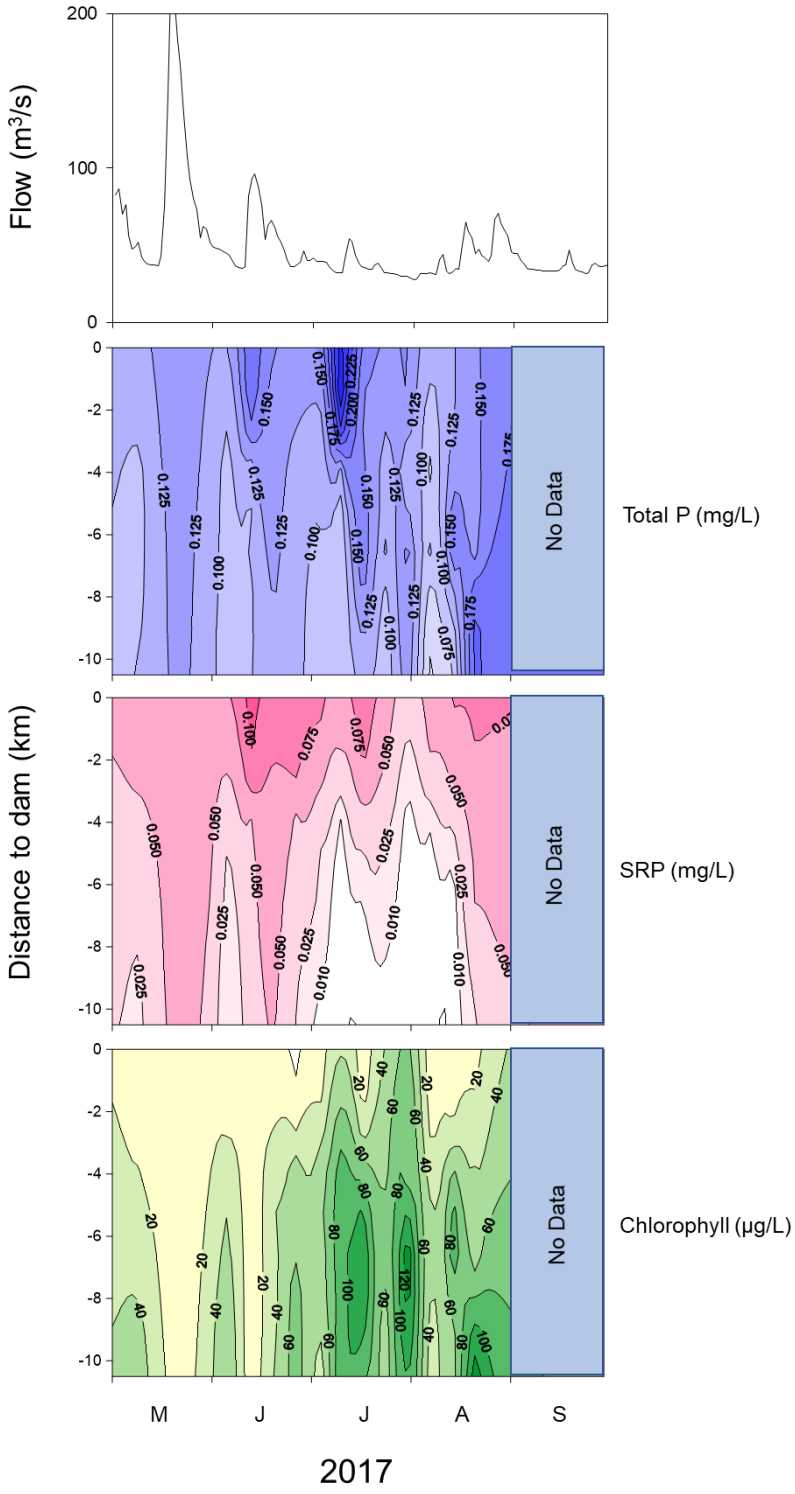

Figure 36. Seasonal variations in mean daily combined (i.e., Red Cedar and Hay Rivers) flow (upper panel) and seasonal and longitudinal variations in surface total phosphorus (P, upper middle panel), surface soluble reactive P (SRP, lower middle panel), and surface chlorophyll (lower panel) in Tainter Lake, 2017.

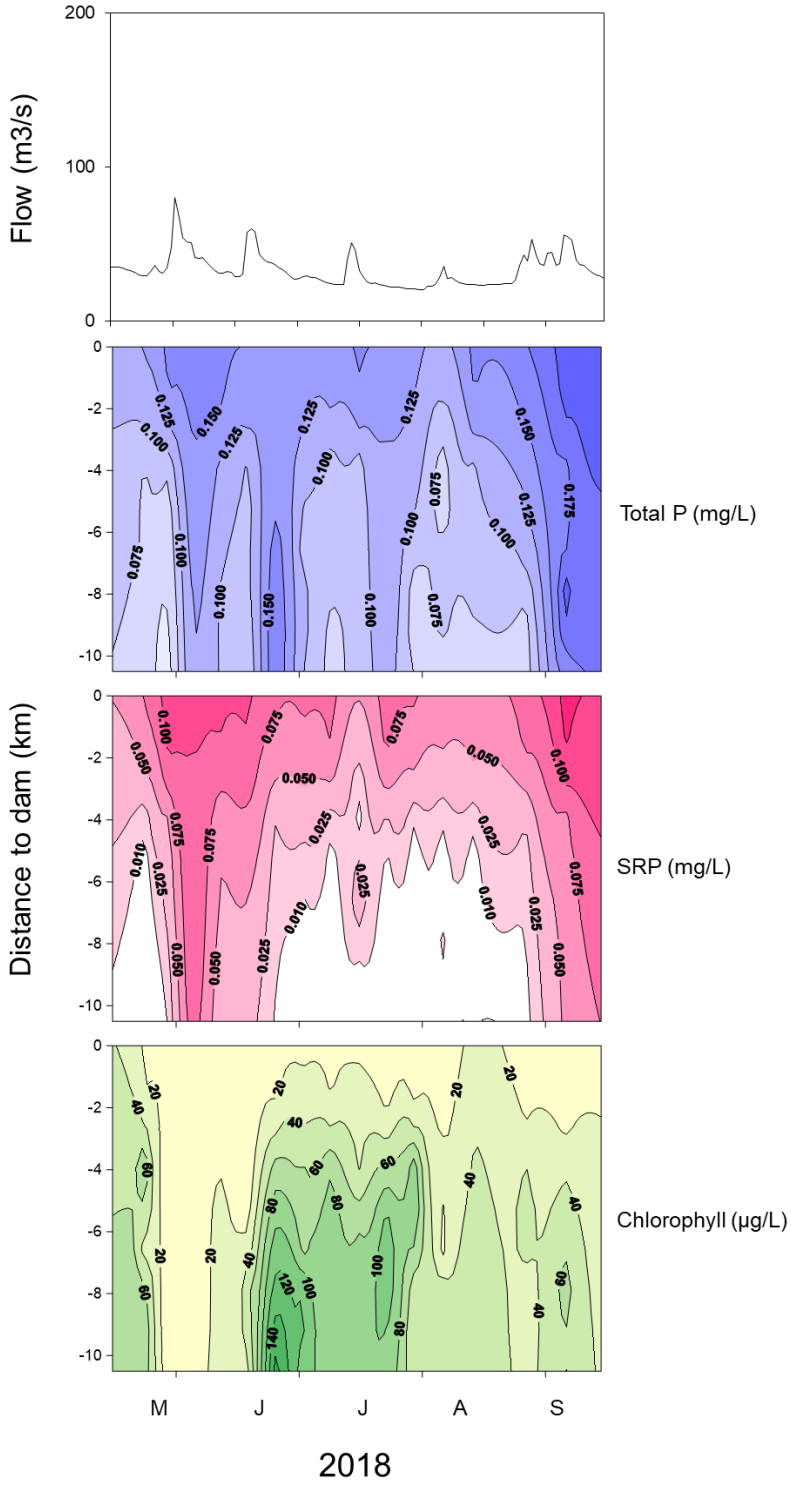

Figure 37. Seasonal variations in mean daily combined (i.e., Red Cedar and Hay Rivers) flow (upper panel) and seasonal and longitudinal variations in surface total phosphorus (P, upper middle panel), surface soluble reactive P (SRP, lower middle panel), and surface chlorophyll (lower panel) in Tainter Lake, 2018.

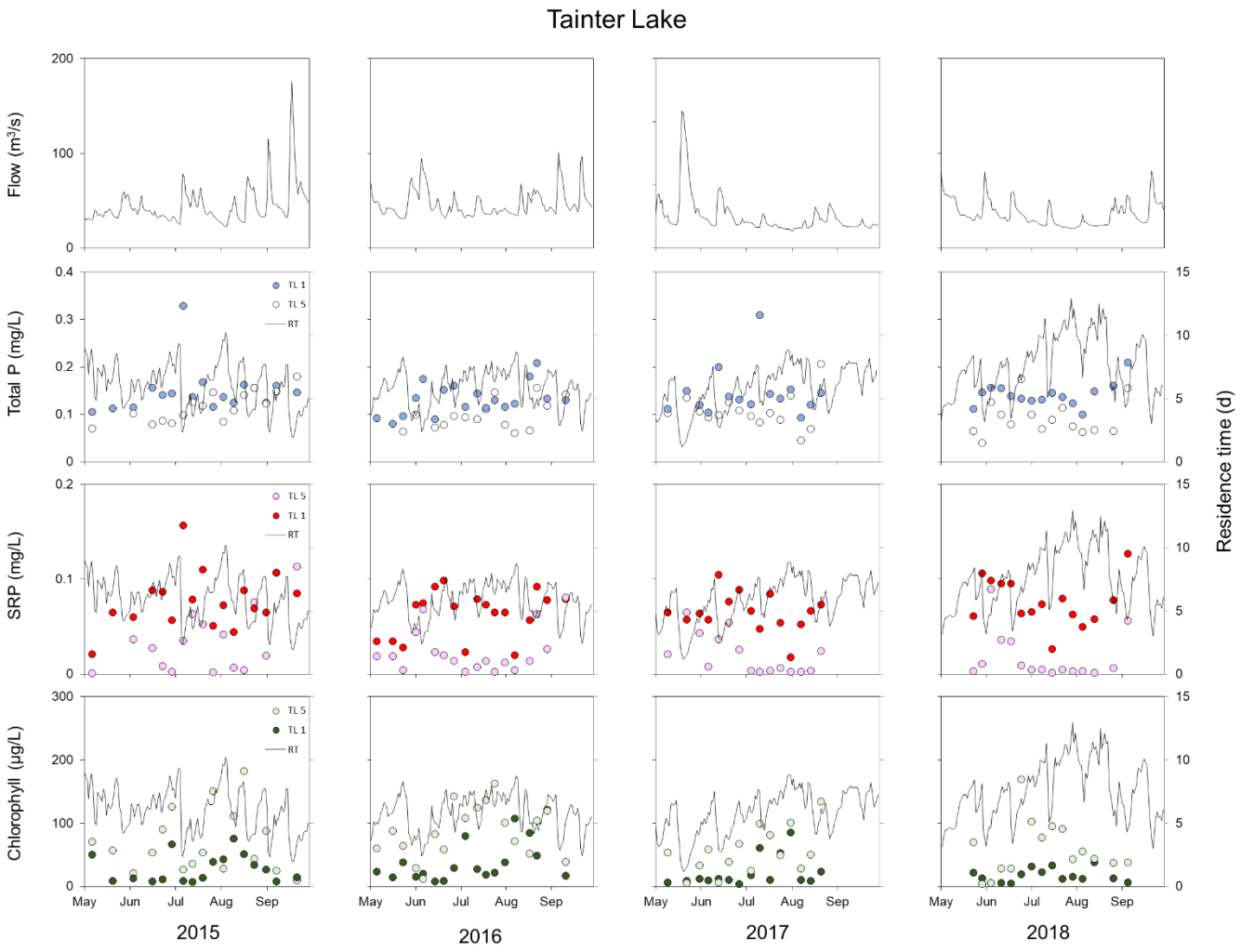

Figure 38. Seasonal variations in mean daily combined (i.e., Red Cedar and Hay Rivers) flow, residence time (RT), surface total phosphorus (P), surface soluble reactive P (SRP), and surface chlorophyll at station TL 1 (headwaters) and TL 5 (near dam) in Tainter Lake in 2015-18.

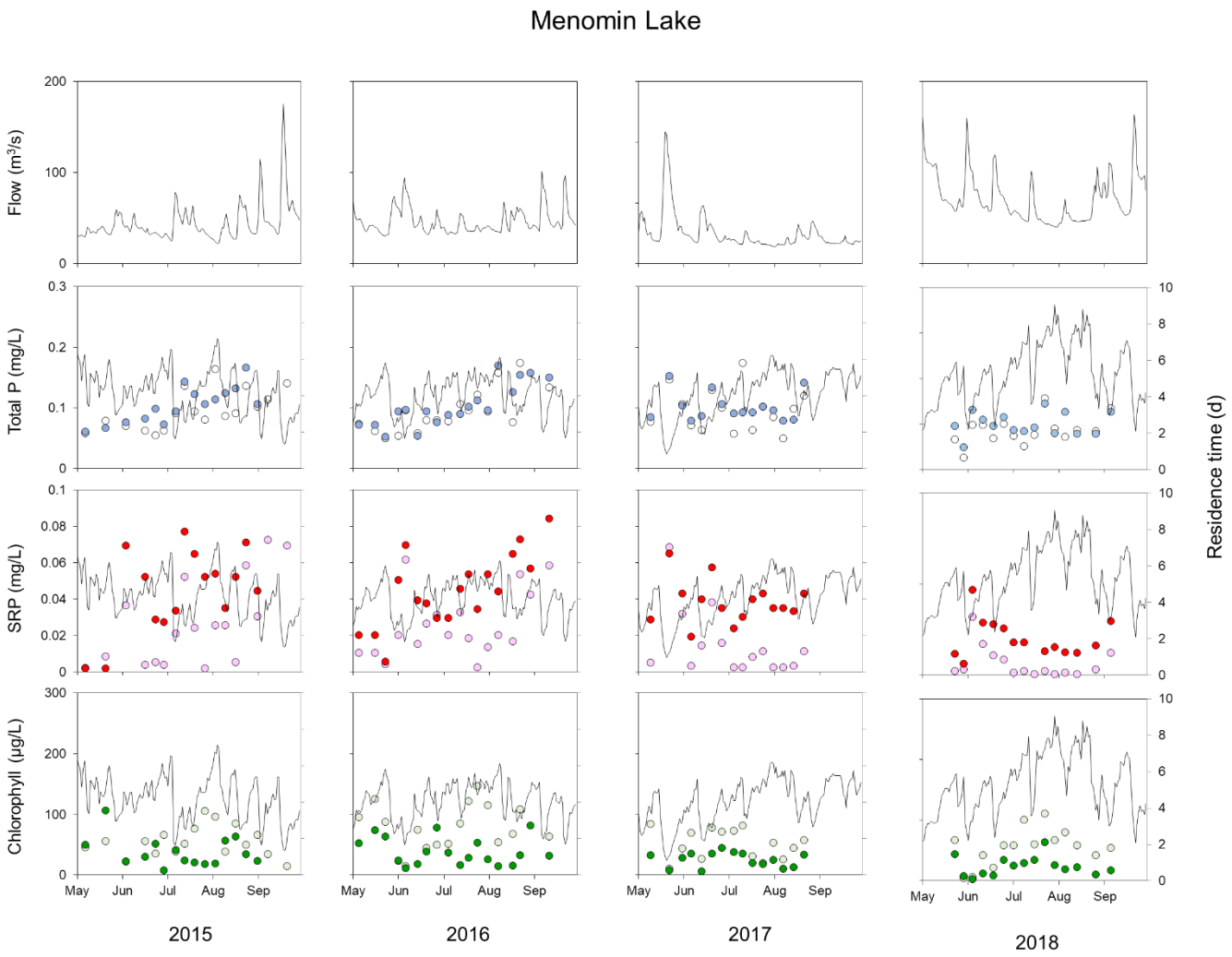

Figure 39. Seasonal variations in mean daily combined (i.e., Red Cedar and Hay Rivers) flow, residence time (RT), surface total phosphorus (P), surface soluble reactive P (SRP), and surface chlorophyll at station ML 1 (headwaters) and ML 5 (near dam) in Menomin Lake in 2015-18.

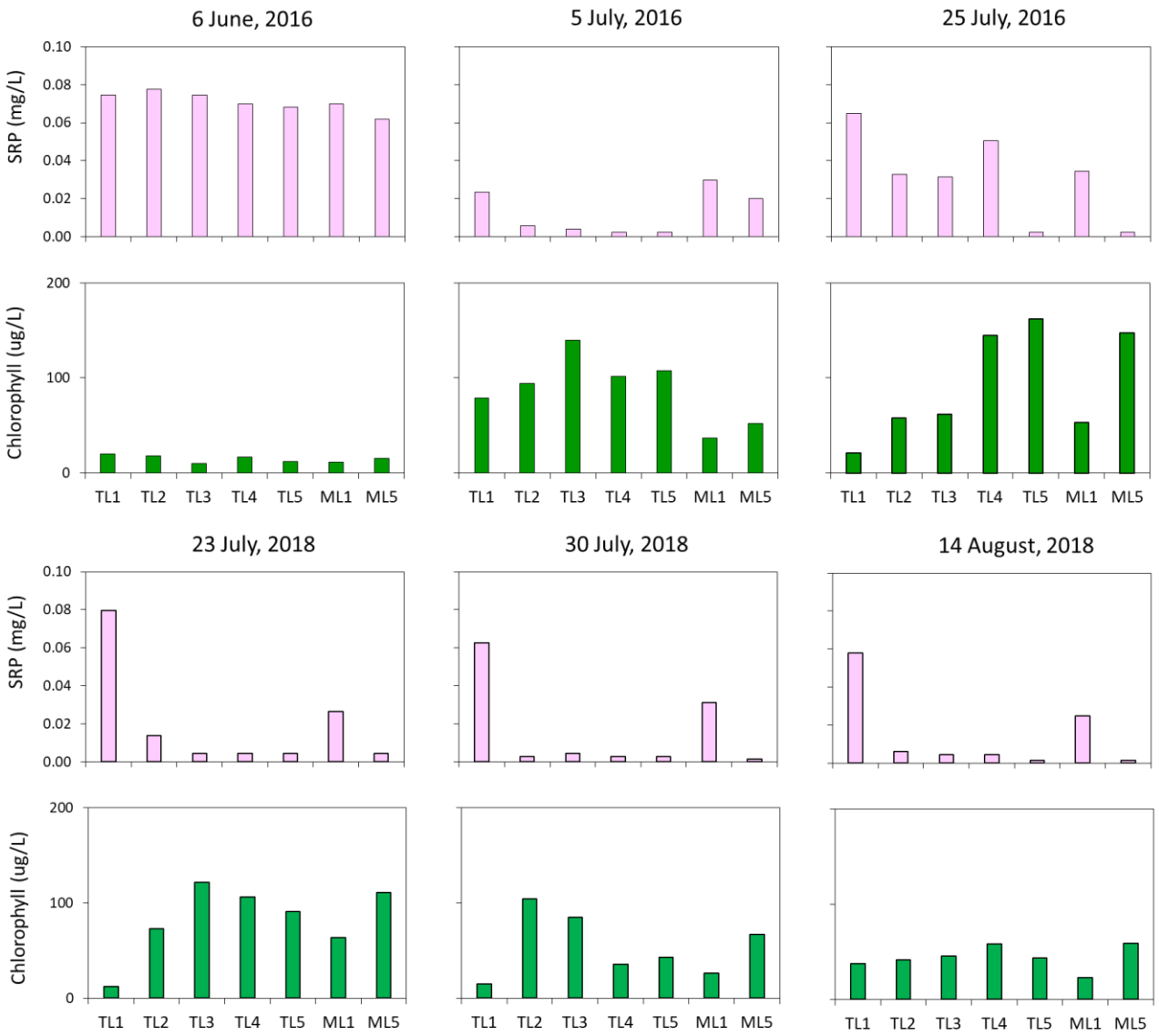

Figure 40. Longitudinal variations in soluble reactive phosphorus (SRP) and chlorophyll on selected dates in 2016 and 2018.

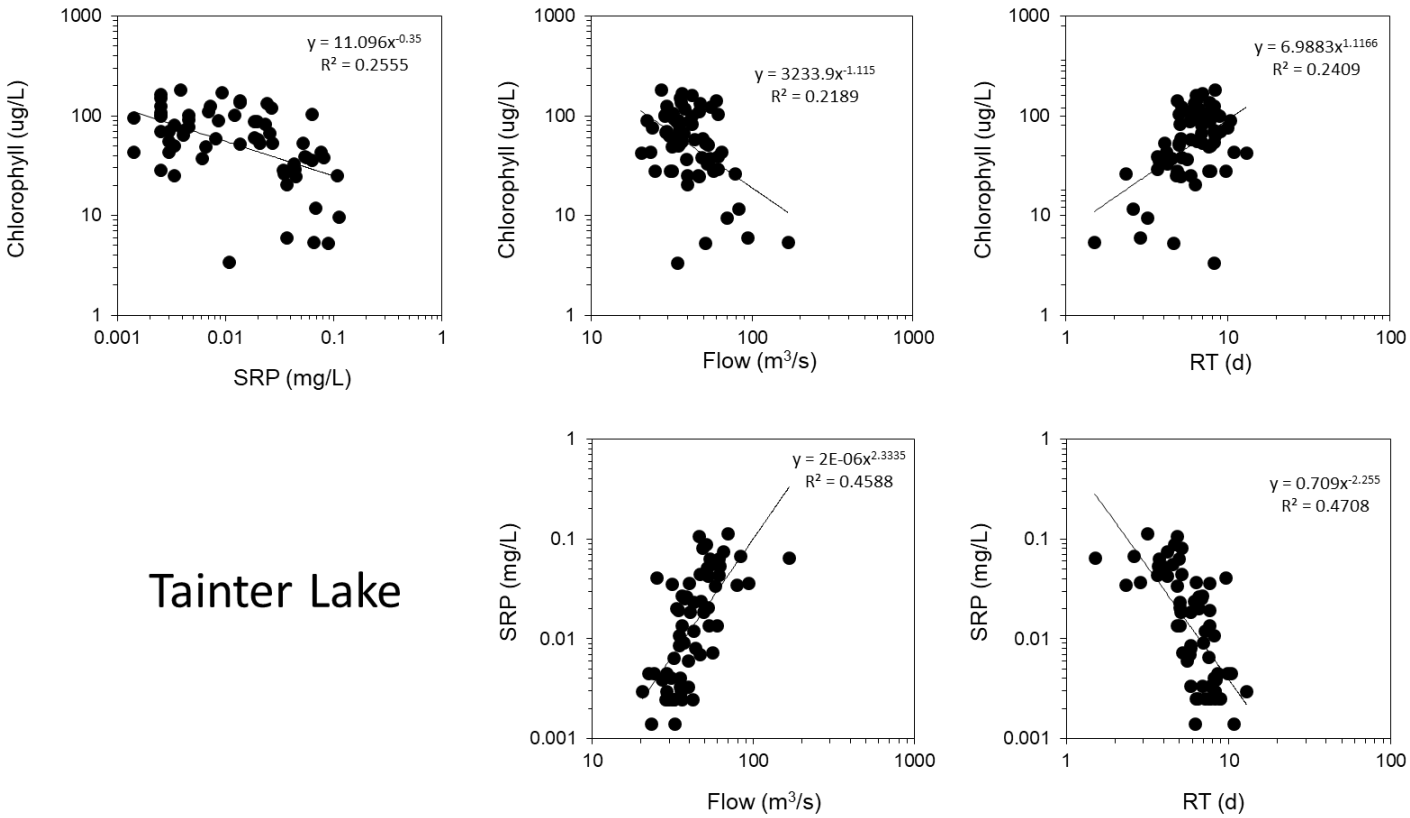

Figure 41. Log-log relationships between soluble reactive phosphorus (SRP) and chlorophyll from station TL 5, combined inflow from the Red Cedar and Hay Rivers, and the residence time (RT) of Tainter Lake.

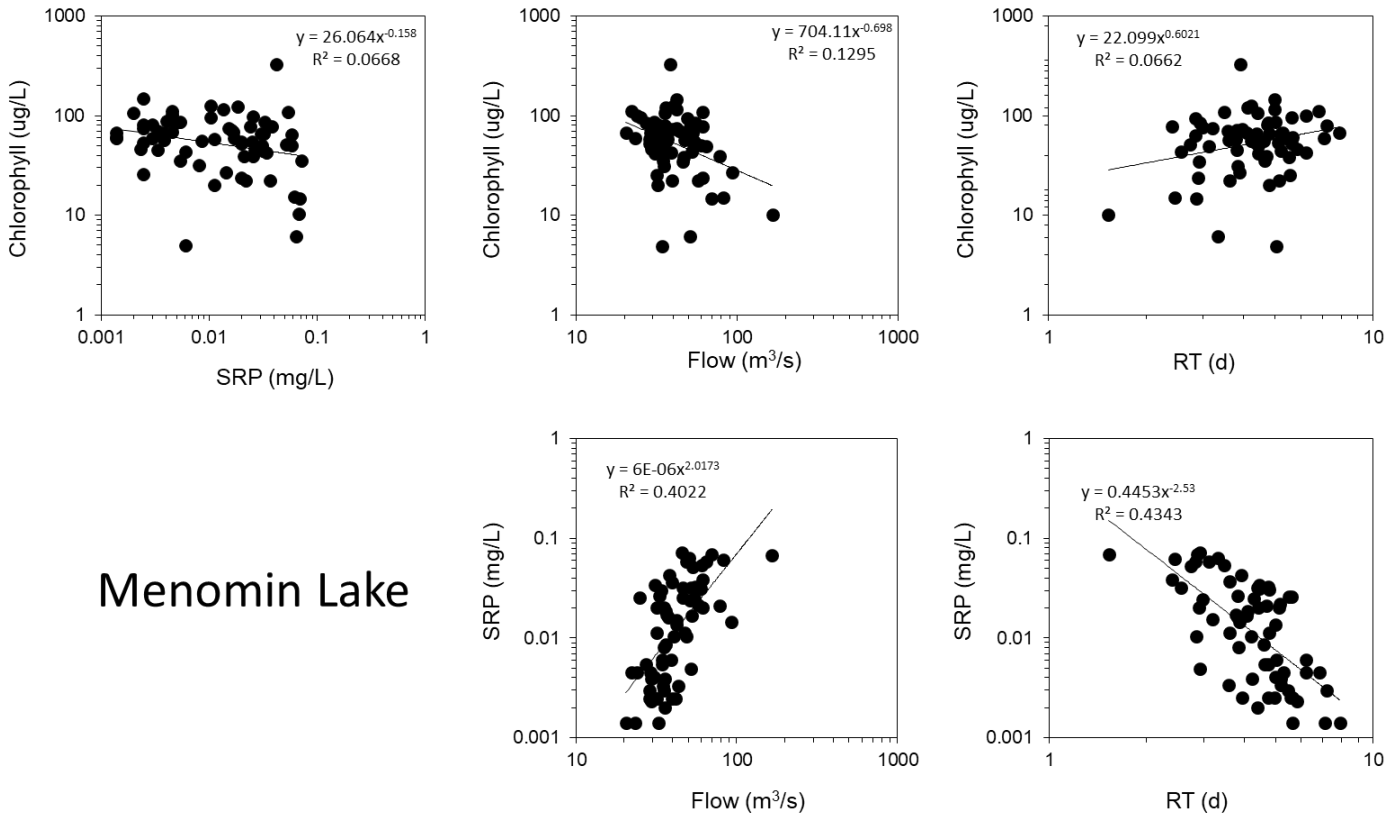

Figure 42. Log-log relationships between soluble reactive phosphorus (SRP) and chlorophyll from station ML 5, combined inflow from the Red Cedar and Hay Rivers, and the residence time (RT) of Menomin Lake.

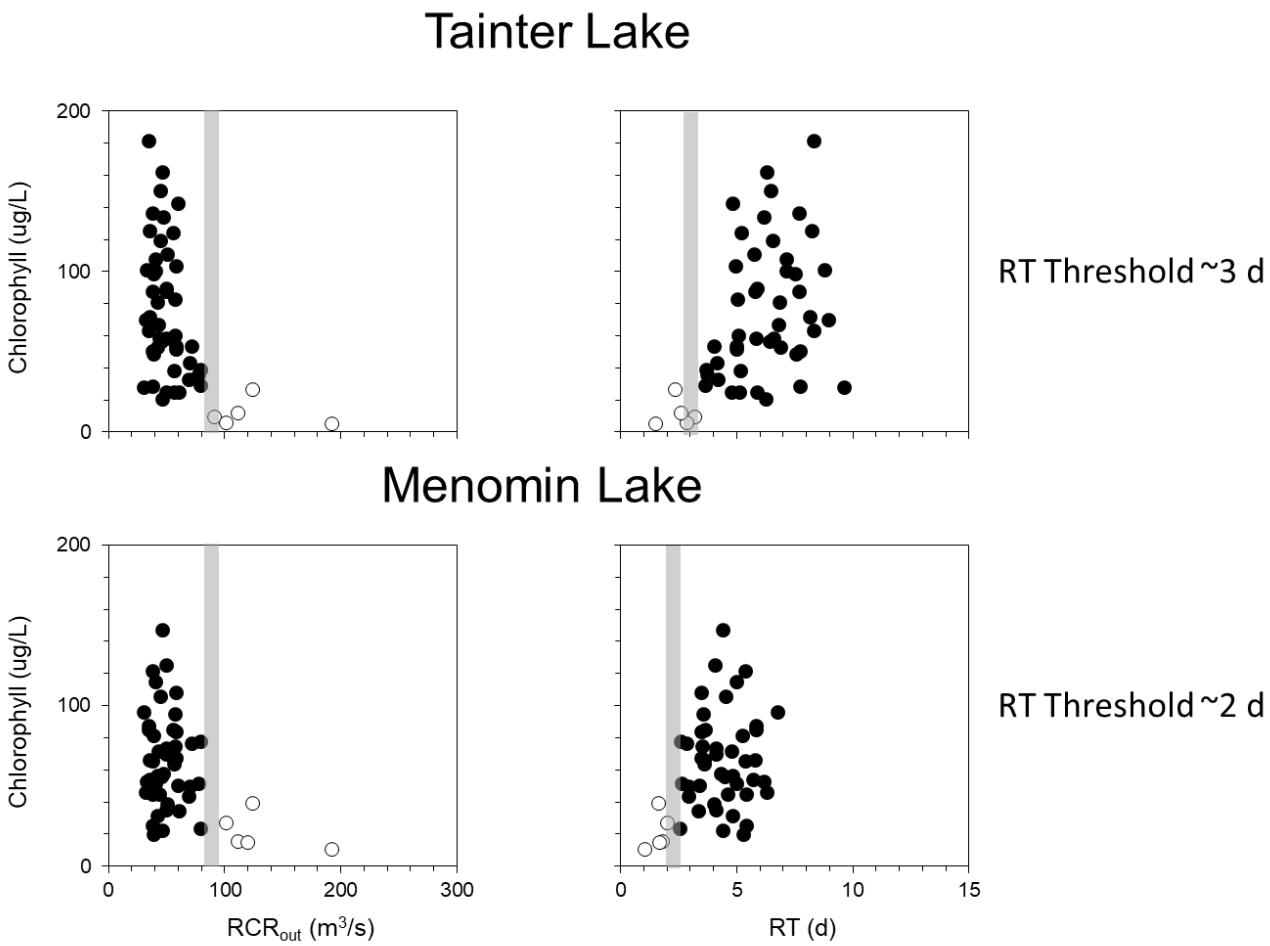

Figure 43. Qualitative relationships between flow for the Red Cedar River at Menomonie, WI (RCR_{out}) or theoretical residence time (RT) and chlorophyll concentration at TL 5 in Tainter Lake (upper panels) and Menomin Lake (lower panels). Trends suggested that blooms develop as RT increases to > 3 d in Tainter Lake and > 2 d in Menomin Lake (gray bar).

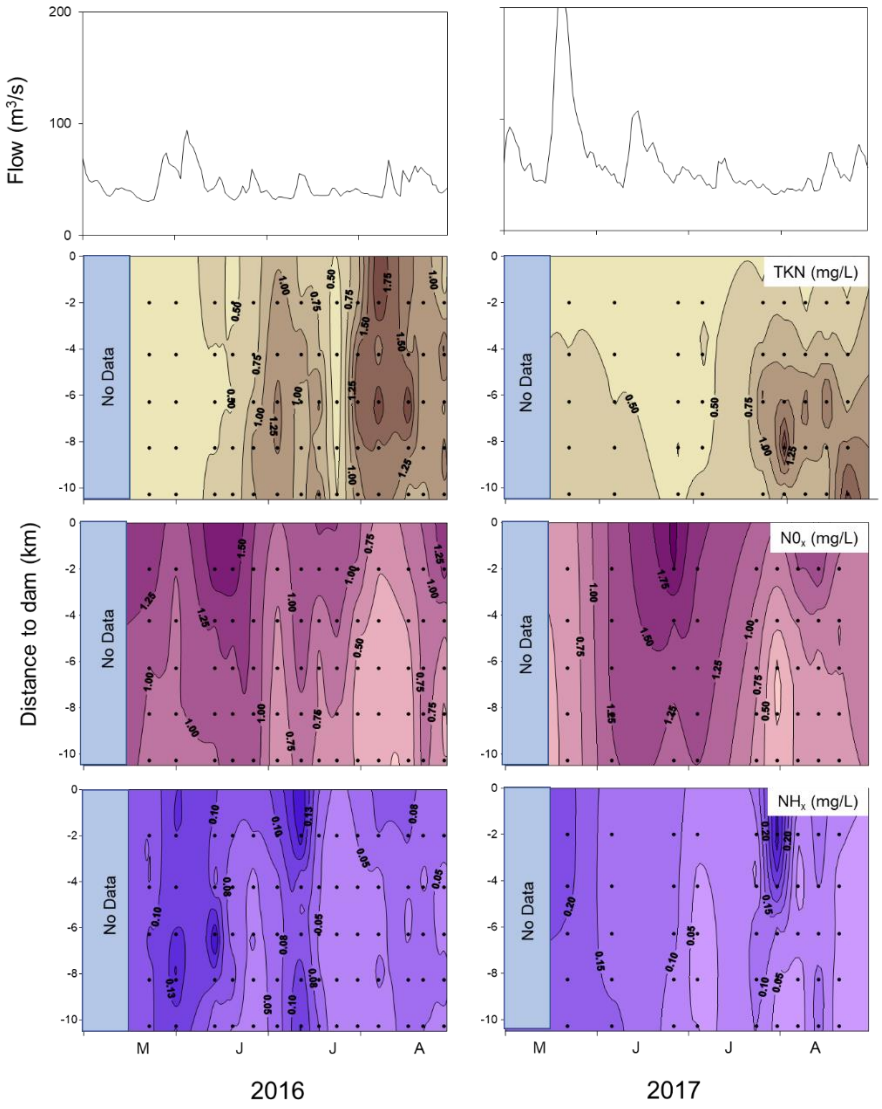

Figure 44. Seasonal variations in mean daily combined (i.e., Red Cedar and Hay Rivers) flow (upper panel) and seasonal and longitudinal variations in surface total Kjeldahl nitrogen (TKN, upper middle panel), surface nitrate-nitrite N (NO_x, lower middle panel), and surface ammonium-nitrogen (NH_x, lower panel) in Tainter Lake, 2016-17.

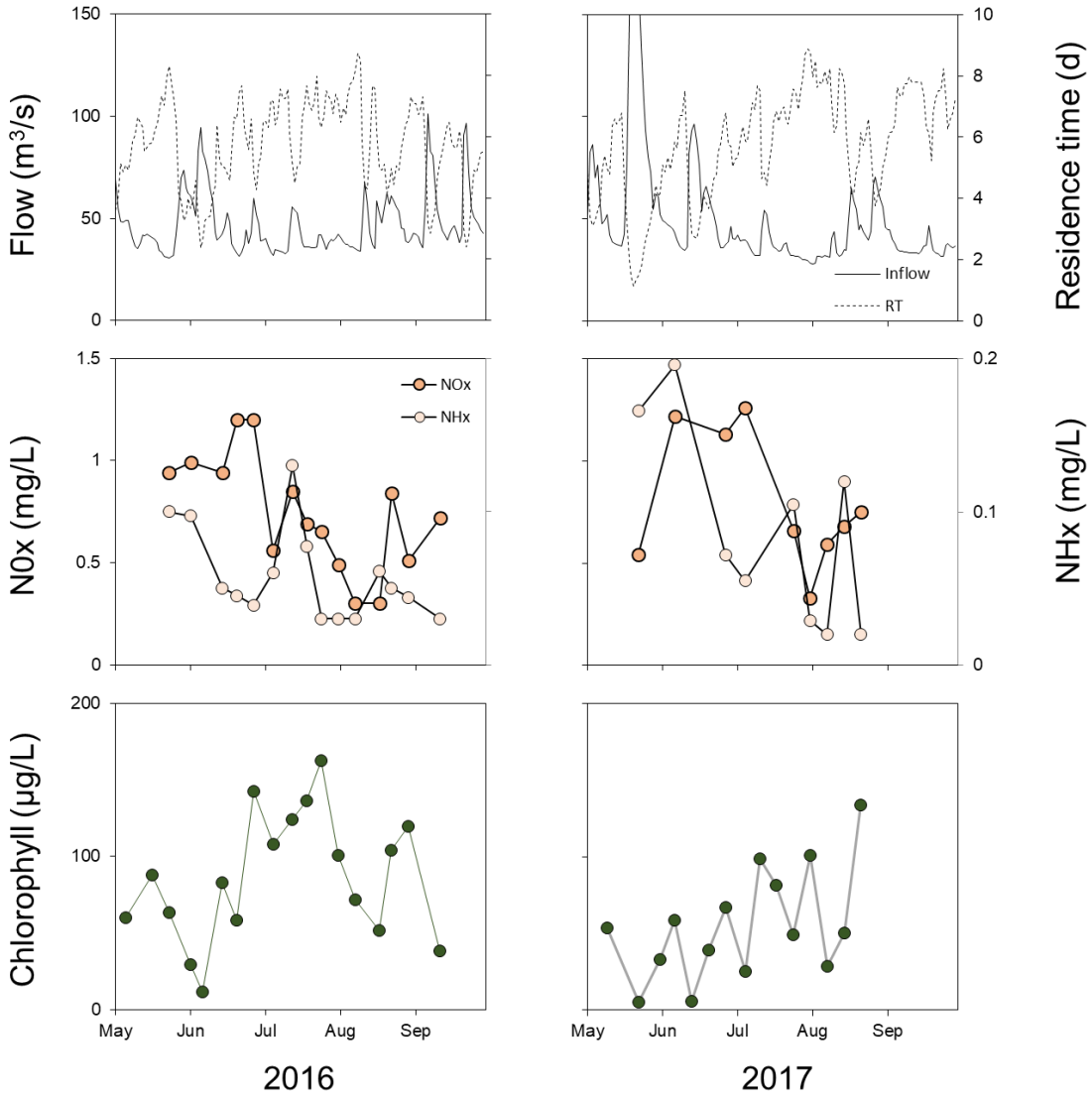

Figure 45. Seasonal variations in mean daily combined (i.e., Red Cedar and Hay Rivers) flow and Tainter Lake residence time (upper panel), Surface nitrate-nitrite nitrogen (NO_x) and ammonium-nitrogen (NH_x, middle panel) and chlorophyll (lower panel) at station TL 5 in 2016-17.

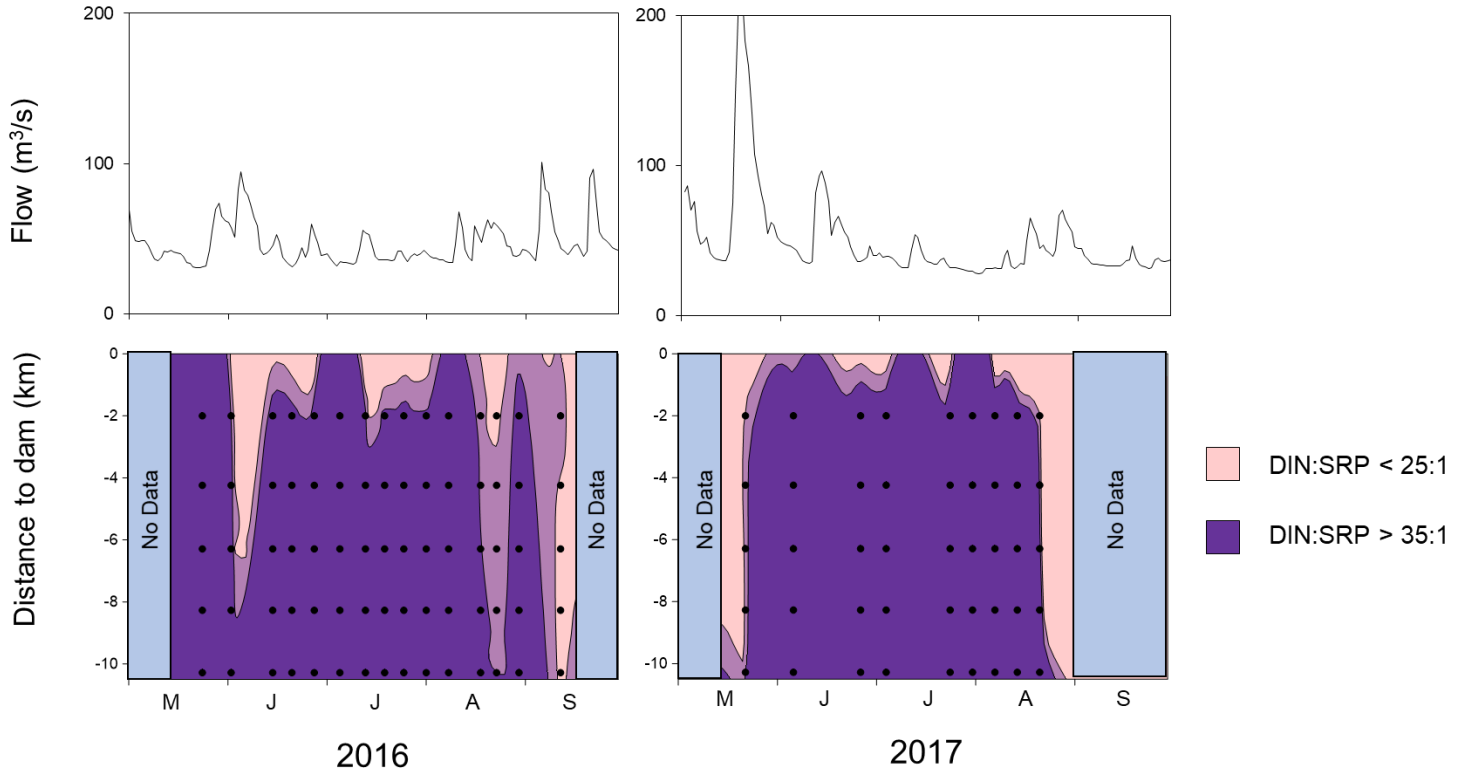

Figure 46. Seasonal variations in mean daily combined (i.e., Red Cedar and Hay Rivers) flow (upper panel) and seasonal and longitudinal variations in surface molar dissolved inorganic nitrogen:soluble reactive phosphorus (DIN:SRP) ratio (middle and lower panels) in Tainter Lake, 2016-17. In the lower panel, the pink areas denote potential N limitation and the purple areas indicate potential phosphorus limitation of cyanobacteria growth.

Figure 47. A comparison of seasonal variations in combined mean daily inflow and Tainter Lake residence time versus soluble reactive phosphorus (P) , chlorophyll, molar dissolved inorganic nitrogen:soluble reactive phosphorus (DIN:SRP) ratio, alkaline phosphatase activity (APA), and biomass specific APA at station TL 5 in Tainter Lake, 2016.

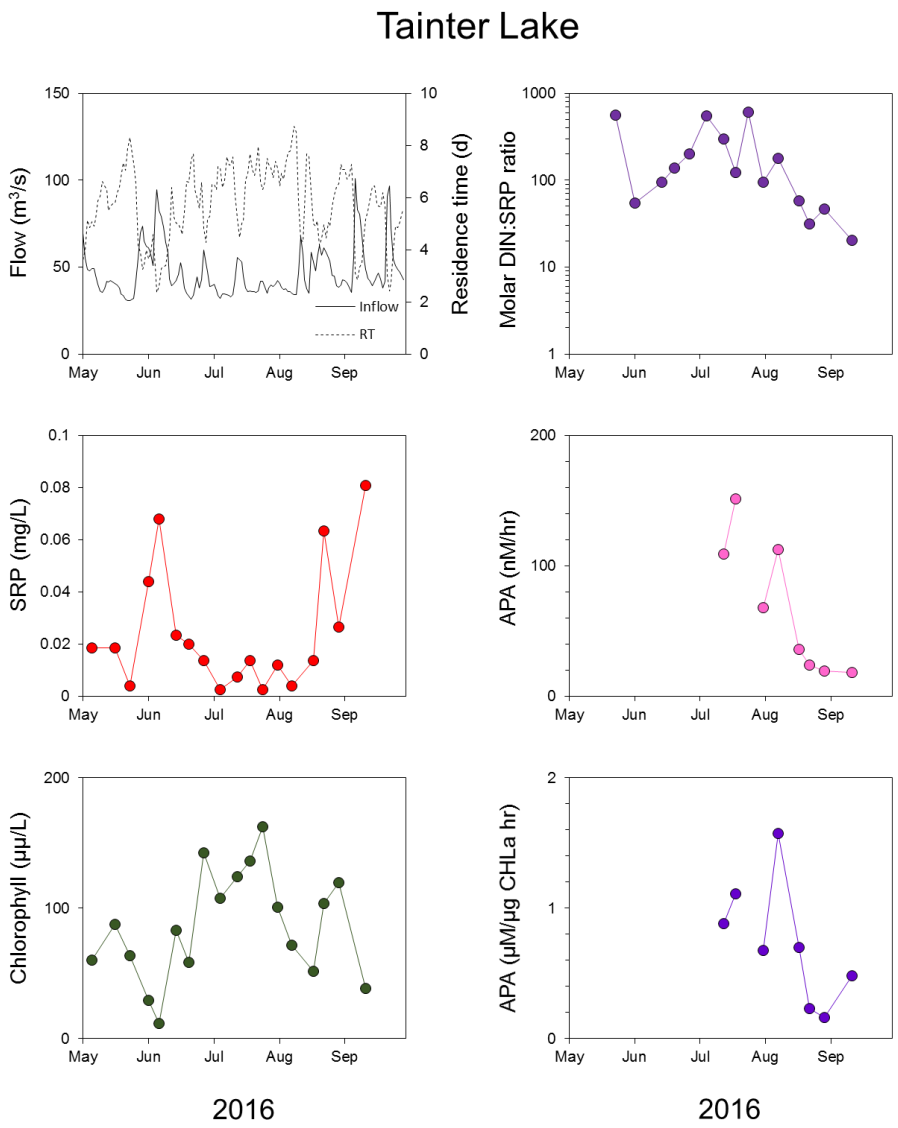

Figure 48. A comparison of seasonal variations in combined mean daily inflow and Menomin Lake residence time versus soluble reactive phosphorus (P), chlorophyll, molar dissolved inorganic nitrogen:soluble reactive phosphorus (DIN:SRP) ratio, alkaline phosphatase activity (APA), and biomass specific APA at station ML 5 in Menomin Lake, 2016.

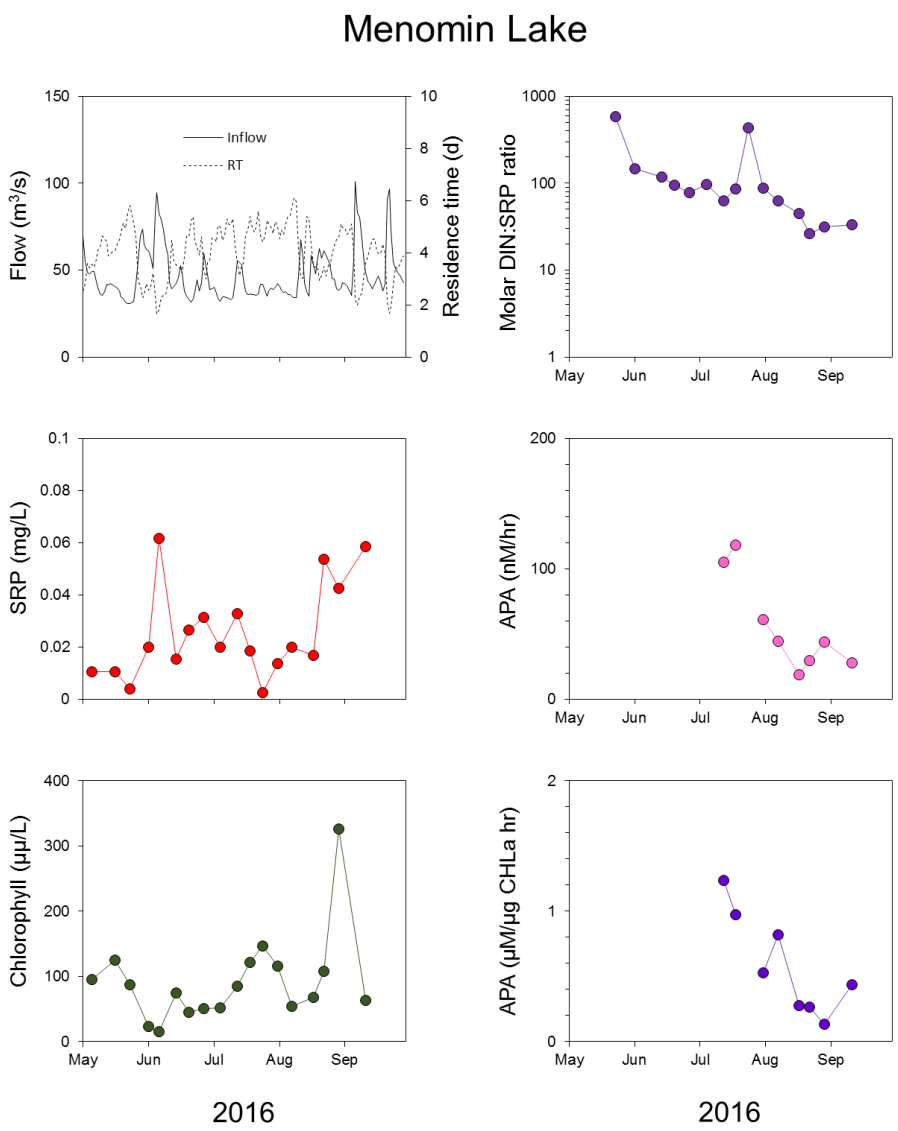

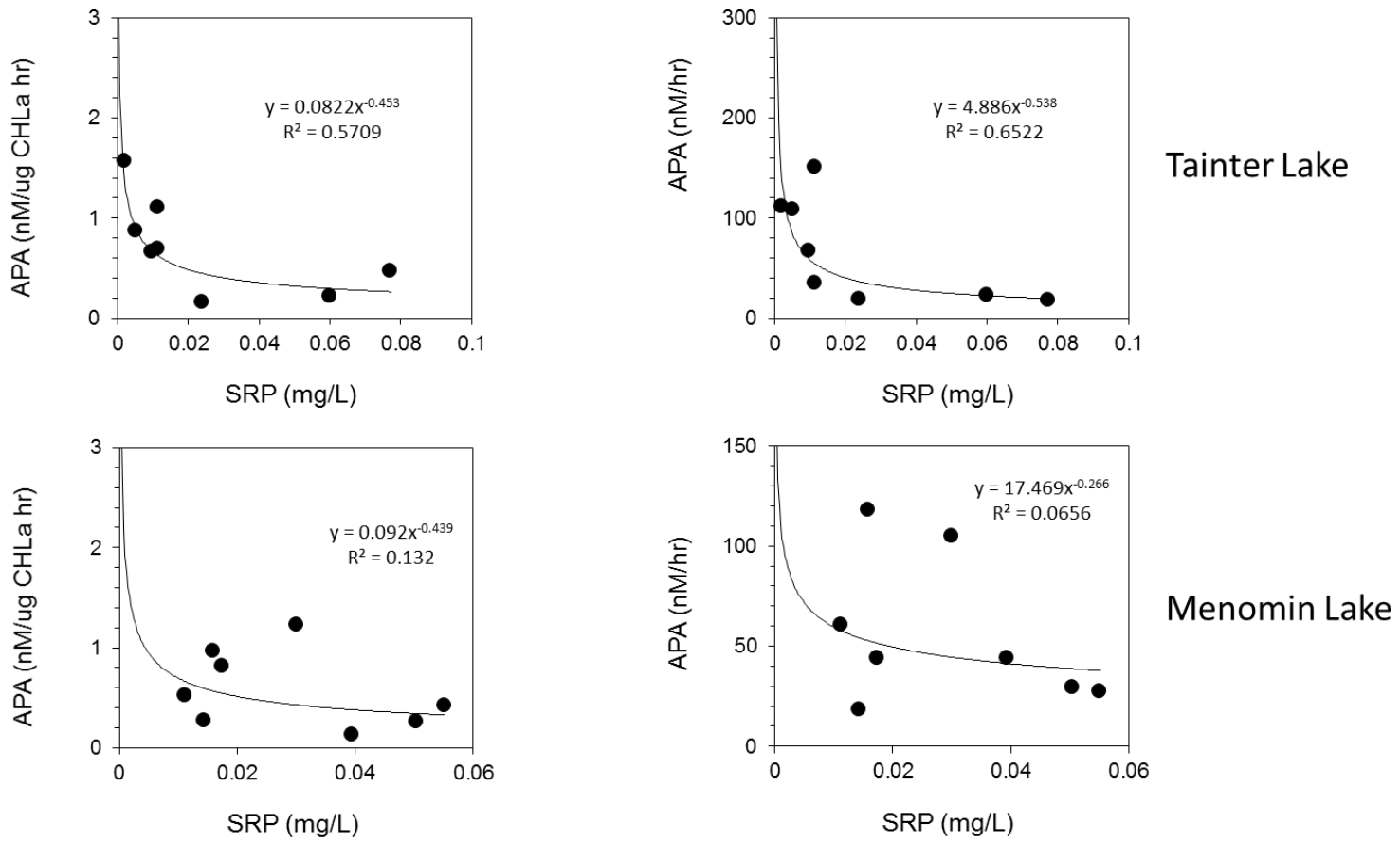

Figure 49. Relationships between soluble reactive phosphorus (SRP) and alkaline phosphatase activity (APA) at station TL5 and ML 5 in Tainter and Menomin Lakes, respectively.

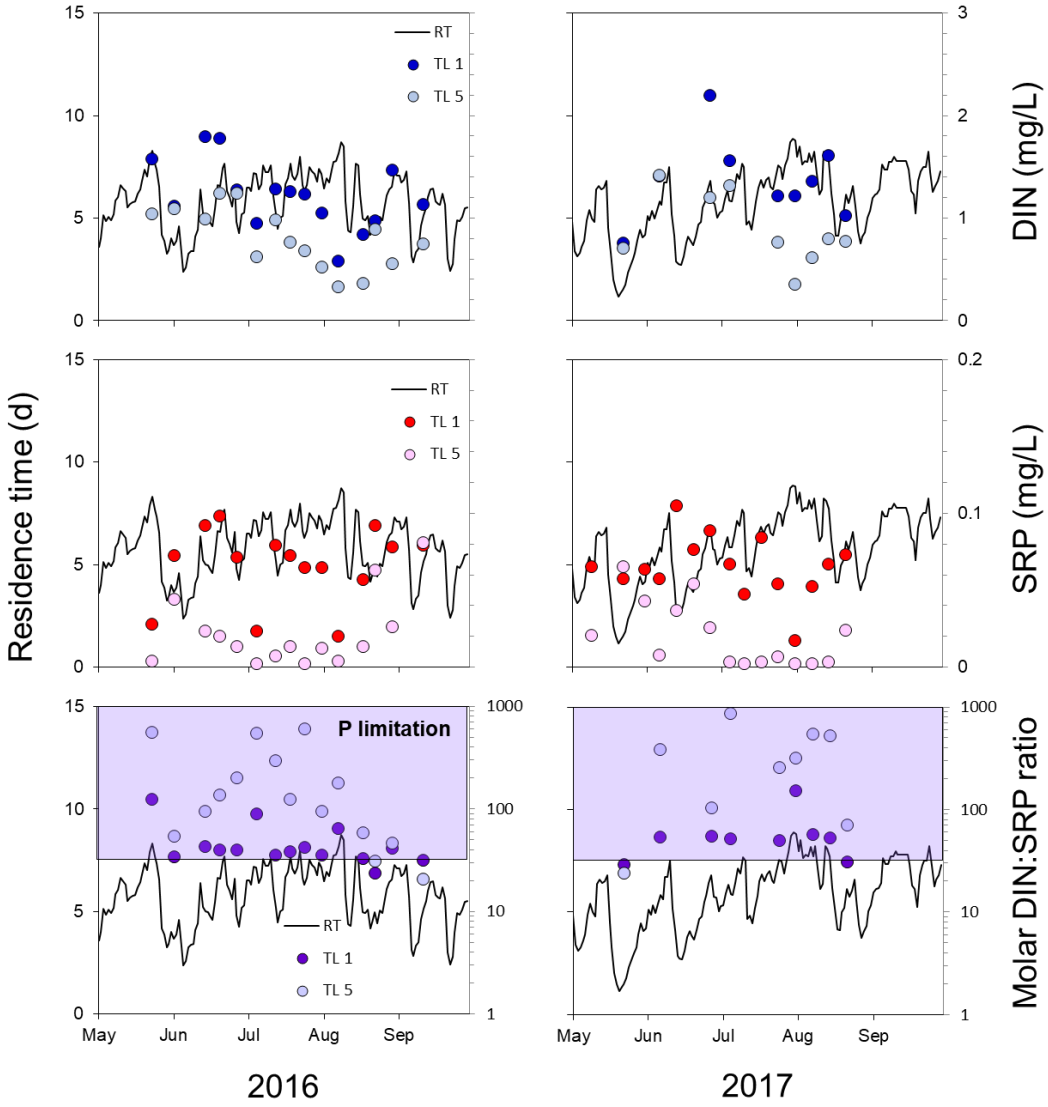

Figure 50. Seasonal variations in Tainter Lake residence time and the concentration of dissolved inorganic nitrogen (DIN, upper panel), soluble reactive phosphorus (SRP, middle panel), and the DIN:SRP ratio (lower panel) at station TL 1 (headwaters) and TL 5 (dam region, upper panel) in Tainter Lake, 2016-17. Purple shaded area in the lower panel denotes DIN:SRP ratio > 30:1 and potential phosphorus limitation of algal growth.

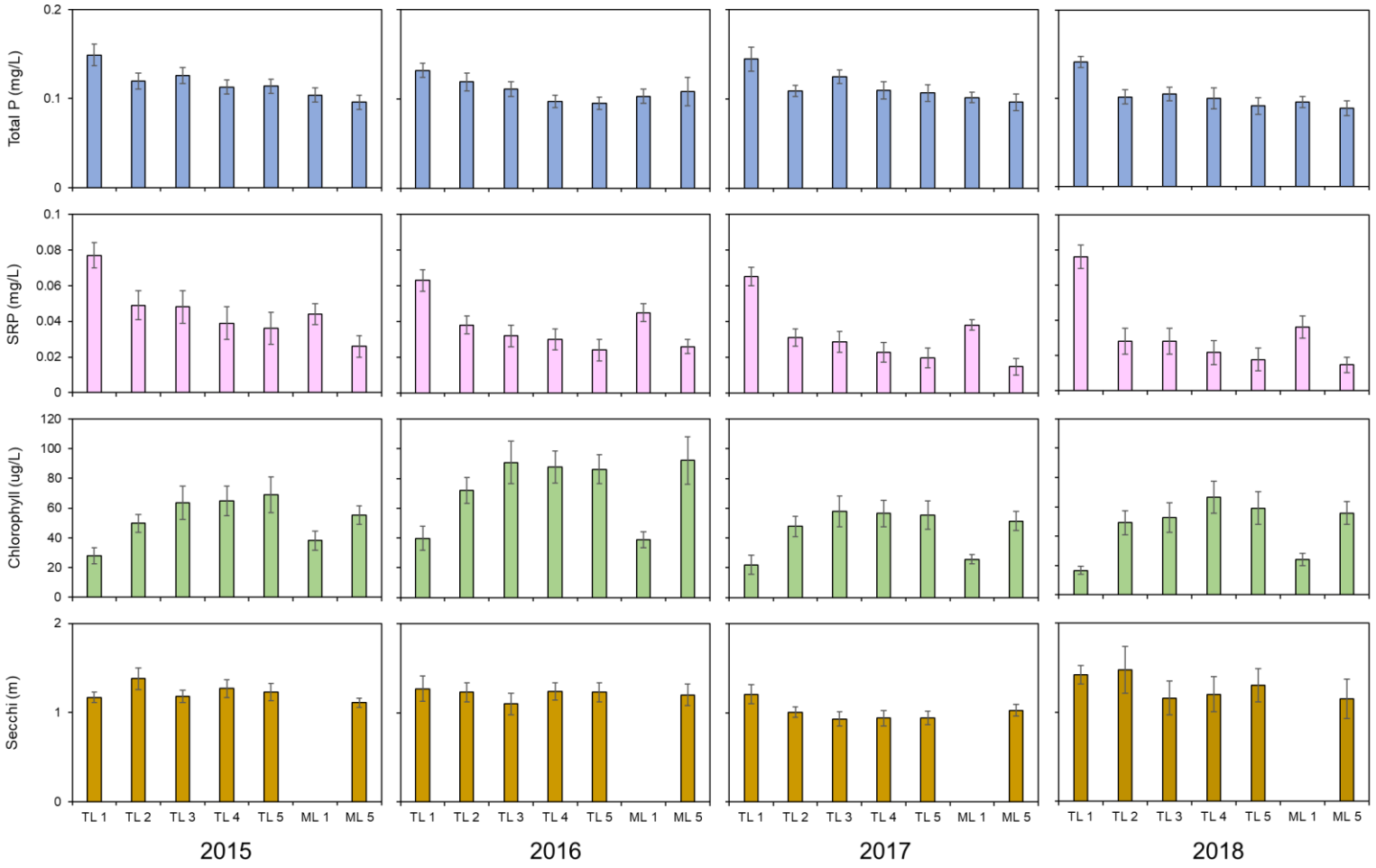

Figure 51. Mean summer concentrations of total phosphorus (P), soluble reactive P (SRP), chlorophyll, and Secchi transparency at various stations in Tainter and Menomin Lakes in 2015-18. Vertical lines represent 1 standard error.

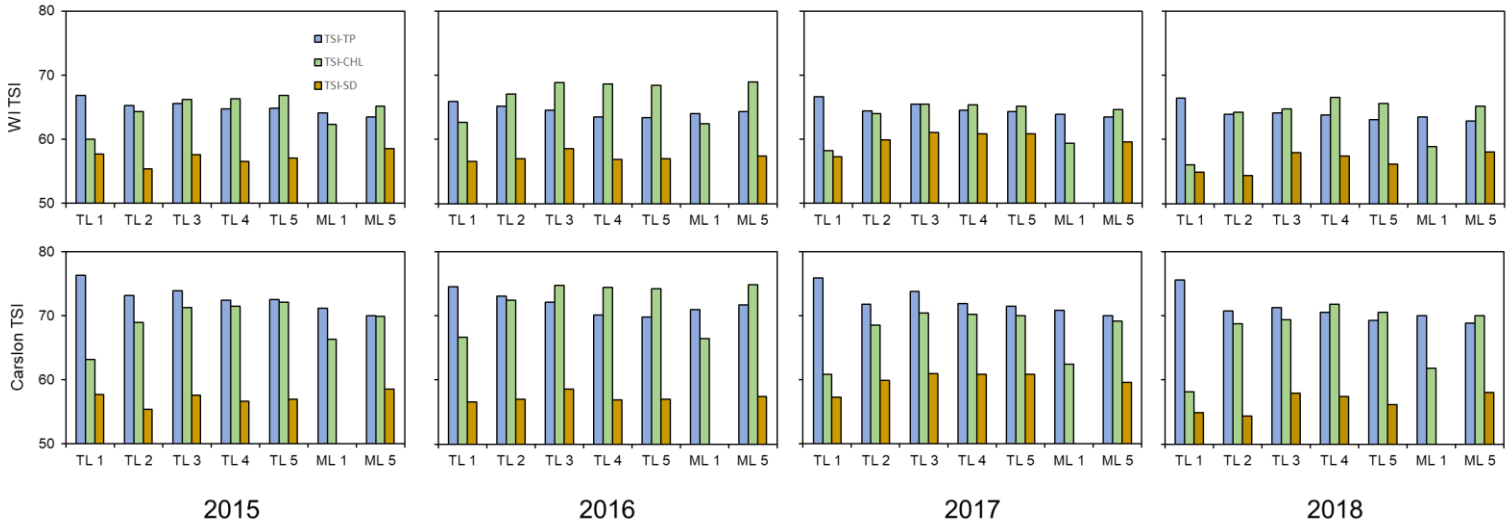

Figure 52. Mean summer Wisconsin and Carlson Trophic State Index (TSI) estimates for total phosphorus (TSI-TP), chlorophyll (TSI-CHL), and Secchi transparency (TSI-SD) at various stations in Tainter and Menomin Lakes in 2015-18.